Neural Correlates of Top-down and Bottom-up Communication in Sensory Networks

Dissertation
zur Erlangung des Doktorgrades
der Naturwissenschaften
(Dr. rer. nat.)

dem Institut für Psychologie
in der Fakultät für Psychologie und Bewegungswissenschaften
an der Universität Hamburg
vorgelegt

von
Liesa Stange

Hamburg, July 2023

Promotionsprüfungsausschuss:

Vorsitzender: Prof. Dr. Frank Rösler

1. Dissertationsgutachterin: Prof. Dr. Brigitte Röder

2. Dissertationsgutachter: PD Dr. Christian Moll

1. Disputationsgutachterin: Prof. Dr. Viola Störmer

2. Disputationsgutachterin: Prof. Dr. Anja Riesel

Tag der Disputation: 14.07.2023

Abstract

What we perceive is not an exact reflection of our surroundings, but rather an interpretation of the noisy and ambiguous information provided by the senses. In the visual system, bottom-up communication occurs in a hierarchical manner, with early areas processing basic features like form and color, and higher areas processing more complex features. On the other hand, top-down communication travels upstream from higher to lower areas, transmitting prior knowledge and influencing our perception of the world. The impact of top-down prior knowledge on perception can be categorized in at least two distinct processes: prediction and attention. Prediction can be understood as prior knowledge about the likelihood of certain stimuli occurring in a particular context or location. On the other hand, attention can be understood as prior knowledge about the relevance of specific stimuli or locations to current behavioral goals. In the present work, we developed two new EEG experiments that investigate top-down and bottom-up communication in sensory networks, controlling either sensory predictions or spatial attention, respectively.

Neuroimaging studies have shown that visual predictions can modulate early visual cortex in a retinotopic specific way. However, the time course of prediction related visual cortex activation is not known yet. In the first study (Chapter II), we implemented a novel event-related potential (ERP) paradigm. A trial started with one of two sounds, which each was associated with one visual stimulus location: either the top left visual field, or the bottom right visual field (‘Standards’). Visual stimuli comprised of gratings, which were presented 750 ms after sound onset. In a small number of trials, the visual stimulus occurred at the unexpected location (‘Deviants’), or was omitted (‘Omissions’). Standards and Deviants elicited a C1 effect, that is, a polarity reversal for lower vs. upper visual field presentation in the latency range between 50-100 ms post stimulus onset. Spatially specific Deviant and Omission effects started with a latency of 150 ms and 230 ms, respectively. The first spatially selective modulation of visual processing was observed as early as 70 ms, as reflected by the *Visual predictive signal*. Spatially specific *Negative* and *Positive error signals* emerged with a latency of 150 and 320 ms, respectively. These results suggest that visual predictions control visual cortex activity in a spatially specific manner, but only after the first sweep of visual processing. However, visual predictions do not elicit neural responses that mimic stimulus-driven activity, but rather, seem to affect early visual cortex via distinct neural mechanisms.

Past research on the relationship between oscillatory activity and attention have consistently found that alpha-power decreases on the contralateral side to the attended stimulus, while showing increases on the ipsilateral side. In contrast to the direction of alpha-lateralization, gamma power shows the complementary pattern. Interestingly, there appears to be a close relationship between alpha and gamma modulation, with alpha power controlling gamma power. In the second study (Chapter III), we used a spatial attention paradigm to investigate whether alpha and gamma lateralization might reflect top-down and bottom-up communication, respectively, as mapped onto endogenous and exogenous spatial attention. We presented letter cues that served as directional (L/R) endogenous cues, which predicted the correct side of the next upcoming target with an 80% probability. Before target presentation, we flashed bright frames around bilateral presented dynamic grating stimuli. These frames served as exogenous cues, which had no predictive value. The presentation of bilateral dynamic grating stimuli resulted in a strong, sustained, band-limited response in the gamma range. During the anticipation of visual stimulation, endogenous spatial attention was found to result in lateralized alpha- and gamma-band responses. However, these effects were not observed after target presentation, which may seem surprising considering the consistent behavioral effects seen with valid and invalid cues. We speculate that the attentional effects were narrow, limited to the task-relevant spatial location, that is the gray circle that was subtended by the dynamic grating stimuli. Therefore, the inhibitory effects of alpha desynchronization observed during the visual stimulation might have been local and did not spread to other regions. Furthermore, since the spatial location of the dynamic grating stimuli were not task relevant the visually induced gamma response was potentially not affected by attention. Overall, both the behavioral and electrophysiological results suggest that endogenous attention (reflecting top-down communication) and exogenous attention (reflecting bottom-up communication) may operate independently from each other.

In conclusion, the findings of this dissertation provide evidence that the initial cortical response in visual processing is independent of top-down control and bottom-up error signals only emerge after the effects of top-down communication. It could be postulated that modulatory top-down effects during anticipation are more widespread, involving a broader assembly of neurons, while modulatory effects during stimulation are limited to more local areas that are behaviorally relevant.

Contents

Abbreviations

BOLD	Blood-oxygenation-level dependent
EEG	Electroencephalography
EPSP	Excitatory postsynaptic potential
ERD	Event-related desynchronization
ERP	Event-related potential
ERS	Event-related synchronization
FFA	Fusiform face area
FFT	Fast Fourier transformation
fMRI	Functional magnetic resonance imaging
ICA	Independent component analysis
IFG	Inferior frontal gyrus
I/I	Invalid/incongruent
ITI	Inter-trial interval
MEG	Magnetoencephalogram
MMN	Mismatch Negativity
PPA	Parahippocampal place area
tACS	Transcranial alternating current stimulation
V/C	Valid/congruent
vMMN	Visual Mismatch Negativity

1

Chapter I: General Introduction

In this introduction, I will shortly introduce the concept of top-down and bottom-up communication in the context of brain activity. I will then mainly focus on the two research fields that are relevant for the empirical work of the present thesis: Sensory predictions in the framework of predictive coding and visual spatial attention.

Top-down and bottom-up communication in the context of brain activity

What we perceive is not the precise reflection of our surrounding world. In fact, the information that our senses provide to us is noisy and ambiguous. Thus, there is a need of inference. Therefore, perception is not a passive registration of the world but instead the integration of bottom-up information, transmitting signals from the external world into the brain, and top-down information, that provides knowledge drawn from prior experiences (Friston, 2005; Summerfield & Koechlin, 2008). In the visual system, bottom-up communication is a hierarchical process. Incoming information is sent downstream via feedforward connections from early to higher-level areas. In the primary visual cortex neurons respond to basic features, such as form and color, whereas in higher areas neurons respond to features with increasing complexity (Lamme et al., 1998). However, information is also travelling upstream via feedback connections from higher to lower areas (Engel et al., 2001), transmitting prior knowledge and inferences about the world, influencing what we actually perceive.

Anatomically top-down and bottom-up communication can be segregated via the layers they target in the cortex. Top-down signals are transmitted via feedback connections which predominantly project to the superficial layers, whereas bottom-up signals are transmitted via feedforward connections which predominantly target the deep layers (Bastos et al., 2015; Buffalo et al., 2011; van Kerkoerle et al., 2014).

A convincing example of how top-down information influences perception are mooney-type images. Without prior knowledge, it might be difficult to recognize what the image in Figure 1 depicts. However, with the additional information that an animal is depicted and that it lives in dry steppes and deserts, one might recognize a camel (Figure 2). The integration of bottom-up and top-down communicated information has behavioral advantages and previous research has shown that prior knowledge not only speeds up reaction times but also lowers detection thresholds (de Lange et al., 2013; Den Ouden et al., 2008; Puri & Wojciulik, 2008; Puri et al., 2009; Rungratsameetaweemana et al., 2018).

Figure 1. Mooney-type image. Created by (Hsieh et al., 2010)

The influence of top-down prior knowledge on perception can be differentiated into at least two distinct processes: prediction and attention. Prediction can be described as prior knowledge about the likelihood of certain stimuli occurring in a particular context, such as a traffic light turning red after turning yellow. It can shape our expectations and guide our understanding of complex stimuli. Research has shown that expectations based on prior knowledge can have a significant impact on early sensory processing and have behavioral advantages (for a review see: Summerfield & Egner, 2009). Attention on the other hand comprises prior knowledge about the relevance of specific stimuli to current behavioral goals and can also affect perception. For example, when searching for a car in a parking lot, knowledge of its color, size and hints about its location (whether it was parked more on the right or the left side of the parking lot) can help to narrow down the set of stimuli that need to be examined, thereby improving search efficiency and behavioral outcomes (for a review see: Carrasco, 2011).

Thus, the integration of bottom-up and top-down information is important to adapt in everyday life. However, it is not yet well understood how top-down and bottom-up information are integrated and interact with each other on a neural level. In the present thesis, I will focus on two approaches to investigate top-down and bottom-up communication, covering both prediction and attention. First, I will investigate sensory predictions in the framework of predictive coding to study the timing and specificity of top-down and bottom-up signals. Secondly, I will examine visual spatial attention using the spatial attention paradigm (also known as the Posner paradigm) to investigate the interaction of top-down and bottom-up sensory signals and their relation to oscillatory activity in specific frequency bands. I will introduce these two topics in the following section.

Figure 2. The grayscale version on which the Mooney-type image in Figure 1 is based. Created by (Hsieh et al., 2010)

Sensory predictions and the predictive coding framework

For a long time, hierarchical feedforward models have been the primary theoretical framework used to guide research investigating the neural basis of perception. These models assume that sensory information are processed through a sequence of increasingly complex feature detectors (DiCarlo et al., 2012; Hubel & Wiesel, 1968; Riesenhuber & Poggio, 1999). This traditional framework has recently been challenged by a different set of theories, known as predictive processing (Friston, 2005; Keller & Mrsic-Flogel, 2018; Rao & Ballard, 1999). They propose that perception is the result of an ongoing process of inference. The brain implements an internal model derived from environmental statistics, enabling the continuous generation of predictions about future incoming sensory events. These predictions reflect the expected sensory information under the assumption that the estimated sensory cause was correct. According to the primary neural computation of predictive processing, called predictive coding, these predictions are sent upstream from high-order to low-order areas. At early sensory stages the actual sensory input is compared to the predictions and only the residual, unexplained sensory information is sent downstream to higher-level areas in form of “prediction errors”. The brain's internal model makes use of error signals to update the likelihood of perceptual hypotheses in an ongoing and iterative manner at all levels of processing hierarchy. This process continues until the network reaches a coherent representation of the underlying sensory stimuli. Therefore, perception can be understood as the selection of the perceptual hypothesis that minimizes prediction error by best predicting incoming sensory information.

This strategy is considered as been especially efficient since, once a high-level representation is formed, only error signals are transmitted through the sensory system and thereby resources needed in processing predictable or stable input are reduced (Alink et al., 2010; Schellekens et al., 2016). In line with this assumption, the repetitive presentation of images reduced spiking activity in the inferior temporal cortex in monkeys (Miller et al., 1991) as well as the hemodynamic activity in the human homologue the lateral occipital cortex (Grill-Spector et al., 2000), as measured with functional magnetic resonance imaging (fMRI).

Furthermore, predictive processing assumes that the error signal does not only represent an unspecific surprise response but that prediction and prediction error units coding for the specific stimulus features exist (Friston, 2005; Rao & Ballard, 1999). On every level of the processing hierarchy error units send the residual mismatch between predictions and actual sensory input downstream and laterally, whereas the prediction units communicate expected input upstream and laterally (Figure 3). The above considerations lead to two main hypotheses: If sensory predictions are updated to minimize the prediction error, stimuli that mismatch the prediction should lead to increased neural responses in comparison to matching stimuli. Also, if prediction units code for specific features of the expected sensory input, in the absence of stimulus-driven activity top-down predictive signals should activate similar neural patterns to the actual expected stimulus.

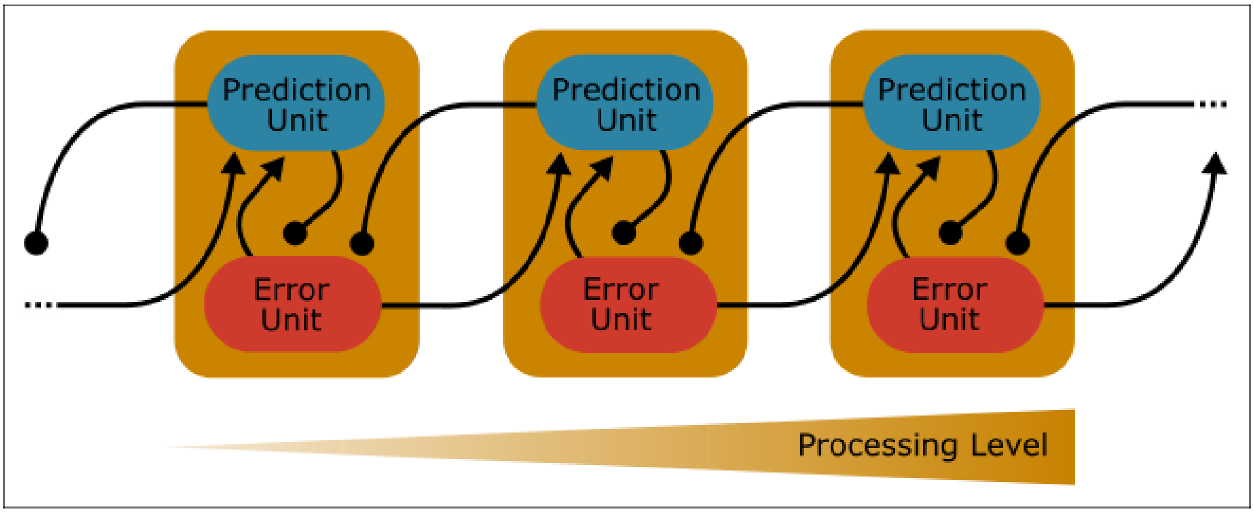

Figure 3. A simplified illustration of the hierarchical predictive coding model proposed by Rao and Ballard (1999). Prediction units send their predictions to the error units located on the same level and one level below. Error units on the other hand send the residual error signal to the predictions unit on the same level and one level above.

Mismatching sensory input increases neural responses

According to predictive coding, the brain constantly predicts upcoming sensory input. It is assumed that at early sensory processing stages the top-down predictive signal is already compared to the actual sensory input. Only the residual is sent feedforward as an error signal. Accordingly, sensory input that violates the prediction, should lead to increased neural responses compared to sensory input that matches the prediction, since an increased or additional error signal is expected. In line with these assumptions, single neuron recordings in monkey inferior temporal cortex, a part of the ventral „what“-path, showed increased firing rates to unexpected than to expected visual input (Meyer & Olson, 2011). fMRI studies in humans (Den Ouden et al., 2010; Egner et al., 2010) found consistently increased blood-oxygenation-level dependent (BOLD) responses to unexpected compared to expected stimulus categories in category-specific regions (fusiform face area vs. parahippocampal place area for presented faces vs. houses). For less complex stimuli increased neural responses were also recorded in early visual and auditory cortex when comparing unexpected to expected stimulation (Alink et al., 2010; Kok, Jehee, & Lange, 2012; Todorovic et al., 2011). Taken together, prediction error signals have been identified as increased responses to unexpected stimuli not only in higher processing areas but also already in primary sensory regions. However, it remains unclear how specific the error signals are and at what time during the processing hierarchy error signals emerge.

Most research investigating the timing and specificity of error signals is conducted in the auditory domain. Mismatching auditory events compared to expected ones typically elicit an increased negative component contralateral to the stimulated side in the time period 100 to 200 ms after stimulus onset, known as the Mismatch Negativity (MMN; Garrido et al., 2009; Winkler, 2007). In the visual domain, a negative component similar to MMN in both latency and topography has been discovered: it is called the Visual Mismatch Negativity (vMMN; Czigler et al., 2006; Sulykos & Czigler, 2011). Both the MMN and vMMN have been assumed to reflect an increased error signal to domain specific stimulation that violates sensory predictions (for a review see: Stefanics et al., 2014). Nevertheless, when it comes to the timing of error responses, especially in the visual domain, results are not consistent. For example, one ERP study that used upper vs. lower visual field stimulation, reported that mismatch effects already started during the late period of the C1 component (Jabar et al., 2017), which is the first visual component associated with early visual processing predominantly stemming from primary visual cortex (Alilović et al., 2019; Di Russo et al., 2002). By stimulating the upper and lower visual field, opposing banks of the calcarine sulcus are targeted, which results in a polarity reversal within a period 50 to 100 ms after stimulation. The C1 effect results in a negative going amplitude by subtracting lower from upper visual field stimulation (for an illustration see: Figure 4). The authors assumed that error signals could emerge already during the first stage of visual processing. However, a recent study with a similar stimulation protocol reported robust effects starting only in the time window of the N1 component (Alilović et al., 2019). It is not yet clear during which stage of visual processing error signals are initiated and how feature specific they are.

A recent proposal opened the discussion whether it is crucial to distinguish the error signals based on the nature of prediction violations. Keller and Mrsic-Flogel (2018) introduce distinct error signals, namely a positive error signal for exceeding sensory input and a negative error signal for missing sensory input. Although the neural circuitry underlying these signals has been described in detail at the cellular level, only one brain-imaging study has yet been conducted to differentiate between the processing of positive and negative error signals (Schliephake et al., 2021). Up to this date, the time course of negative and positive error processing has not been studied.

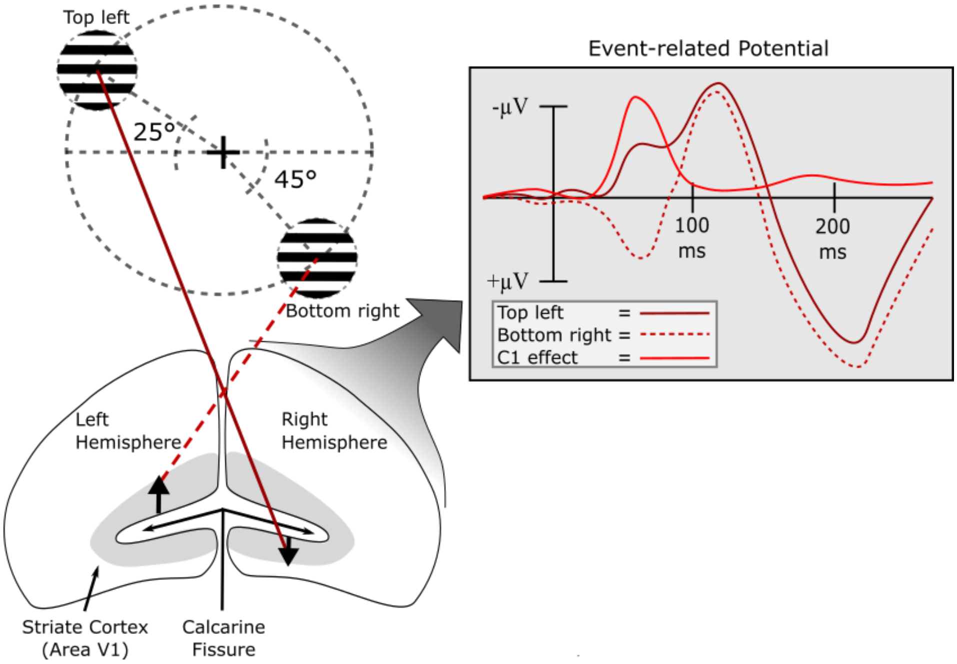

Figure 4. Relationship of stimulus position and C1 polarity and the resulting C1 effect. Visual stimuli presented in the upper or lower visual field hit opposing banks of the calcarine sulcus. The alignment of pyramidal cells in the cortex results in a negative or positive potential. The difference of the ERPs to upper and lower visual field presentation results in a negative going amplitude.

Unexpected sensory omissions reflect top-down predictions

To assess the top-down predictive signal is more challenging than to examine the bottom-up error signal. One approach has been to eliminate any confounding bottom-up sensory-driven activity by investigating neural responses to unexpected sensory omissions. In the auditory domain, sound omissions reliably elicited neural responses comparable to the activation pattern of veridical stimuli. For example, SanMiguel et al. (2013) showed that the unexpected omission of self-generated tones, triggered by button-presses, lead to an auditory-like ERP response. Furthermore, Bendixen et al. (2009) reported that neural responses to unexpected tone omissions were indistinguishable from the neural responses to the actual tones. Interestingly, intracranial recordings in humans also showed localized cortical responses to missing tones that were topographically similar to the responses evoked by actual tones (Hughes et al., 2001).

These studies suggest that the recorded neural responses during omissions represent the pure top-down signal and that top-down predictions are not only unspecific surprise responses, but carry feature-specific information. However, in the visual domain omission studies are not that consistent. Intracranial recordings in mouse V1 have shown that the omission of an image, that was preceded by an associated image, elicited a neural response that was indistinguishable from the neural response to the actual image (Gavornik & Bear, 2014). In humans, fMRI studies reported similar findings: The omission of learned visual stimulus configurations elicited similar neural response patterns as the presentation of the actual stimuli (Ekman et al., 2017; Kok et al., 2014; Muckli et al., 2015). For example, in a recent study by Kok et al. (2014) the omission of line gratings tilted to an expected degree with either 45° or 135° elicited the same activation pattern as the actual stimuli. These findings are in line with the assumption that neural responses to omissions reflect top-down predictions because in the absence of stimulus-driven bottom-up activity they contain feature specific information and activate similar neural assemblies. However, to this date there has been a lack of studies investigating whether the timing of visual omission responses is equivalent to the timing of actual visual stimuli. In other words, we need studies investigating whether the timing of top-down visual predictions recorded during visual omissions follow the same activation course as neural responses recorded during stimulus presentation, and are in fact indistinguishable. It should be noted, that recent research is challenging the view that omission responses correspond to the pure top-down signal, since the absence of the expected sensory input should elicit additional negative error processing as introduced in the section above.

Visual spatial attention

Spatial attention is an important process in order to select relevant information due to the limited computational capacities of the brain. It is a crucial mechanism in gain-control by amplifying the neural signal evoked by attended stimuli (Hillyard et al., 1998) and which might account for the behavioral benefits and costs reported in spatial attention paradigms (Posner, 1980; Posner et al., 1978). Spatial attention can be differentiated into overt and covert attention. During overt attention, observers move their eyes to the relevant location, with the focus of attention covering a rather limited area. Covert attention describes the shift of attention to a broader space in the visual field, typically in the periphery, without moving the eyes nor directing the gaze to a specific point in space. Studying covert attention has the big advantage that attention can be directed without the necessity of eye movements. Especially when recording electroencephalogram (EEG) a stable gaze improves data quality and thereby the signal-to-noise ratio. Furthermore, in contrast to overt attention that can only be shifted in serial because eye movements are inevitably sequential, covert attention can cover more than one location at a time.

Endogenous and exogenous attention

Covert attention can be oriented in two different ways: either under voluntary control and directed by our goals, expectations, and prior knowledge or it is captured by salient stimuli in the environment, regardless of our goals or intentions. The first type of attention, also known as endogenous or top-down attention is directed by higher-level cognitive processes, such as memory, decision-making, and language. For example, when driving in a new city, you might use endogenous attention to focus on the street signs that are relevant to your search, i.e., those that are close to your destination. The second type, also known as exogenous attention is directed by sensory stimuli that are especially salient, such as sudden noise or a flashing light. Exogenous attention is generally transient and can easily disrupt ongoing attentional processes. For example, if you are driving and concentrating on the traffic and suddenly hear a loud noise, such as the car behind you honking, your attention will be automatically captured by the noise, even if you were focused on the traffic before. Both endogenous and exogenous attention involve communication between different parts of the brain. Endogenous attention relies on top-down communication between higher-level areas and lower-level sensory areas, while exogenous attention relies on bottom-up communication between sensory areas and higher-level areas. These two types of attention can work together to help us selectively attend to important stimuli in our environment.

In the paradigm invented by Posner (1980) known as the spatial cueing paradigm, endogenous and exogenous attention are investigated by comparing behavioral costs and benefits to cued and uncued locations, e.g. speeding up reaction times to targets. Endogenous attention is directed by symbolic cues, presented in the center of the visual field. Exogenous attention on the other hand is controlled by flashing a salient stimulus in the periphery. Usually these two attentional types are studied in isolation (Carrasco, 2011). However, utilizing a double-cue paradigm (Figure 5), a variant of the Posner paradigm that cues in each trial both endogenous and exogenous attention makes it possible to additionally investigate their interaction. At the beginning of each trial, an endogenous symbolic cue is presented at the center of the visual field. Then, the exogenous cue (a salient stimulus, e.g. a bright dot or frame) is flashed in the periphery at the location of a subsequent target. Finally, the target is presented either on the left or on the right side. Endogenous cues typically predict with a high probability the correct location of the target, whereas exogenous cues have no predictive value. Most studies include neutral endogenous and exogenous cueing conditions allowing to study not only the interaction of both attentional types but also the isolated effects by keeping one cue at a time uninformative or neutral, respectively. For this purpose, at the beginning of the trial, the letter N is presented serving as a neutral endogenous cue and the salient stimulus is simultaneously flashed at both locations for a neutral exogenous cueing condition (Figure 5).

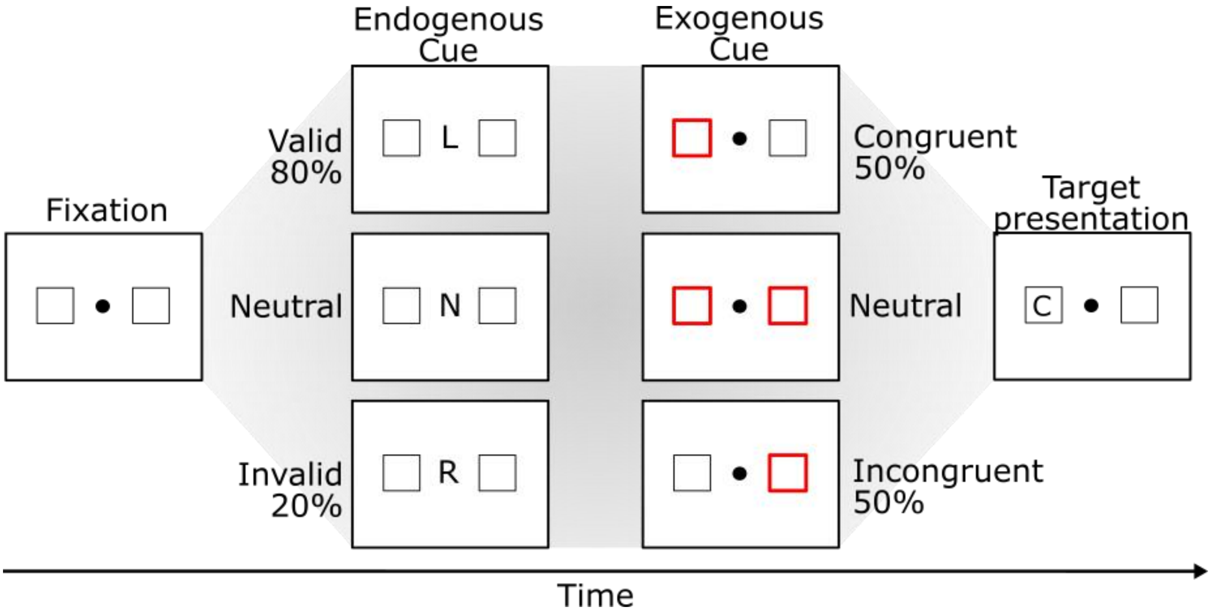

Figure 5. Illustration of a double-cue paradigm. Each trial starts with the presentation of a fixation point or cross and two placeholders (in this example two squares in which the target can appear). Next, either a valid, invalid or a neutral endogenous cue is presented. Directional cues (in this example the letters L and R) predict with a high probability (in this example 80%) the correct target location. Neutral or uninformative endogenous cues have no predictive value. Then a congruent or incongruent exogenous cue with no predictive value but directing attention to either the left or the right is presented. The neutral or uninformative exogenous cueing condition consists of the simultaneous presentation of the cue (in this example a flashing frame) on both sides. Finally, the target is presented inside either the left or the right square.

Both endogenous and exogenous attention show behavioral benefits for cued versus uncued locations by e.g. speeding up reactions times, increasing performance and lowering detection thresholds (for a review see: Carrasco, 2011). However, they do so independently without interacting with each other (Berger et al., 2005). Moreover, they show essential differences. Behavioral studies that used double-cueing paradigms allowing the investigation of the interaction of endogenous and exogenous attention have shown that cognitive load has a greater impact on endogenous orienting than on exogenous orienting (Jonides, 1981). Furthermore, while participants were able to disregard endogenous cues, they were unable to do so when exogenous cues were presented (Jonides, 1981; Müller & Rabbitt, 1989). Moreover, the effects of exogenous cues were more pronounced than those of endogenous cues (Müller & Rabbitt, 1989). Finally, the cue validity and predictability had a greater impact on endogenous orienting compared to exogenous orienting (Müller & Findlay, 1988). An additional major difference is their time course. Endogenous attention is most effective after long latencies (> 300 ms) and can be maintained for a long period up to seconds (Müller & Findlay, 1988; Müller & Rabbitt, 1989). In contrast, exogenous attention builds up quickly (< 200 ms) and sustains only for a short period of time with an initial facilitation followed by inhibition at longer latencies. This phenomenon is referred to as "inhibition of return" (Klein, 2000; Posner et al., 1985). The observed differences and the lack of interactions lead to the proposal that spatial attention relies on two separate mechanisms that deploy from the same capacity-limited attention system: voluntary goal-directed endogenous and reflexive stimulus-driven exogenous attention (Chica et al., 2013).

In line with the findings in behavioral data, current models of attention assume that endogenous and exogenous attention rely on two independent neural systems. They propose a dorsal fronto-parietal network that primarily serves endogenous orienting, and a ventral network that mainly subserves faster exogenous orienting (Chica et al., 2013; Corbetta & Shulman, 2002; Funes et al., 2005). It is important to note, however, that these effects may act on various stages of sensory processing (Müller & Rabbitt, 1989), as ERP studies have demonstrated.

Most ERP studies have examined the neural substrates of endogenous and exogenous attention in isolation. It has been shown that both endogenous and exogenous attentional effects are observable already in the early phase of the P1 component, starting as early as 70 ms after stimulus onset (Di Russo et al., 2002; Martinez et al., 1999). Compared to invalid cues, valid cues increase the amplitude of the P1 component, which is thought to result from a sensory gain-control mechanism that enhances the processing of validly cued stimuli (Mangun & Hillyard, 1991). The subsequent N1 component is only modulated by endogenous attention under specific task conditions: Valid cues elicited increased amplitudes contralateral to the target stimulus only for difficult discrimination tasks, that demanded a high cognitive load, (Hopfinger & West, 2006; Mangun & Hillyard, 1991; Vogel & Luck, 2000). The P300 component, which is associated with higher processing and related to working memory and decision making, is again affected by both endogenous and exogenous attention (Hopfinger & Mangun, 1998, 2001; Hopfinger & West, 2006). Valid cues elicited higher P300 amplitudes compared to invalid cues, indicating that the target location is treated as more relevant than the uncued location.

Neurophysiological and imaging studies that investigated the interaction of endogenous and exogenous attention are sparse. In line with the assumption that endogenous and exogenous attention engage independent neural circuits, a fMRI study that concurrently engaged endogenous and exogenous attention in the same trial reported that for orienting as well as reorienting, both attention modes activated different brain structures independently of each other (Natale et al., 2009). In contrast, an ERP study showed that although endogenous and exogenous attention dominated different processing stages (exogenous the late phase of P1 and endogenous the subsequent N1 component), they did not do so completely independently of each other, as endogenous and exogenous cueing effects interacted (Hopfinger & West, 2006). The authors concluded that endogenous and exogenous attention might rely on partially separate but interacting neural networks, which can be active concurrently and influence sensory processing at various overlapping stages.

In summary, endogenous and exogenous attention show both similar behavioral costs and benefits, although the latter seems to be less susceptible to interference and to be a more automatic process. Both attention types seem to affect similar processing stages when investigated in isolation. However, concurrently modulated results are not as consistent. Although endogenous and exogenous attention seem to deploy different brain regions and dominate different stages of sensory processing, they do not do so completely independently of each other. Further research is needed to clarify whether the neural systems that endogenous and exogenous attention rely on are in fact partially overlapping and interact, or whether they are completely separate and independent from each other.

Communication through coherence

Endogenous and exogenous attention reflect top-down and bottom-up processes, which seem to rely on different neural networks but interact with each other on several sensory processing stages. However, the question remains how attended information that is amplified by these two attentional types is transmitted. Furthermore, it is still not clear how these information streams interact with each other when operating simultaneously and how they are integrated into a coherent percept. Maintaining information in small as well as in large scale is one major challenge for neural communication: within brain areas, only related information has to be integrated whereas between brain areas, information has to travel big distances without being altered. A growing body of literature supports the proposal that reliable neural communication is established via synchronized oscillatory activity. For example the so called “communication trough coherence” theory assumes that selective communication among neural networks might be implemented via oscillatory phase-coherent activations (Fries, 2005). An illustration of the proposed mechanism is given in Figure 6. Neural assemblies fluctuate between states of high and low excitability. Just before and at the peak of excitability the neural group is easily excited, whereas around the through excitation is improbable. In Figure 6, the red neural groups at processing level X and X +/-1 encode coherent information, whereas the blue neural group encodes incoherent information. Therefore, the communication between the red neural groups should be facilitated, whereas communication between mismatching colored groups should be hindered. The red neural group at processing level X spikes at the peak of the red neural group at processing level X +/- 1 and vis versa, thereby they fluctuate coherently and their communication is effective. In contrast, the blue neural group spikes while the receiving red neural group is currently at the trough of excitability. Their communication is not effective or even prohibited. The processing levels are not only representative of different brain regions but also of neural groups in different layers of the cortex. Furthermore, information transmission via coherent spiking is not limited to the representation of identical objects but extends also to other cognitive processes such as attention or memory. In summary, ‘communication through coherence’ provides a simple mechanism to explain effective neural communication both between and within cortical regions.

Recently, this theory was extended by the proposal that oscillatory activity in different frequency bands serve different tasks (Fries, 2015; Wang et al., 2016). It has been proposed that lower frequencies, specifically in the alpha- and beta-band could be involved in communication within brain areas and top-down communication, as well as in inhibitory processes. On the other hand, higher frequencies in the gamma range are suggested to reflect local as well as bottom-up communication (Bastos et al., 2015; Chao et al., 2022; Michalareas et al., 2016). This proposal is anatomically plausible: feedback connections predominantly target the superficial layers of the cortex and exert gamma-band synchronization, whereas feedforward connections mostly project to deep layers and show alpha- and beta-band synchronization (Bastos et al., 2015; Buffalo et al., 2011; van Kerkoerle et al., 2014). How oscillatory activity in the alpha and gamma range map onto top-down and bottom-up processing and how they relate to endogenous and exogenous attention will be discussed in the next section.

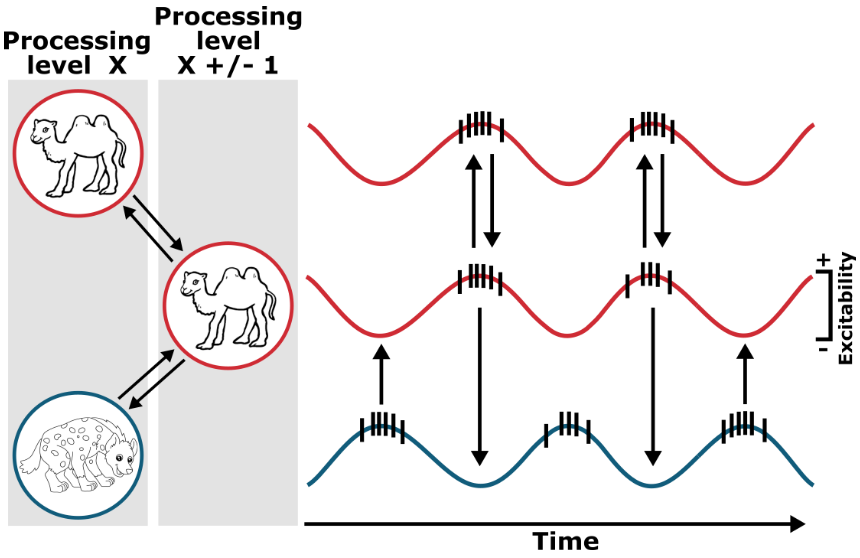

Figure 6. Illustration of communication through coherence. Two neural assemblies at the same processing level X encode different information (red and blue). At processing level X +/- 1, the neural assembly is encoding the same information of only one of the latter (red). The excitability of neural assemblies fluctuates over time. At peaks, excitability is probable and at troughs, it is improbable. If the receiving and sending neural assembly fluctuate coherently, their communication is effective (both red groups). Neural groups that show incoherent fluctuations (red and blue groups) communicate in a less effective way or their communication is even prohibited. Arrows depict the direction of information transmission and moment of spiking. Short vertical lines represent spiking activity.

Oscillatory activity and its association with endogenous and exogenous attention

It was Berger (1929) who first reported the typical rhythmic activity visible even in raw EEG recordings, called alpha rhythm. Since Adrian and Matthews (1934), this dominant activity was interpreted as reflecting an “idling” state of the brain without specific function in neural computation. Nowadays activity in the alpha-band is better understood and has been related to perception and several different cognitive processes (for a review see: Başar, 2012). As one of the first ones Pfurtscheller et al. (1994) reported that engaging in a visual task enhanced resulted in event-related alpha desynchronization (ERD) over occipital regions. The authors interpreted their findings as reflecting intentionally enhanced excitability of these areas. In line with this interpretation, studies investigating spatial visual attention reported increased ERD contralateral to the attended side (Sauseng et al., 2005; Thut et al., 2006). However, it was only Rihs et al. (2007) who emphasized the importance of event-related alpha synchronization (ERS) as a mechanism of selective inhibition. Together, ERD and ERS have been widely interpreted as reflecting top-down inhibitory control processes (for a review see: Jensen & Mazaheri, 2010; Klimesch et al., 2007). In line with this assumption, increased alpha modulation has been linked to improved behavioral performance by increasing detection and discrimination performance (Thut et al., 2006; van Dijk et al., 2008), as well as to reduced reaction times (Gould et al., 2011; Kelly et al., 2009) and distractor inferences (Okazaki et al., 2014).

It was also Berger (1937) who reported the first effects in higher frequency ranges (40 to 90 Hz) when comparing spontaneous EEG activity with EEG activity during mental calculations. Later empirical work emphasized the involvement of high frequency or gamma synchronization in feature-binding and object-representation (for a review see: Tallon-Baudry, 2009). More recent research has stressed its role in a variety of cognitive processes as e.g. attention, memory and error processing (Jensen et al., 2007; Vinck et al., 2022). Taken together neural activity in the gamma-band seems not only to reflect perception but also to be involved in more complex cognitive operations.

On a physiological level, oscillatory activity in the gamma range is a good candidate for transmitting bottom-up information. The duration of excitatory post-synaptic potentials (EPSPs) is approximately 10 ms (Williams & Johnston, 1991), only fitting around 1 to 3 times in a gamma cycle (10 to 30 ms). Thus, EPSPs synchronized in gamma frequency provide a high temporal precision and add up more easily as compared to lower frequencies, which are more temporally smeared. Accordingly, oscillatory activity in the gamma range has an efficient and temporally precise impact on subsequent (downstream) neurons, which is especially important in bottom-up communication, which transmits incoming potentially behaviorally relevant information.

It has been proposed that attention works by boosting the impact of neurons that encode attended stimuli within sensory cortices, thereby increasing the strength of their influence on other cortical areas further downstream (Treue, 2001). In line with this idea and the proposed role of gamma-band activity being especially efficient in transmitting bottom-up information, studies in monkeys (Bichot et al., 2005; Engel et al., 2001) as well as in humans have shown that attended compared to unattended stimuli increased oscillatory activity in the gamma-band (Gruber et al., 1999; Müller et al., 2000). Furthermore, this increase was spatially specific as gamma-band power increased only contralateral to the attended side (Fries et al., 2001; Müller et al., 2000) and was positively correlated with performance (Hoogenboom et al., 2010; Siegel et al., 2008). More recent studies, consistently showed that spatial attention also increased the amplitude of visually induced gamma responses over occipital regions contralateral to the attended hemisphere (Bauer et al., 2012; Magazzini & Singh, 2018; Marshall, O'Shea et al., 2015; Marshall, Bergmann, & Jensen, 2015; Siegel et al., 2008). However, to date only the effect of endogenous attention on gamma-band activity has been investigated. There remains a lack of studies investigating the effect of exogenous attention on gamma-band activity, which would be important to get a deeper understanding of the role of gamma-band oscillations in bottom-up communication.

Alpha- and gamma-band modulation might be closely related, as alpha power decreases contralateral and increases ipsilateral to the attended side, whereas gamma power shows the complementary pattern (Marshall, Bergmann, & Jensen, 2015). Furthermore, alpha power seems to control gamma power (Herring et al., 2019; Popov et al., 2017; Siegel et al., 2008). Popov et al. (2017) reported that stronger modulation in both alpha and gamma power predicted the performance in a detection task. More importantly, in anticipation of the target display the decrease of alpha predicted stimulus-induced gamma-band activity. More recently, Herring et al. (2019) conducted a study using transcranial alternating current stimulation (tACS) in the alpha range over the occipital cortex while recording a magnetoencephalogram (MEG). They observed that alpha tACS suppressed visually induced gamma oscillations and found a negative correlation between the degree of gamma suppression and performance in a visual detection task. Taken together these observations suggest that alpha oscillations reflecting top-down inhibitory control may regulate the bottom-up sensory processing that is conveyed by high frequency gamma oscillations. However, it is still not clear whether visually induced gamma-band activity can be modulated by exogenous attention and whether one can thereby argue that gamma-band activity reflects bottom-up processing.

Summary and Outlook of the Thesis

What we perceive results from the integrative process of top-down and bottom-up information. Bottom-up communication carries new sensory information from the world into the system, top-down communication transmits prior knowledge about the surrounding world to analyze and interpret incoming information. To understand how top-down and bottom-up communication interact and are integrated is fundamental to understand human perception.

For a long time, perception was understood as a solely feedforward process, from the specific to the more general. However, a new set of theories that emphasize the significance of feedback processing, called predictive coding or processing, is challenging this view. They assume that top-down predictions and bottom-up sensory information are compared at every level of the processing hierarchy and that only the residual is sent downstream as an error signal, updating future predictions. Studies have shown that early sensory areas are modulated by top-down predictions in a stimulus specific manner. In the auditory domain, these modulations are reported to be early in time and to be indistinguishable from the neural activity corresponding to the actual stimulus. However, studies in the visual domain found equivocal results. One study reported effects as early as the first ERP response of primary visual cortex, whereas the majority of studies reported later effects. It remains an open question which stages of visual processing are under top-down control and whether top-down sensory predictions represent neural activity associated with veridical stimuli.

It has been proposed that reliable communication of top-down and bottom-up information is established via synchronized oscillatory activity. Oscillatory activity in lower frequency-bands (alpha-/ beta-band) are hypothesized to subserve top-down communication and higher frequencies (gamma-band) are hypothesized to index bottom-up communication. A commonly used paradigm to investigate top-down and bottom-up communication is the Posner paradigm, in which endogenous and exogenous attention, respectively, map onto top-down and bottom-up processing. It has been shown that alpha-band power decreases contralateral and increases ipsilateral to the attended side, whereas gamma-band power is modulated in the opposite direction: it increases contralateral and decreases ipsilateral. These observations lead to the proposal that alpha and gamma modulations might be closely related and that alpha power controls gamma power. Although their interaction might play a key role not only in spatial attention but also in perception, studies that investigate simultaneously the effects of endogenous and exogenous attention on oscillatory activity in the alpha- and gamma-band are lacking. Furthermore, no study to date examined directly whether oscillatory activity in the gamma-band reflects exogenous attention and thereby bottom-up processing.

The aim of the present dissertation is to examine the timing and specificity of top-down information, and to investigate whether power in the alpha- and gamma-band, respectively, map onto top-down and bottom-up communication. In chapter II, a novel ERP omission paradigm is used to test the hypothesis that the timing of top-down predictions and bottom-up generated sensory cortex activity in primary visual cortex are in fact indistinguishable. The timing and specificity of error signals are examined. We investigated whether error signals can be differentiated depending on how they violate sensory predictions. A new proposal provides a detailed description of the neural circuits underlying positive (sensory input that exceeds sensory predictions) and negative error processing (missing sensory input). To date empirical work that tried to distinguish both is limited. In chapter III, a spatial attention paradigm is used to investigate whether lateralized responses in the alpha-band that reflect top-down inhibitory control may regulate bottom-up sensory processing that is conveyed by lateralized gamma-band activity. We examine whether visually induced gamma-band activity is modulated by exogenous attention and thereby argue that oscillatory activity in the gamma-band indicates bottom-up processing. Visual stimuli are tailored to yield an adequate response in the gamma-band, since in EEG it is challenging to obtain a sufficient response. In addition, we tested whether the behavioral outcomes can be explained by the observed alpha- and gamma-band modulations.

Chapter II: Crossmodal Visual Predictions elicit spatially specific early Visual Cortex Activity but later than real Visual Stimuli[1]

---

[1] Parts of this chapter are submitted as Stange et al. (2022)

1. Introduction

Expectations about forthcoming sensory input in a continuously changing environment are essential for efficient behavior: Sensory predictions have been reported to lower detection thresholds and to increase processing speed for sensory events (de Lange et al., 2013; Den Ouden et al., 2008; Puri & Wojciulik, 2008; Puri et al., 2009). One framework that offers a potential explanation of the underlying neural mechanisms of these beneficial behavioral effects is predictive coding. This framework proposes that top-down predictions are compared to bottom-up sensory input at sensory processing stages. A mismatch between both would generate an error signal which travels downstream to update future predictions (Bastos et al., 2012; de Lange et al., 2018). In line with this assumption, that mispredicted stimuli evoke error signals, both brain imaging (Alink et al., 2010; Den Ouden et al., 2008) and electrophysiological studies (Todorovic & Lange, 2012; Wacongne et al., 2011) have revealed enhanced neural responses to unexpected compared to expected sensory events, which were interpreted as reflecting the error signal. Recently, different error signals have been proposed depending on how predictions are violated (Keller & Mrsic-Flogel, 2018): one to encode sensory input that exceeds the predicted input (positive error signal) and a second one to encode missing sensory input (negative error signal). While Keller and Mrsic-Flogel (2018) provided a detailed description of the neural circuitry of negative and positive error signals at the cellular level, no neurophysiological study in humans has yet tried to distinguish positive and negative error processing.

Assessing neural activity related to top-down predictions is even more experimentally challenging. One approach has been to remove any confounding stimulus-driven activity by investigating the neural signature to expected but omitted stimuli. For example, fMRI studies have confirmed that predictions of expected but omitted visual stimuli modulate the primary visual cortex in a retinotopic specific manner (Kok et al., 2014; Muckli et al., 2015). These results as well as analogous results in the auditory system (Todorovic et al., 2011) converge to the hypothesis that predictions are sent upstream and that they alter activity of early sensory cortex in a stimulus specific manner. However, the precise timing of how predictions unfold their influence is yet unknown. The time resolution of brain imaging techniques is not sufficient to dissociate visual cortex activity within subsecond resolution. Thus, even if early visual cortex is known to be subject of top-down modulation, it is yet unclear when such a modulation emerges and when spatially selective error signals are generated. Some authors have suggested that prediction related sensory cortex activity mimics the sensory-driven activity of the expected stimulus. Thus, it is assumed that top-down and bottom-up generated sensory cortex activity are indistinguishable (Bendixen et al., 2009). Testing this proposal requires an experimental protocol that allows tracking neural activity in early visual cortex with a millisecond resolution within the first few hundred milliseconds of stimulus processing.

The present ERP study made use of a visual ERP effect named as C1 effect. A polarity reversal of the ERPs for upper vs. lower visual field stimulation emerges as early as 50 –100 ms. The polarity reversal is considered to indicate activity in opposing banks of the calcarine sulcus and thus to reflect early retinotopic processing, likely stemming from primary visual cortex (Di Russo et al., 2002). In two separate runs, we first recorded ERPs to two sounds differing in pitch and two circular gratings, one presented in the top left (TL) and the other in the bottom right (BR) quadrant of the visual field. In the next run, crossmodal associations were created to investigate the effect of spatially specific visual predictions, e.g. the high pitched tone was followed with a high likelihood by the TL grating and the lower pitched tone by the BR grating (‘Standards’) or vis versa. In rare trials, the visual stimulus was presented at the unexpected location (‘Deviants’) or not at all (‘Omissions’).

We expected to find a C1 effect for both Standards and Deviants. If visual predictions mimic stimulus-driven activity with an indistinguishable timing, we would expect to observe a typical C1 effect within the time window 50 - 100 ms for Omissions too. Furthermore, if error signals are generated at the initial stage of visual processing we would expect a larger C1 effect for Deviants compared to Standards. Consequently, both negative and positive error signals were hypothesized to emerge as early, too. Pre-stimulus alpha lateralization has been shown to indicate top-down processes as sensory predictions and spatial attention (Alilović et al., 2019; Sauseng et al., 2005; Worden et al., 2000). To examine the time course of visual prediction built up we finally analyzed alpha oscillatory activity and ERPs following the sound but preceding the visual stimulation.

2. Methods and Materials

2.1 Subjects

Forty-five students of the University of Hamburg participated in the study. They all reported normal or corrected to normal vision, normal hearing and no history of psychiatric or neurological disorders. Data of two participants were excluded because of a too noisy electroencephalogram (EEG) signal (in more than three adjacent occipital electrodes, see below in section: EEG recording and preprocessing). Two other participants' datasets were disregarded because data were missing for one condition, and one participant's data were removed due to extensive blinking. The remaining forty participants had an average age of 23.8 years (range: 18 to 45 years, SD = 5.8, 27 females, 5 left-handed). The Local Ethics board of the Faculty of Psychology and Movement Science of the University of Hamburg (Germany) had approved the study (No. 2018_190). All participants gave informed consent and received course credit as compensation.

2.2 Stimuli and Apparatus

All stimuli were generated using the Psychophysics Toolbox for MATLAB (Brainard, 1997; Kleiner et al., 2007). The visual stimuli were presented with a 23.5’’ Eizo FG2421 LCD monitor (Ishikawa, Japan) with a refresh-rate of 120 Hz. They consisted of full contrast circular grating patterns subtending an angle of 2.5°. The grating patterns were black and white horizontally oriented stripes with a spatial frequency of 2 cycles/°. In addition, some grating patterns were presented with vertically oriented stripes, which served either alone or in combination with an auditory stimulus as behavioral targets. The grating stimuli were presented one at a time for 500 ms. They were positioned either in the top left (TL) or bottom right (BR) visual quadrant at an eccentricity of 4°. In the top quadrant, the grating stimuli were presented at an angle of 25° from the center (V1), and in the lower quadrant at an angle of 45° (V2; Figure 7A), to best target the opposing banks of the calcarine sulcus (Sourav et al., 2018). The auditory stimuli consisted of two, easily to differentiate sinusoidal tones (A1/A2: 1000 and 400 Hz, respectively) with a duration of 1.25 s (including 83 ms linear rise and fall envelopes) presented at 70 dB(A) (as measured at the ear level of participants) from two loudspeakers centrally positioned under the screen. In the auditory run, these continuous tones were additionally presented with a gap implemented 750 ms post onset, serving as behavioral targets (see below). During the whole experiment, participants were asked to indicate targets by pressing a Buddy Button (AbleNet, Inc., Minneapolis, United States of America) operated by their dominant hand.

To ensure precise timing of the stimuli with respect to the event-trigger signal stored with the EEG file, a photodiode connected to a custom-made Arduino microcontroller (Banzi & Shiloh, 2014) was installed. A fixed delay of 23.74 ms (SD = 1.88) between the trigger event mark and the visual presentation was observed which was removed during the pre-processing of the EEG data.

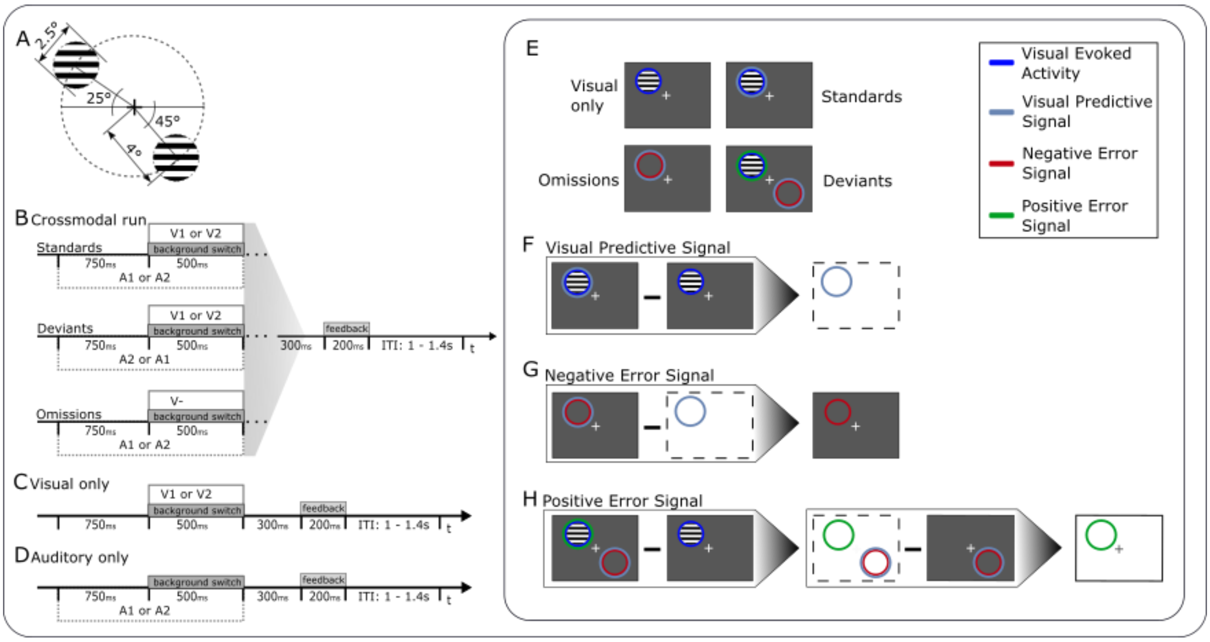

Figure 7. Study design and definition of the three ERP effects of interest exemplary depicted for top left (TL) grating location. (A) The visual stimuli comprised full contrast circular grating patterns, which were presented in either the TL or the bottom right quadrant arranged such that they best hit opposite banks of the calcarine sulcus. (B) Trial structure of the crossmodal run separately illustrated for each of the five possible conditions; from top to bottom: Standards, Deviants and Omissions. V- represents the omission of the grating stimulus. (C) Trial structure of the Visual only trials. (D) Trial structure of the Auditory only trials. (B,C,D) A1/A2 represent the two possible auditory stimuli and V1/V2 indicate the two possible locations of the visual grating stimuli. All trials ended with a random intertrial interval (ITI). (E) Visual only trials were hypothesized to contain only visually evoked activity (blue). In contrast, Standards were considered additionally to contain the Visual predictive signal (gray). Omissions were assumed to comprise the Visual predictive signal and the Negative error signal (red). Deviants were hypothesized to elicit the Visual predictive signal and the Negative error signal related to the expected stimulus location and in addition visually evoked activity and the Positive error signal related to the visual stimulus at the unexpected location (green). Definition of the three effects of interest, exemplary for the TL location: (F) Visual predictive signal TL. (G) Negative error signal TL. (H) Positive error signal TL.

2.3 Design

2.3.1 Crossmodal run

The trial structure was the same for all conditions (Figure 7B): trials started with the simultaneous presentation of a white central fixation cross (size 0.25°) on a black background and the onset of the auditory stimulus. The fixation cross remained visible until the end of a trial. After 750 ms the background was inverted from black to gray (called ‘background switch’ in the following) and simultaneously a grating stimulus was presented at one of the two possible locations. The grating and auditory stimulus were extinguished after 500 ms and the background changed back to black.

There were two frequent combination of tone and grating location (termed “Standards”; A1V1/A2V2); which tone and grating location were paired was counterbalanced across subjects. Standards were presented in 70% of the trials. In 4% of the trials, the tones and grating locations were recombined (called “Deviants”: A1V2/A2V1). In both conditions, gratings were presented with vertically oriented stripes. In 18% of the trials, the grating stimulus was omitted (called “Omissions” in the following: A1V-/A2V-; see Table 1 for a summary of all conditions). Since the background switch still occurred, the timing of the omission was obvious to the subjects. In fact, the background switch was introduced to reduce temporal uncertainty in omission trials.

In order to guarantee that the frequent crossmodal combinations were task relevant, we presented additional 8% of the trials with vertically oriented gratings. The tone-grating location combination of half of these trials corresponded to Standards (called “Targets” in the following) and the other half corresponded to Deviants (called “Distractors” in the following). The task of the participants was to respond to trials that presented vertically oriented gratings but only if the tone-grating location combination corresponded to Standards. Participants had to respond within 800 ms after the background switch. After a correct response, the fixation cross remained white for another 200 ms; after an incorrect response the fixation cross turned red instead. After a random interstimulus interval (ITI), ranging between 1 and 1.4 s (uniform distribution), the next trial started.

Table 1

Probabilities for each condition in the crossmodal run

Stimuli	Proportion		Condition (number of trials)
A1V1 A2V2	0.35 0.35	0.70	Standards (1120)
A1V2 A2V1	0.02 0.02	0.04	Deviants (64)
A1V- A2V-	0.09 0.09	0.18	Omissions (288)
A1V1vertical A2V2vertical	0.02 0.02	0.04	Targets (64)
A1V2vertical A2V1vertical	0.02 0.02	0.04	Distractors (64)

2.3.2 Unimodal runs

Prior to the crossmodal run, the visual grating stimuli (V1/V2) and the auditory stimuli (A1/A2) were presented in two separate unimodal baseline runs. The trial structure of the unimodal runs (Figure 7C and 7D) were the same as for crossmodal runs (Figure 7B), except that either only the auditory or only the grating stimuli were presented.

In the visual run, trials started with the presentation of the fixation cross on a black background for 750 ms. Simultaneously with the background switch the grating stimuli was presented at one of the two possible locations (V1/V2) for 500 ms. Upon stimulus extinction, the background changed back to black. In twenty out of 220 trials (9.1%), vertically oriented gratings were presented: Participants were asked to respond to vertical grating stimuli, irrespectively of stimulus location. In the remaining trials, horizontally oriented gratings were presented (called “Visual only” in the following). As in crossmodal runs, participants had to respond within 800 ms following the background switch. Feedback was provided as in the crossmodal runs. The trial ended with a random ITI, ranging between 1 and 1.4 s (uniform distribution).

In the auditory run, the trials started with the presentation of the fixation cross on a black background and the onset of one of the two auditory stimuli (A1/A2). After 750 ms, the background switched from black to gray. The auditory stimulus terminated after an additional 500 ms and the background changed back to black. In twenty of the 220 trials (9.1%), the auditory stimuli contained a gap; these sounds served as targets and required a response. In the remaining trials, the auditory stimuli were presented without the gap (called “Auditory only” in the following). Participants had to respond within 800 ms following the onset of the gap. Feedback was provided as in the crossmodal run. After a random ITI, ranging between 1 and 1.4 s (uniform distribution), the next trial started. Auditory only trials were physically identical to Omissions (A1V-/A2V-; see Figure 7A and 7C).

2.4 Procedure

Participants were comfortably seated in a dimly lit room at a 60 cm distance from the screen. The experimental session always began with the unimodal baseline runs. The order of unimodal runs was counterbalanced across participants. Each unimodal run comprised 220 trials. Trials were randomly presented in two blocks of 110 trials each.

After the completion of both unimodal runs, the crossmodal run followed with 16 blocks each consisting of 100 trials. Crossmodal trials were randomized in sets of four subsequent blocks guaranteeing that relative trial probabilities were equally distributed across the whole crossmodal run. Before the crossmodal run started, participants were informed about the likelihood of the frequent combinations of tone and grating location.

2.5 EEG recording and Preprocessing

The electroencephalogram (EEG) was recorded from 74 Ag/AgCl electrodes positioned according to the 10-10 system (Acharya et al., 2016) and mounted in an elastic cap (EASYCAP GmbH, Herrsching, Germany), with location AFz serving as ground and the left earlobe as reference. The EEG signal was recorded at a sampling rate of 1000 Hz with a BrainAmp DC amplifier (Brain Products GmbH, Gilching, Germany); with a hardware bandpass filter with a passband of 0.0167 to 250 Hz. The electrode impedances were kept below 15kΩ.

Offline EEG data were preprocessed using custom scripts and the EEGLAB toolbox version 14.1.1b (Delorme & Makeig, 2004) for MATLAB version R2015a (MathWorks Inc., Natick, MA, USA). First, we epoched the data from -1.75 to 1 s centered at the onset of the background switch and baselined each trial by subtracting the average activity of the -1,75 to 0 ms baseline epoch from each time point. Subsequently, data were low-pass filtered with a finite impulse response filter and an upper cutoff frequency of 110 Hz (6dB cut off at 123.75 Hz, 27.5 Hz transition bandwidth) using the pop_eegfiltnew function in EEGLAB. Electrodes with artefacts (e.g., muscle activity, movement of the electrode, electrode saturation) in more than 15% of the trials were removed (0.18 channels per subject, range: 0 to 2 channels, *SD* = 0.5) and later substituted by spherical linear interpolation of the three closest neighboring channels.

Next, to remove typical biological (blink, eye movement, muscle, heart) and other (line noise) artefacts we used the Independent Component Analysis (ICA, as implemented by EEGLAB *runica* function; Lee et al., 1999). Components representing artifacts were identified by employing the ICLabel classifier (Pion-Tonachini et al., 2019). This classifier calculates for each Independent Component the probability that it captures brain activity or rather activity related to artifacts. A component was considered as representing an artefact if the probability exceeded 0.8 for one of the artifact categories muscle, eye, heart and line noise. Additionally, based on the scalp topography and power spectrum of eye-movement related Independent

Components (Plöchl et al., 2012) we subsequently added or adapted the labels for components that were not classified as eye components (additional 0.43 components per subject, range: 0 to 3, SD = 0.8). All independent components identified as artifacts were removed (on average 13.55 components per subject, range: 4 to 33, *SD* = 6.60).

To ensure that participants had perceived the critical time point of visual stimulation, we removed trials in which the participants had blinked during or near the onset of the background switch. This was achieved by removing trials in which the activity of the independent component related to blinks exceeded a threshold of +/- 25 standard deviations in a time window of +/-150 ms around the onset of the background switch.

Next, the EEG data were average-referenced and the onset of the event-mark for the background switch was corrected (see Stimuli and Apparatus). Subsequently, we interpolated the previously rejected electrodes. Thereafter we applied a low-pass filter with an upper cut-off at 40 Hz (6 dB cut off at 59.64 Hz, 39.29 Hz transition bandwidth). Epochs were baseline corrected to the average activity between -100 and 0 ms. This baseline was used for statistical analyses. Finally, trials which still contained values exceeding +/- 100 µV were removed. Only Standards, Deviants and Omissions of the crossmodal run (see Table 1) and non-target trials of the two unimodal runs (Auditory only and Visual only) were analyzed. Thus, only trials without manual responses and thus motor-related activity were considered. In total, 94.7% of trials of the Auditory only condition, (range = 57% to 100%, *SD* = 8.51), 95.2% of trials of the Visual Only condition (range = 55% to 100%, *SD* = 8.13), 95.1% of trials of the Standard condition (range = 67.14 to 99.82%, *SD* = 8.13), 95.6% of trials in the Deviant condition (range = 68.75 to 100%, *SD* = 6.92) and 94.7% of trials in the Omission condition (range = 67.36 to 100%, *SD* = 6.77) remained for the statistical analysis.

2.6 Behavioral analysis

The hit rate for targets was defined separately for the crossmodal, visual and auditory runs as the percentage of correct responses to targets divided by the absolute number of target trials. Correspondingly, the false alarm rate was calculated by dividing the number of responses in non-target trials by the total number of non-target trials (absolute number of trials minus number of target trials).

2.7 ERP Analysis

ERP data were analyzed using the Fieldtrip toolbox (Oostenveld et al., 2011) and customized MATLAB scripts.

2.7.1 C1 effect

To investigate neural activity at the first cortical stages of visual processing we calculated the C1 effect by subtracting the ERPs elicited by BR visual stimulation from the ERPs elicited by TL visual stimulation, separately for Standards and Deviants. Separately for Omissions (crossmodal run) and Auditory only trials (unimodal run), we subtracted the ERPs to tones associated with the BR from the ERPs to tones associated with the TL location.

The C1 effect was parameterized by calculating the average voltage of the 50-100 ms post background switch epoch across 20 posterior electrodes (CPz/1/3/5, Pz/1/3/5/7/9, POz/3/7/9, Oz/1/9, Iz, TP7/9, see Figure 8B). The time epoch and the posterior electrode selection were adapted from (Sourav et al., 2018; see also: Di Russo et al., 2002). We analyzed the C1 at left hemisphere electrodes that is, at electrodes ipsilateral to the upper and contralateral to the bottom visual stimulation. This decision was based on previous results indicating that the C1 wave is largest for upper visual field stimulation at ipsilateral posterior electrodes and lager for lower visual field stimulation at contralateral ipsilateral electrodes (Baumgartner et al., 2018; Di Russo et al., 2002; Kelly et al., 2008). Consequently, the largest C1 effect (ERP difference between upper and lower visual field stimulation) for the stimulus locations employed in the present experiment is expected for the left hemisphere recordings. The existence of a C1 effect in Standards, Deviants and Omissions was evaluated with one-tailed t-tests against zero after applying a Bonferroni Correction for multiple testing. To compare the size of the C1 effect across conditions, a one-way repeated measures ANOVA with the repeated measures factor condition (four levels: Standards, Deviants, Omissions and Auditory only) was run. If the main effect was significant, we conducted post-hoc two-tailed t-tests with Bonferroni correction to compare the C1 effect between conditions.

2.7.2 Cluster-based permutation analyses

Separate cluster-based permutation tests (Maris & Oostenveld, 2007) as implemented in the Fieldtrip toolbox were employed to evaluate Mismatch and Omission effects after the first cortical stages of visual processing (see below). To investigate ERP correlates of *Visual prediction*, and of both the *Negative* and *Positive error signal* (see below), we employed cluster-based permutation tests too. All cluster-based permutation tests were run over the 500 ms post background switch time epoch including all scalp electrodes. We defined positive and negative clusters according to the polarity of the difference waves. We defined effects as follows.

2.7.2.1 Omission effect

We compared ERPs to the omission of expected visual stimuli separately for TL and BR trials. By comparing these two conditions, we were able to investigate the time course and spatial specificity of visual omission responses. The Omission effect was defined as follows:

Omission effect = ERP(Omission TL) – ERP(Omission BR) (1)

To confirm that the Omission effect was exclusively driven by visual expectations, the same difference was defined for the Auditory only trials and both signals were subsequently compare with an additional cluster-based permutation test.

2.7.2.2 Mismatch effect

ERPs to visual gratings which mismatched (Deviants) vs. matched (Standards) the visual expectation were compared separately for TL and BR grating stimuli. Mismatch effects were defined as follows:

$$\mathit{Mismatch\ effect\ TL} = \mathit{ERP(Deviant\ TL)} - \mathit{ERP(Standard\ TL)}\ (2.1)$$

$$\mathit{Mismatch\ effect\ BR} = \mathit{ERP(Deviant\ BR)} - \mathit{ERP(Standard\ BR)}\ (2.2)$$

The resulting Mismatch effects indicate a stimulus driven violation of the crossmodal expectation and the difference of both conditions indicates any spatially specific aspect of this the mismatch response. The spatially specific Mismatch effect was defined as follows:

$$\mathit{Spatially\ specific\ mismatch\ effect} = \mathit{Mismatch\ effect\ TL} - \mathit{Mismatch\ effect\ BR} = (\mathit{ERP(Deviant\ TL)} - \mathit{ERP(Standard\ TL)}) - (\mathit{ERP(Deviant\ BR)} - \mathit{ERP(Standard\ BR)})\ (2.3)$$

This comparison allowed us to examine electrophysiological activity that was temporally and spatially specific with respect to the original visual prediction.

2.7.2.3 Visual predictive signal

ERPs to Standards were assumed to comprise the visually evoked activity and neural activity related to visual predictions. Whereas ERPs to the Visual only trials were assumed to only comprise the visually evoked activity. We defined the *Visual predictive signal* separately for the TL and BR location by subtracting ERPs to the Visual only trials from the ERPs to Standards (Figure 7F):

$$\mathit{Visual\ predictive\ signal\ TL} = \mathit{ERP(Standards\ TL)} - \mathit{ERP(Visual\ only\ TL)}\ (3.1)$$

$$\mathit{Visual\ predictive\ signal\ BR} = \mathit{ERP(Standard\ BR)} - \mathit{ERP(Visual\ only\ BR)}\ (3.2)$$

These effects indicate spatially specific processing differences due to valid visual predictions. The *Visual predictive signal* was thus defined as follows:

Spatially specific Visual predictive signal =

Visual predictive signal TL – Visual predictive signal BR =

(ERP(Standards TL) - ERP(Visual only TL)) – (ERP(Standards BR) -

ERP(Visual only BR)) (3.3)

2.7.2.4 Negative error signal

ERPs to Omissions were assumed to comprise the *Visual predictive signal* and the *Negative error signal*. The Negative error signal was defined separately for the TL and BR location by subtracting the *Visual predictive signal* (Eq. 3.1 and 3.2) from the ERP to Omissions (Figure 7G):

Negative error signal TL =

ERP(Omissions TL) – (ERP(Standards TL) – ERP(Visual only TL)) (4.1)

Negative error signal BR =

ERP(Omissions BR) – (ERP(Standards BR) – ERP(Visual only BR)) (4.2)

Since two ERPs are subtracted from one ERP in equation 4.1, the resulting difference cannot be unambiguously interpreted. As demonstrated by Gondan et al. (2004), there might be additional shared “common activity” in the ERPs, which would be subtracted twice and would possibly result in an artificially introduced negative difference. However, the spatial selective *Negative error signal* can be unambiguously interpreted since any possible common activity is subtracted out. The spatially specific *Negative error signal* was defined as:

Spatially specific Negative error signal =

Negative error signal TL – Negative error signal BR =

(ERP(Omissions TL) – (ERP(Standards TL) – ERP(Visual only TL)) -

(ERP(Omissions BR) – (ERP(Standards BR) – ERP(Visual only BR)) (4.3)

2.7.2.5 Positive error signal

ERPs to Deviants were assumed to comprise not only visually evoked activity, the *Visual predictive signal* and the *Negative error signal*, but also additionally the *Positive error signal* (Figure 7H). For example, if an ERP to a Deviant in the TL visual location is elicited, this ERP comprises the visual prediction effect for the expected visual stimulus in the BR visual field, but additionally the visually evoked activity to the unexpected grating in the TL visual field. The latter is presumed to result in a *Positive error signal*. Assuming an additive model, we thus eliminated first activity related to visually evoked processing by subtracting the ERPs to Visual only trials from the ERPs to Deviants. Next, we subtracted from the resulting difference the Omission ERPs to eliminate both the *Visual predictive signal* and the *Negative error signal*. We defined the *Positive error signal* separately for TL and BR visual locations as follows:

Positive error signal TL =

ERP(Deviants TL) – ERP(Visual only TL) – ERP(Omissions BR) (5.1)

Positive error signal BR =

ERP(Deviants BR) – ERP(Visual only BR) – ERP(Omissions TL) (5.2)

The *Positive error signal* TL and the *Positive error signal* BR where then compared to investigate whether the defined *Positive error signals* were spatially specific:

Spatially specific Positive error signal =

Positive error signal TL –Positive error signal BR =

(ERP(Deviants TL) – ERP(Visual only TL) – ERP(Omissions BR)) -

(ERP(Deviants BR) – ERP(Visual only BR) – ERP(Omissions TL)) (5.3)

2.7.2.6 Pre-background switch epoch

To investigate the neural correlates of top-down spatial predictions we analyzed the period prior to the presentation of the grating stimulus that is the pre-background switch epoch.

We compared ERPs to crossmodal trials in which the pitch of the tone predicted the location of the consecutive grating stimulus in the TL (A1) vs. in the BR (A2) location. Accordingly, we averaged ERPs to Standards and Omissions at the TL location as well as to Deviants at the BR locations (trials that presented A1) and ERPs to Standards and Omissions at the BR location as well as Deviants at the TL location (trials that presented A2). The resulting ERPs were baselined to -0.85 to -0.75 s time epoch prior to the onset of the background switch, this corresponds to a 100 ms time epoch prior to the onset of the auditory tone. As a next step, we employed a cluster-based permutation test with all electrodes starting at -0.75 s prior to the background switch and ending at the onset of the background switch. To test whether potential differences were due to spatially specific visual predictions or represented only a temporal expectation of visual stimulation (e.g. the background switch with any of the two possible grating locations), we applied the same analysis to the Auditory only trials (comparing A1 and A2), which were physically identical to the crossmodal trials until the background switch.

2.8 Time-frequency analysis

A time-frequency analysis was performed with a sliding window single-taper analysis (Hanning taper, 300 ms window length, frequency resolution 3.33 Hz, 10 ms step size). The resulting spectra were baseline corrected to decibels (dB) with respect to the period from – 1.35 to – 0.9 s before grating stimulus onset (that is, at least 150 ms before the start of the auditory stimulus). To investigate effects of spatial predictions on alpha modulation, we compared trials in which the tone predicted the TL (A1) and BR (A2) locations of the consecutive grating stimulus for the crossmodal run. A cluster-based permutation test was run over a time window from -750 to 0 s according to the onset of the background switch on the average power in the alpha-band (8 to 12 Hz). The same procedure was applied to the Auditory only and Visual only trials from the unimodal runs. For the comparison in the Auditory only run, we compared trials that presented A1 with trials that presented A2. For the comparison in the Visual only run, we compared trials that presented V1 with trials that presented V2.

3. Results

3.1 Behavior

In both unimodal runs, we asked participants to detect rare targets (auditory run: tone containing a short gap in 20 out of 220 trials, visual run: vertically oriented gratings independent of their location in 20 out of 220 trials). In the crossmodal run, we asked participants to respond to Targets. Targets corresponded to the frequent combination of tone and visual stimulus location but used vertically oriented gratings (A1V1v/A2V2v, see also Table 1). A high hit rate (auditory run: M = 98.38%, SD = 3.28; visual run: M = 96.88%, SD = 3.87; crossmodal run: M = 84.34%, SD = 12.11) and a low false alarm rate (auditory run: M = 1.20%, SD = 4.60; visual run: M = 0.30%, SD = 0.48; crossmodal run: 1.00%, SD = 0.98) in each run indicated that participants were engaged and able to perform the tasks successfully.

3.2 C1 effects

To investigate whether visual predictions modulate neural activity at the first stages of visual processing we analyzed the C1 effect separately for Standards, Deviants, Omissions and Auditory only trials. First, we tested whether a significant C1 effect was obtained for each of these four conditions. A significant C1 effect was found for Standards (M = -0.67 µV, SD = 0.75; $t(39) = -5.64$, $p < .001$) and for Deviants (M = -0.47 µV, SD = 1.07; $t(39) = -2.80$, $p = .004$; Figure 8A). In contrast, no C1 effect was observed for Omissions (M = -0.01 µV, SD = 0.40; $t(39) = -0.01$, $p = .46$) nor for Auditory only trials (M = -0.02 µV, SD = 0.46; $t(39) = 0.05$, $p = .52$; Figure 8A). A repeated measures ANOVA with the within-subjects factor condition (Standards, Deviants, Omissions, Auditory only) was significant ($F(3,36) = 8.53$,

$p < .001$; Figure 8B and 8C). Subsequent t-tests confirmed significantly larger C1 effects for Standards and Deviants compared to Omissions ($t(39) = -5.64, p < .001$; $t(39) = -2.82, p = .007$) and Auditory only trials ($t(39) = -4.54, p < .001$; $t(39) = -2.66, p = .011$). By contrast, the C1 effect was indistinguishable for Omissions and Auditory only trials ($t(39) = 0.13, p = .90$) and for Standards and Deviants ($t(39) = -1.53, p = .13$).

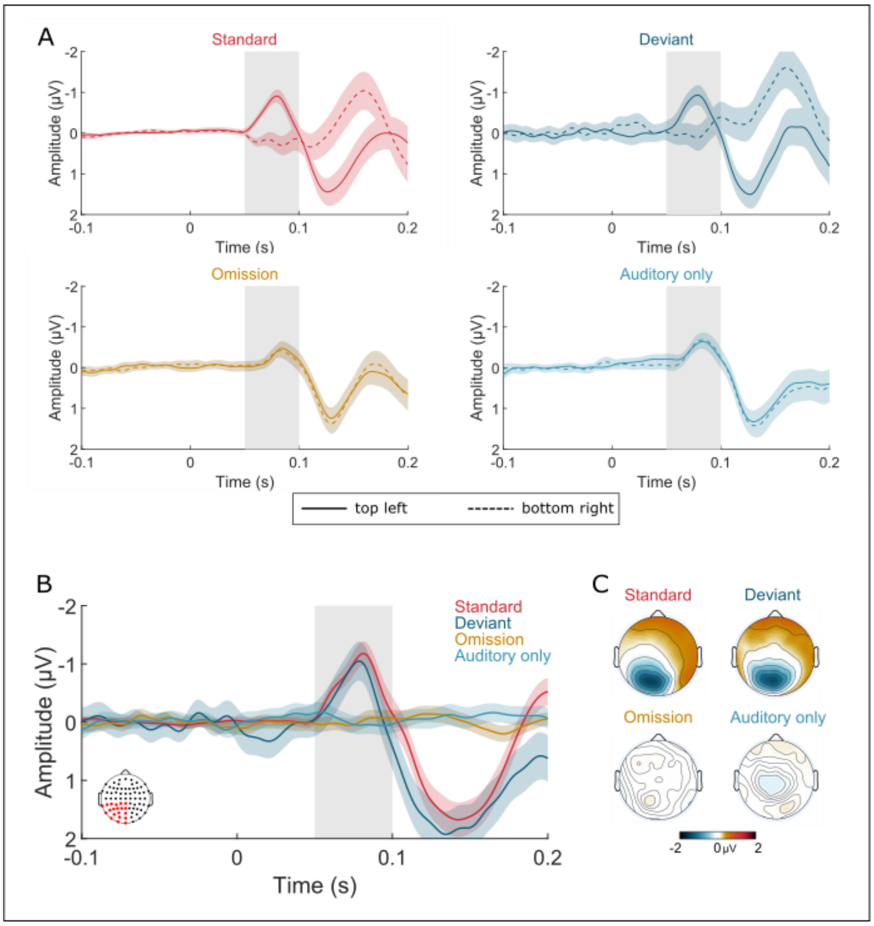

Figure 8. Grand average C1 effects. (A) First row: ERPs elicited by top left (TL) (solid line) and bottom right (BR) (dashed line) grating stimuli by Standards (left) and Deviants (right). Second row: ERPs elicited by Omissions (left) and Auditory only trials (right) to tones which were associated with TL (solid line) and BR (dashed line) location, respectively. The C1 latency is shaded in gray. Error bands represent the standard error of the mean. Time zero is the onset of the background switch. The shown traces are averages across 20 posterior electrodes depicted in the insert in (B). (B) Grand averages of the C1 effect (difference ERP derived by subtracting ERPs for BR from ERPs for TL locations). (C) ERP topographies displaying the C1 effect for each condition in the C1 latency (50-100 ms).

3.3 Omission effect

In order to investigate the time course and spatial specificity of visual omission responses, we compared the ERPs to Omissions associated with the top left (TL) vs. Omissions associated with the bottom right (BR) location. The Omission effect started around 230 ms with a negative difference potential over the left and a positive difference potential over the right hemisphere (positive cluster: from 235 to 500 ms, $p < .001$; negative cluster: from 245 to 500 ms, $p = .002$; Figure 9, Table 2). In contrast, the equivalent comparison of ERPs to Auditory only trials did not reveal any significant effect ($p = .15$ for the first positive, and $p = .16$ for the first negative cluster). Correspondingly, the Omission effect was significantly larger for the crossmodal than for the Auditory only run (positive cluster: from 223 to 500 ms; $p = .01$; negative cluster: from 238 to 500 ms, $p = .01$; Figure 10).

Table 2
Latency, topography and end of the investigated ERP effects

	Latency (ms)	Topography (lateralization)	End (ms)
Omission effect (Figure 9)	230	Contralateral positivity	500
Mismatch effect TL (Figure 11)	140	Contralateral negativity	500
Mismatch effect BR (Figure A.1)	140	Contralateral negativity	500
Spatially specific Mismatch effect (TL-BR; Figure 12)	170	Contralateral negativity	380
Visual predictive signal (Figure 13)	70	Contralateral positivity	500
Negative error signal (Figure 14)	140	Contralateral negativity	410
Positive error signal (Figure 15)	320	Contralateral positivity	500
Pre-background switch epoch (Figure 16)	-525	Contralateral negativity	0

Note. This table lists all observed effects, their latencies, topographies and ends. 500 ms was the end of the analyzed time epoch window.

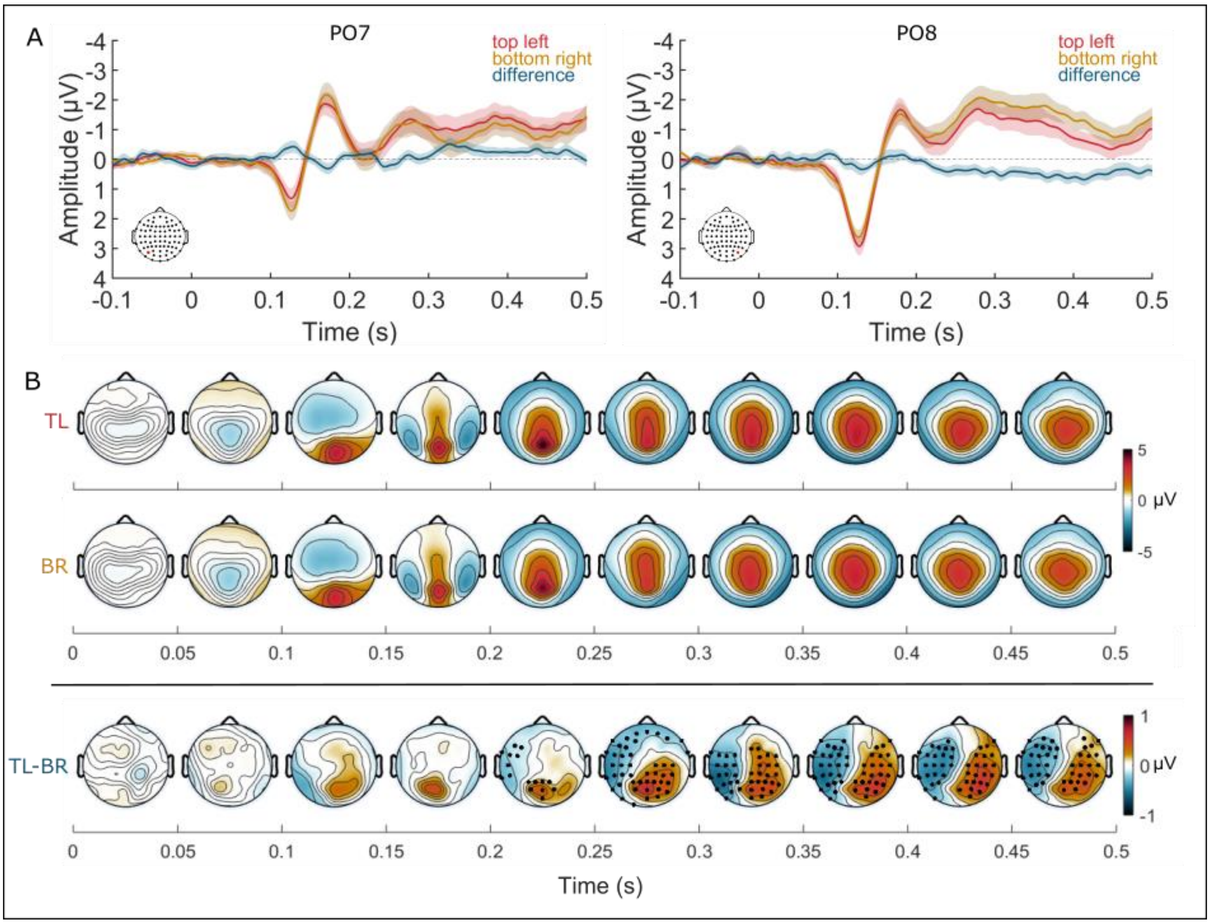

Figure 9. Grand averages of the ERPs to Omissions associated with the top left (TL) and bottom right (BR) locations. (A) Omission ERPs for TL (red) and BR (yellow) locations and the TL-BR difference (blue) at electrodes PO7 (left) and PO8 (right) (see red marked electrodes in the schematic drawing of the electrode montage). Error bands represent the standard error of the mean. Time zero is the moment of the background switch. (B) ERP topographies to Omissions associated with the TL (first row) and BR (second row) location as well as the difference ERP of both conditions (TL-BR; last row) for the post background switch time epoch 0 to 500 ms in 50 ms steps. Stars in the ERP topographies in the last row indicate electrodes that survived tests for multiple comparisons ($p < .05$).

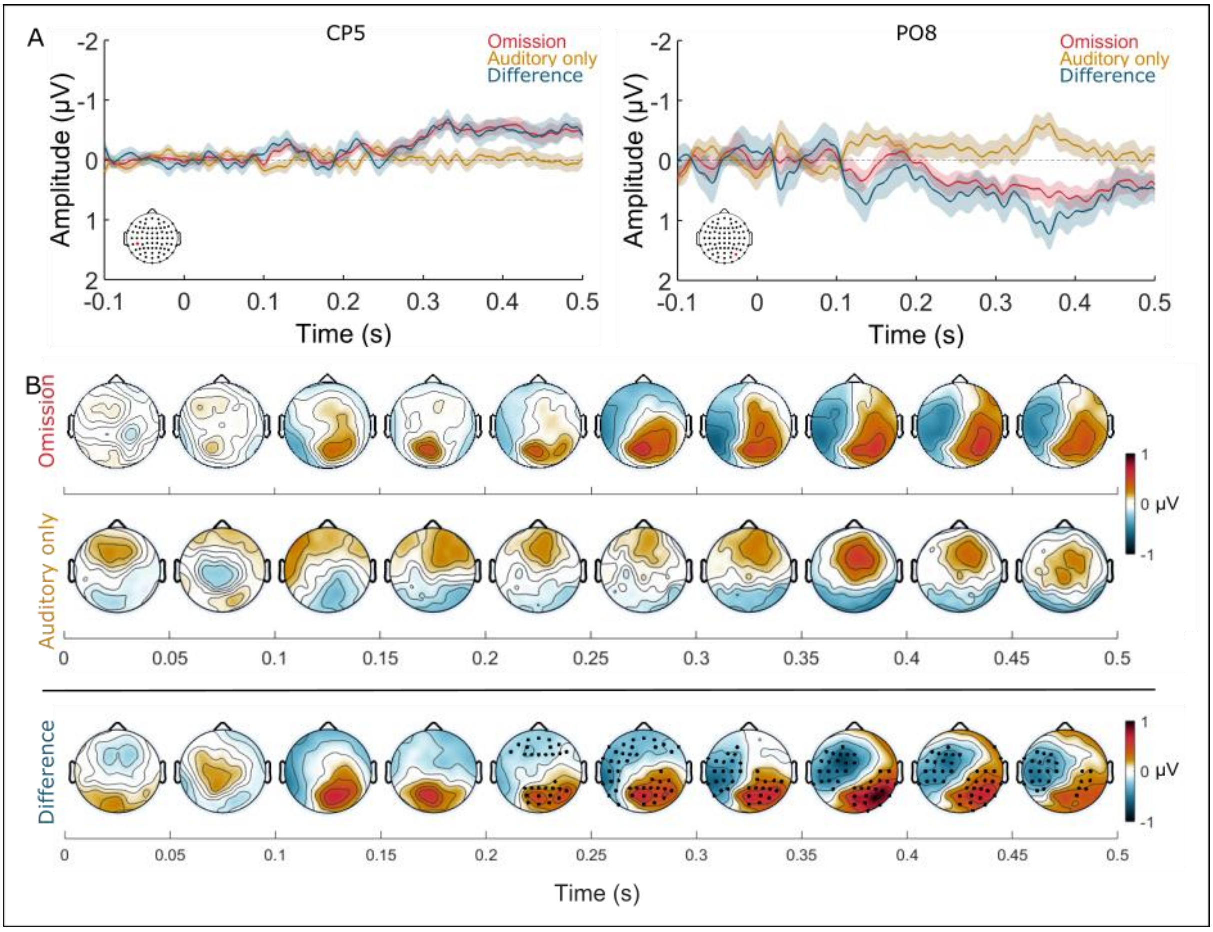

Figure 10. Grand averages of the ERPs to Omissions and Auditory only. (A) Difference ERPs to top left (TL) Omissions minus bottom right (BR) Omissions (red) and difference ERPs to TL Auditory only minus BR Auditory only (yellow) and the difference ERP (blue) derived by subtracting the difference ERPs to Auditory only from the difference ERPs for Omissions. ERPs are at electrodes CP5 (left) and PO8 (right) (see red marked electrodes in the schematic drawing of the electrode montage). Error bands represent the standard error of the mean. Time zero is the moment of the background switch. (B) ERP topographies display the difference ERPs for Omissions (TL-BR; first row) and for Auditory only (TL-BR; second row) and as well as the difference ERP of both conditions ((TL-BR)Omissions-(TL-BR)Auditory only; last row) for the post background switch time epoch 0 to 500 ms in 50 ms steps. Stars on the ERP topographies in the last row indicate electrodes that survived tests for multiple comparisons (p < .05).

3.4 Mismatch effects

To investigate Mismatch effects we compared ERPs to Deviants and Standards separately for TL and BR grating. ERPs to Deviants and Standards to gratings presented at the TL differed over the fronto-central and posterior scalp starting at about 140 ms after the onset of the background switch (positive cluster: from 142 to 500 ms, $p < .001$; first negative cluster: from 176 to 379 ms, $p < .001$; second negative cluster: from 385 to 500 ms, $p = .005$; Figure 11, Table 2). Corresponding results were obtained for the analogous analysis for ERPs elicited by visual stimulation at the BR location (positive cluster: from 142 to 454 ms, $p < .001$; first negative cluster: from 143 to 351 ms, $p = .002$; second negative cluster: from 339 to 500 ms, $p = .018$; Figure A.1). Grating stimuli that mismatched the predicted input, elicited larger ERPs than gratings that matched the predicted input. To investigate the spatially specific aspects of the Mismatch effects we compared the difference ERPs to Mismatch TL and Mismatch BR. A significant spatially specific Mismatch response started after around 170 ms after stimulus onset (positive cluster: from 177 to 384 ms, $p = .006$, negative cluster: from 178 to 286 ms, $p = .021$) with a positive polarity over the left hemisphere and a negative polarity over the right hemisphere (Figure 12).

3.5 Visual predictive signal

To isolate the *Visual predictive signal* we subtracted ERPs to the Visual only trials from the corresponding ERPs to Standard trials (see Eq. 3.1 and Eq. 3.2; Figure 7F). *Visual predictive signals* for the TL and BR locations significantly differed at two clusters starting with a latency of approximately 70 ms (positive cluster: from 71 to 500 ms, $p < .001$; negative cluster: from 76 to 500 ms, $p < .001$). The *Visual predictive signal* was characterized by a lateralized response with a negative difference potential over the left hemisphere and a positive difference potential over the right hemisphere (Figure 13; Table 2).

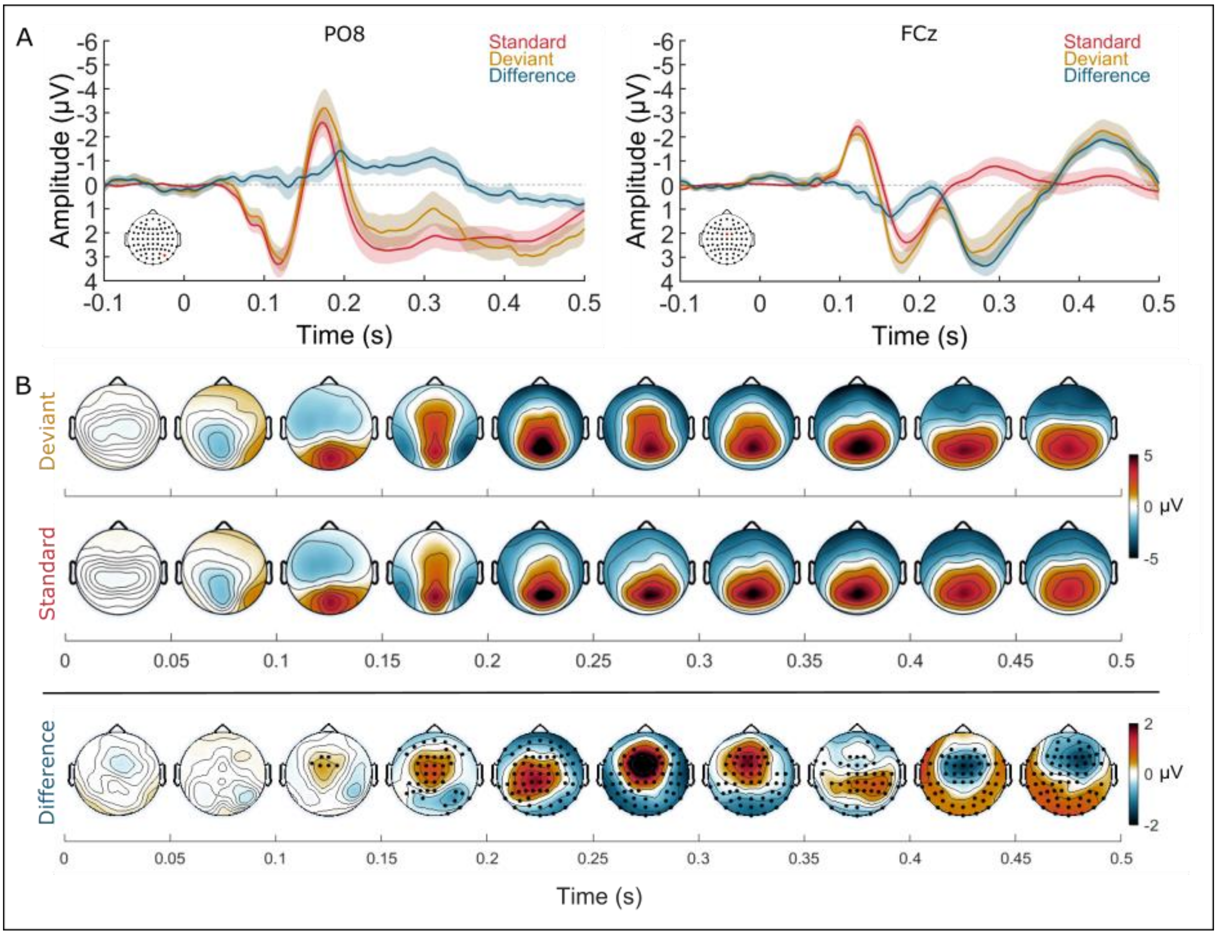

Figure 11. Grand averages of the ERPs to top left (TL) Standards and Deviants. (A) ERPs to TL Standards (red) and Deviants (yellow) and the difference ERP (blue) derived by subtracting ERPs to TL Deviants from ERPs to TL Standards at electrodes PO8 (left) and FCz (right) (see red marked electrodes in the schematic drawing of the electrode montage). Error bands represent the standard error of the mean. Time zero is the moment of the background switch. (B) ERP topographies display the ERPs to TL Deviants (first row) and Standards (second row) and the difference of ERPs to TL Standards minus ERPs to TL Deviants (last row) for the post background switch time epoch 0 to 500 ms in 50 ms steps. Stars in the ERP topographies in the last row indicate electrodes that survived tests for multiple comparisons ($p < .05$).

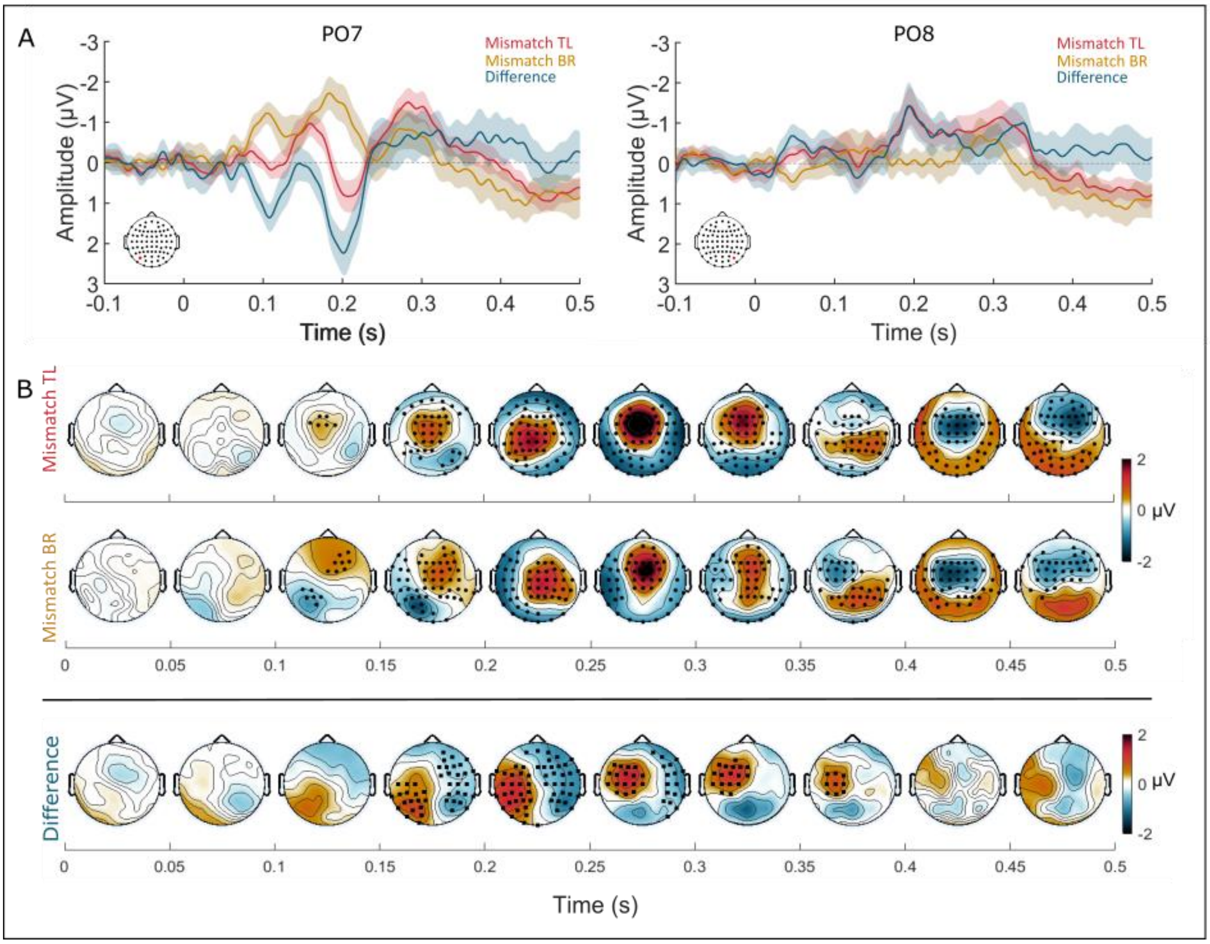

Figure 12. Grand averages of the ERPs for the Mismatch effect TL and BR. (A) ERPs to Mismatch effect TL (red) and BR (yellow) and the difference ERP (blue) derived by subtracting ERPs to Mismatch TL from ERPs to Mismatch BR at electrodes PO7 (left) and PO8 (right) (see red marked electrodes in the schematic drawing of the electrode montage). Error bands represent the standard error of the mean. Time zero is the moment of the background switch. (B) ERP topographies display the ERPs to Mismatch TL (first row) and Mismatch BR (second row) and the difference of ERPs to Mismatch TL minus ERPs to Mismatch BR (last row) for the post background switch time epoch 0 to 500 ms in 50 ms steps. Stars in the ERP topographies indicate electrodes that survived tests for multiple comparisons ($p < .05$).

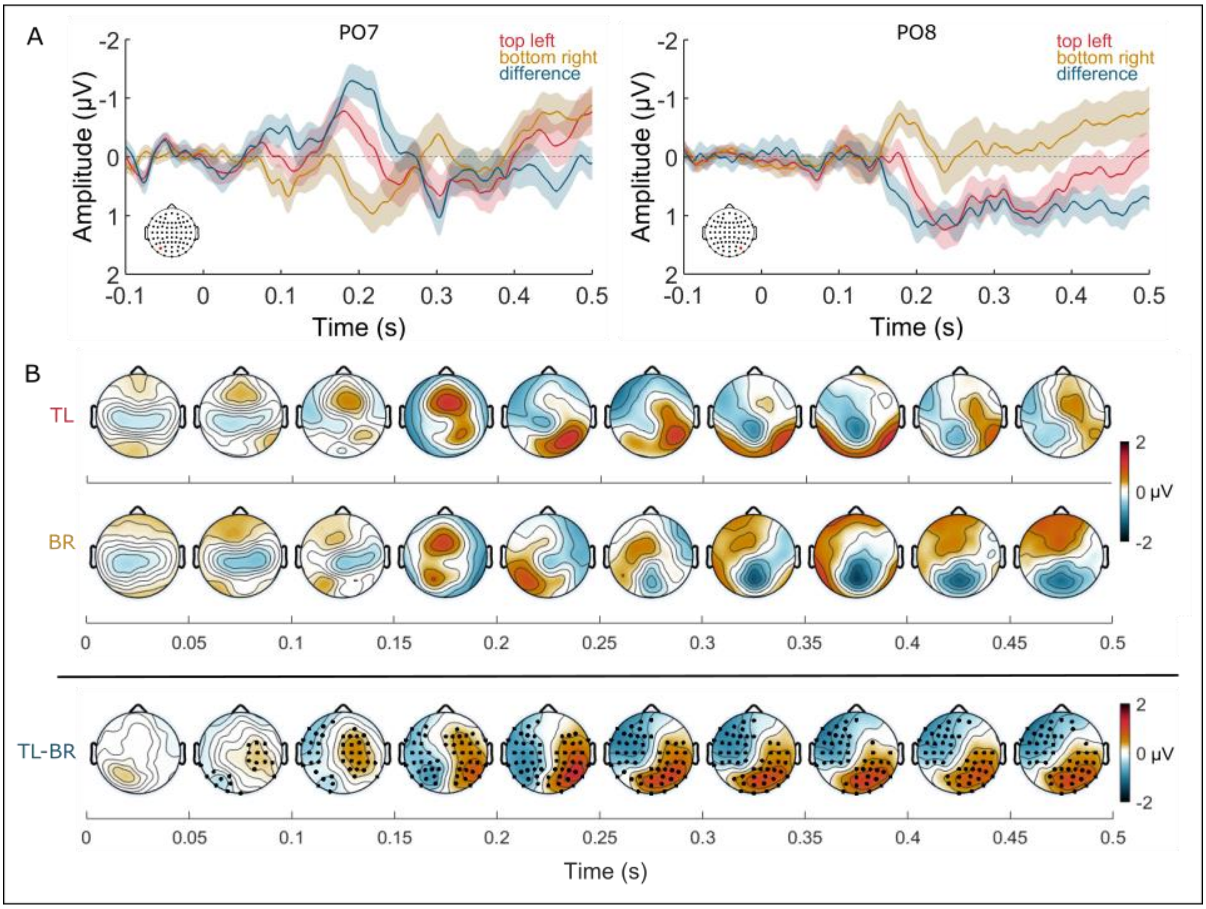

Figure 13. Grand averages of the ERPs for Visual predictive signals associated with the top left (TL) and bottom right (BR) locations. (A) Visual predictive signal ERPs for TL (red) and BR (yellow) locations and the TL-BR difference (blue) at electrodes PO7 (left) and PO8 (right) (see red marked electrodes in the schematic drawing of the electrode montage). Error bands represent the standard error of the mean. Time zero is the moment of the background switch. (B) ERP topographies to Omissions associated with the TL (first row) and BR (second row) location as well as the difference ERP of both conditions (TL-BR; last row) for the post background switch time epoch 0 to 500 ms in 50 ms steps. Dots on the ERP topographies in the last row indicate electrodes that survived tests for multiple comparisons ($p < .05$).

3.6 Negative error signal

To isolate the *Negative error signal* we subtracted the *Visual predictive signal* from the corresponding Omission ERPs (see Eq. 4.1 and Eq. 4.2; Figure 7G). To examine the spatial and temporal properties of the *Negative error signal*, we compared the *Negative error signal* for the TL and the BR location (see Eq. 4.3). The *Negative error signal* started with a latency of approximately 140 ms and was characterized by a lateralized response with a positive difference potential over the left hemisphere and a negative difference potential over the right hemisphere (positive cluster: from 142 to 408 ms, p <.001; negative cluster: from 155 to 390 ms, p = 0.004; Figure 14; Table 2).

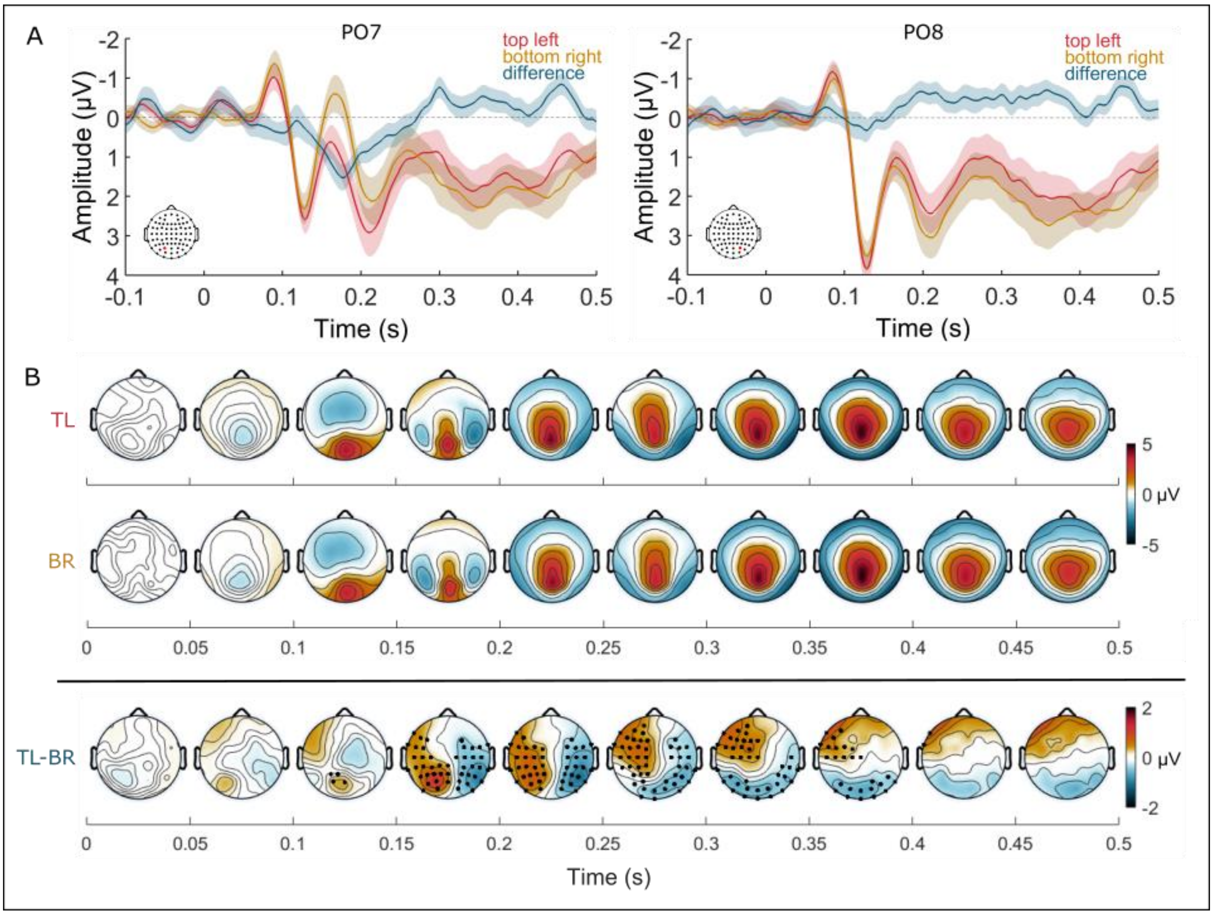

Figure 14. Grand averages of the ERPs for Negative error signal associated with the top left (TL) and bottom right (BR) locations. (A) Negative error signal ERPs for TL (red) and BR (yellow) locations and the TL-BR difference (blue) at electrodes PO7 (left) and PO8 (right) (see red marked electrodes in the schematic drawing of the electrode montage). Error bands represent the standard error of the mean. Time zero is the moment of the background switch. (B) ERP topographies of Negative error signals associated with the TL (first row) and BR (second row) location as well as the difference ERP of both signals (TL-BR; last row) for the post background switch time epoch 0 to 500 ms in 50 ms steps. Dots on the ERP topographies in the last row indicate electrodes that survived tests for multiple comparisons (p < .05).

3.7 Positive error signal

To define the *Positive error signal* we subtracted from the ERPs to Deviants the sum of the ERPs to Visual only and Omission trials (see Eq. 5.1 and Eq. 5.2; Figure 7H). We compared the *Positive error signal* for the TL and BR location (see Eq. 5.3). The *Positive error signal* comprised a lateralized response with the positive difference potential being most prominent at right electrodes and the negative difference potential at left electrodes, which started approximately with a latency of 320 ms (positive cluster: from 320 to 500 ms, *p* = 0.008; negative cluster: from 355 to 500 ms, *p* = 0.033; Figure 15; Table 2).

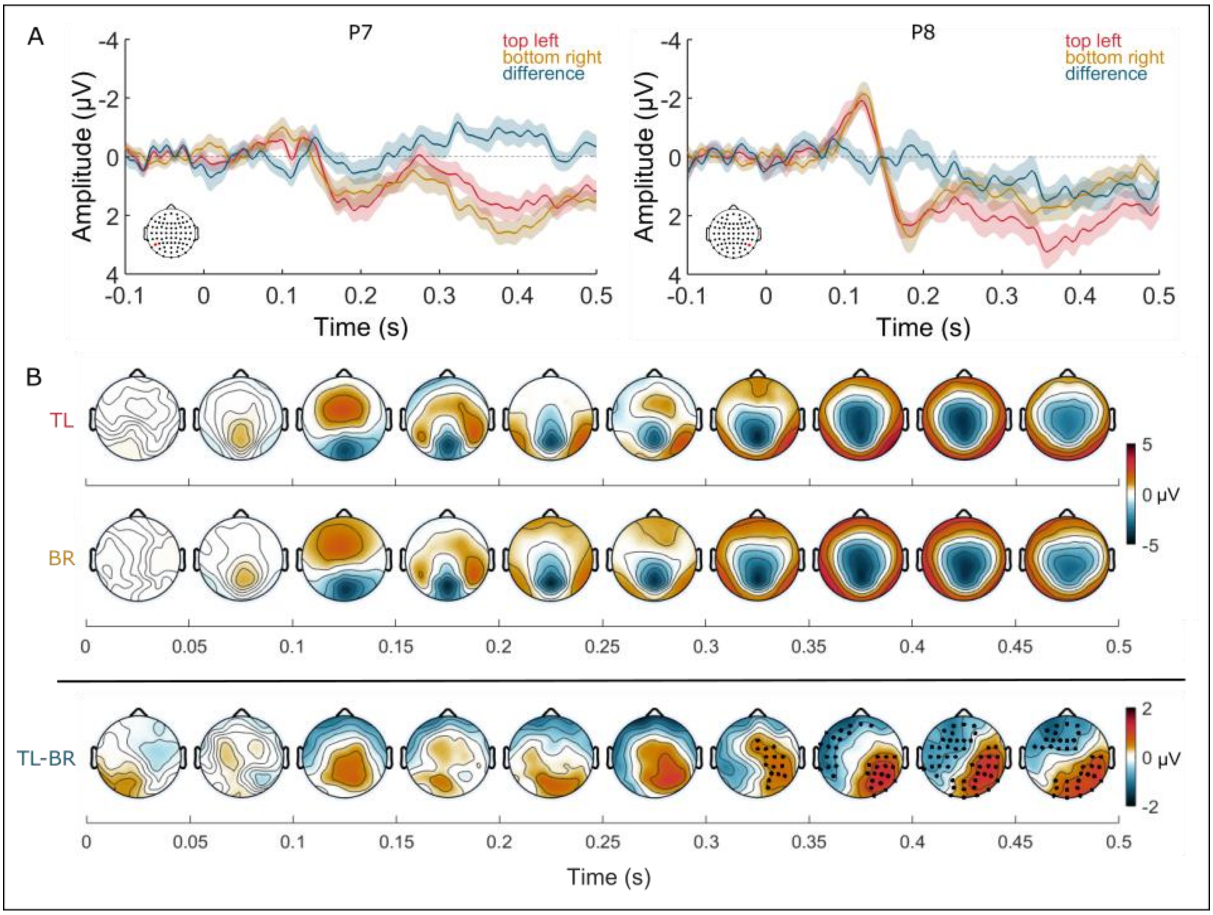

Figure 15. Grand averages of the ERPs for Positive error signal associated with the top left (TL) and bottom right (BR) locations. (A) Positive error signal ERPs for TL (red) and BR (yellow) locations and the TL-BR difference (blue) at electrodes PO7 (left) and PO8 (right) (see red marked electrodes in the schematic drawing of the electrode montage). Error bands represent the standard error of the mean. Time zero is the moment of the background switch. (B) ERP topographies for Positive error signals associated with the TL (first row) and BR (second row) location as well as the difference ERP of both signals (TL-BR; last row) for the post background switch time epoch 0 to 500 ms in 50 ms steps. Dots on the ERP topographies in the last row indicate electrodes that survived tests for multiple comparisons (p < .05).

3.8 Pre-background switch phase

To investigate whether top-down visual predictions modulate neural activity already in the anticipation of the expected stimulus we compared ERPs to the tones that were associated with the TL (A1) and BR (A2) grating location prior to the background switch. A cluster-based permutation test revealed a significant difference between trials in which the TL vs. the BR grating location was expected (including the corresponding Standard, Omission and Deviant trials). We found both positive (positive cluster: from -450 to 0 ms, $p < .001$) and negative difference potentials (negative cluster: from -527 to 0 ms, $p < .001$) with the positive differences most prominent over the left frontal scalp and the negative difference potential over the right posterior scalp (Figure 16, Table 2). The same analysis was run for the Auditory only trials. As seen in Figure A.2 the cluster based permutation test did not reveal any significant differences between the two Auditory only conditions (A1 vs. A2, physically identical in that period to the crossmodal trials) validating that any effect reported for crossmodal trials was genuinely linked to visual predictions.

3.9 Alpha activity indicating visual predictions prior to background switch

To examine whether spatial visual predictions affect pre-background switch alpha modulation we contrasted trials in which the TL and BR grating location were expected. We observed two significant clusters over parieto-occipital regions (positive cluster: from -530 ms to 0 ms, $p = .014$; negative cluster: from -530 ms to -110 ms, $p = .032$), compatible with a reduction of alpha power contralateral to the side of the expected grating (Figure 17A and 17B). Furthermore, alpha power seemed to be stronger for TL compared BR grating expectation over frontal regions (second positive cluster: from -370 ms to 0 ms, $p = .047$). In contrast, in the unimodal runs in which the auditory tones (A1 and A2) were either not yet associated to visual stimuli (Auditory only trials) or not presented at all (Visual only trials), there was no difference in alpha power between the two types of trials (Auditory only: $p = .17$,Figure 17C; Visual only: $p = .19$, Figure 17D). Thus, spatial visual predictions seemed to bias visual areas in anticipation of an upcoming visual stimulus in a spatially specific way.

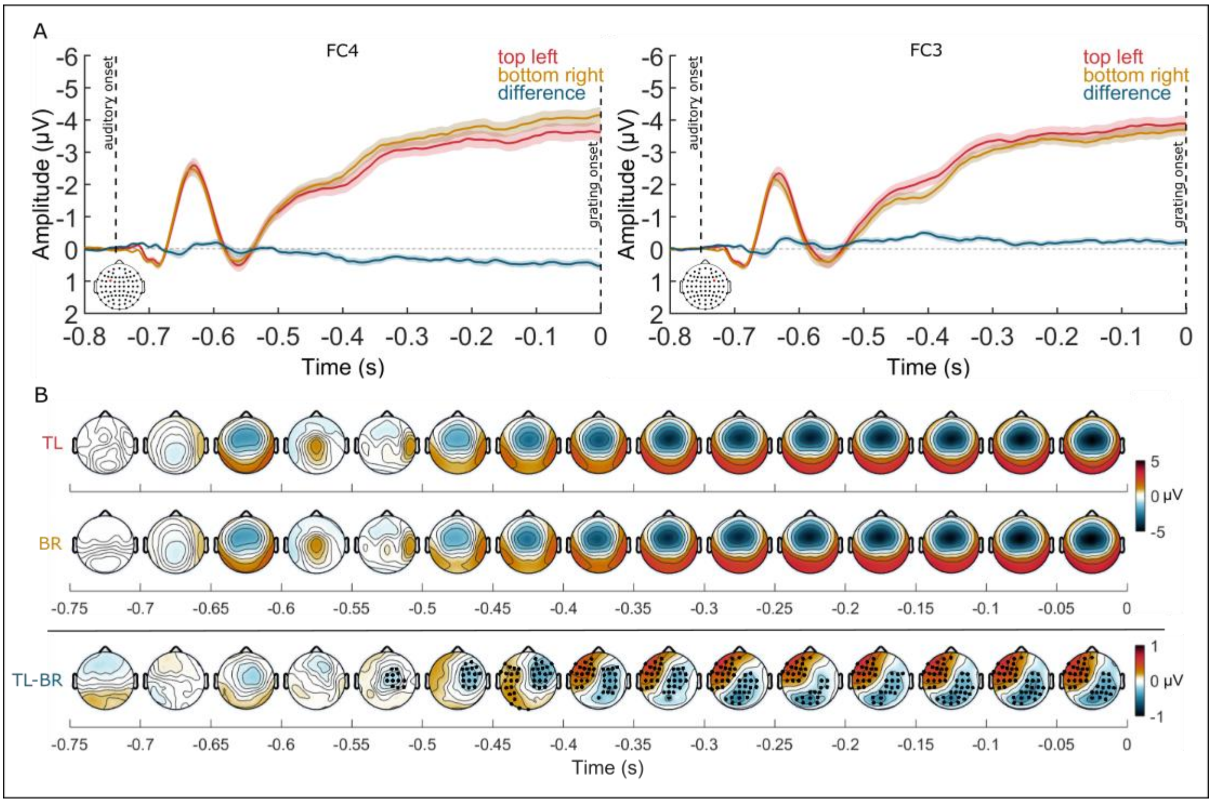

Figure 16. Grand averages of the ERPs to auditory stimulation associated with top left (TL) and bottom right (BR) locations. (A) ERPs following auditory stimulation associated with TL (red) and BR (yellow) locations and the difference TL-BR (blue) at electrodes FC3 (left) and FC4 (right) (see red marked electrodes in the schematic drawing of the electrode montage). Error bands represent the standard error of the mean. The first dashed line indicates the onset of auditory stimulus. Time zero is the moment of the background switch. (B) ERP topographies to auditory stimuli (A1/A2) associated with the TL (first row) and BR (second row) location as well as the difference ERP of both conditions (TL-BR; last row) for the pre background switch time epoch -750 to 0 ms in 50 ms steps. Stars in the ERP topographies in the last row indicate electrodes that survived tests for multiple comparisons (p < .05).

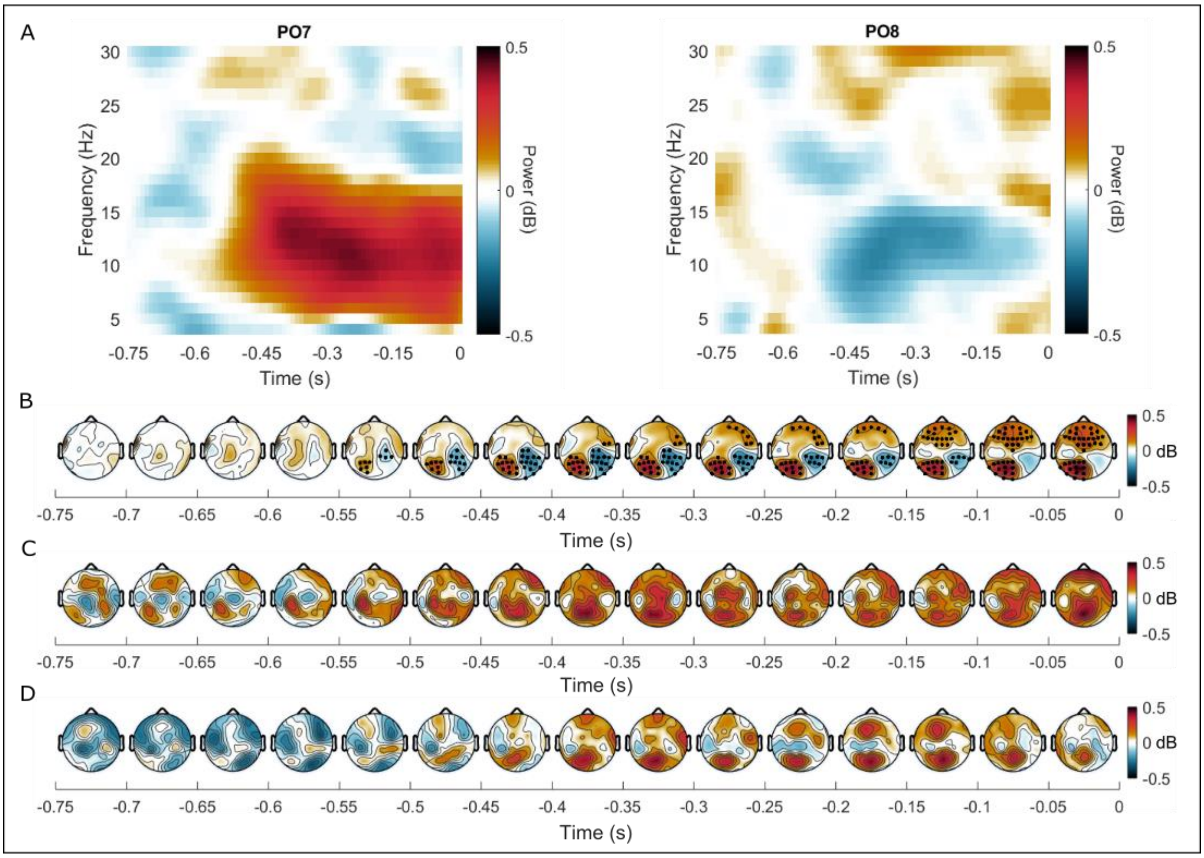

Figure 17. Grand averages of pre background switch alpha-band (8 to 12 Hz) power. Power is displayed in dB with respect to a baseline period between –1.35 to -0.9 s before the background switch. Time zero is the moment of the background switch. (A) Color maps of alpha power differences of trials associated with top left (TL) and bottom right (BR) locations in the crossmodal run at electrode PO7 (right) mad PO8 (left). (B,C,D) Topographies display the pre background switch time epoch -750 to 0 ms in 50 ms steps. Stars in the topographies indicate electrodes that survived tests for multiple comparisons (p < .05). (B) Topographies display the scalp distribution of the alpha power difference of trials associated with TL and the BR locations in the crossmodal run. (C) Topographies display the scalp distribution of the alpha power difference of trials that presented TL and the BR locations in the Visual only run. (D) Topographies display the scalp distribution of the alpha power difference of trials that presented auditory stimuli later associated with TL and the BR locations in the Auditory only run.

4. Discussion

The present study aimed at investigating how top-down spatial visual predictions modulate visual cortical processing. In particular, we were interested in the timing of visual predictive signals and associated error signals. Here we implemented a novel crossmodal omission paradigm while recording ERPs. In this paradigm, auditory stimuli were associated with the location of subsequent grating stimuli, presented in either the top left (TL) or the bottom right (BR) quadrant of the visual field (‘Standards’). In rare trials, a mismatching visual stimulus was presented (‘Deviants’) or no visual stimulus was presented at all (‘Omissions’). By stimulating the upper vs. lower visual field we were able to assess the first visual ERP (50-100 ms), known as the C1. Since the C1 reverses in polarity for upper and lower visual field stimulation, the C1 is considered as reflecting activity of early visual cortex, likely predominantly generated as the initial wave of primary visual cortex activation (Di Russo et al., 2002). While Standards and Deviants elicited robust C1 effects, Omissions did not. The first spatially specific omission response was recorded at 230 ms. Stimulus specific mismatch responses emerged at 140 ms and spatially specific Mismatch responses started at about 170 ms. Based on a recent model describing the neural circuits that may underlie predictive coding, we defined a *Visual predictive signal* and two error signals: a *Negative* and a *Positive error signal* (Keller & Mrsic-Flogel, 2018). The *Visual predictive signal* started with a latency of 70 ms that is within the early time epoch of the P1. Error signals emerged as lateralized responses with a latency of approximately 140 ms (*Negative error signal*) and 320 ms (*Positive error signal*). Finally, the pre-stimulus phase, that is the epoch between presenting the sound associated with a spatial location and the genuine visual stimulus was analyzed: typical lateralized pre-stimulus potentials were observed with a relative contralateral negativity. Time-frequency analysis revealed a decrease in pre-stimulus alpha power contralateral to the expected location of the visual stimulus.

Whereas fMRI studies have supported the idea that primary visual cortex is susceptible to top-down effects such as spatial prediction (Alink et al., 2010; Den Ouden et al., 2010; Kok et al., 2014; Muckli et al., 2015) and spatial attention (Brefczynski & DeYoe, 1999; Kanwisher & Wojciulik, 2000; Martinez et al., 1999), the precise timing of prediction effects within visual cortical processing has yet been unknown. One reason was that fMRI measures do not have the temporal resolution to distinguish activity within the first 500 ms. Another reason was that the employed ERP methods did not use the stimulation protocols necessary to dissociate striate from extrastriate processing or stimulus related processing (e.g. of the auditory cues) from effects of visual predictions. Neural activity to highly expected but omitted visual stimuli are considered to reflect the “pure” visual prediction effect (Egner et al., 2010). The majority of electrophysiological studies in humans have investigated omission responses in the auditory domain (for a review see: Walsh et al., 2020). For example, Bendixen et al. (2009) reported a high similarity of early (<100 ms) ERPs to omissions and to veridical stimuli. However, the experiment of Bendixen et al. (2009) and other previous studies (SanMiguel et al., 2013; Todorovic & Lange, 2012; Todorovic et al., 2011; Wacongne et al., 2011) were not designed to isolate neural activity associated with the first cortical response of sensory processing.

The present study implemented a stimulation protocol that unambiguously allowed us to assess the first neural response in visual cortex by investigating the existence of a C1 effect to real expected (and unexpected) visual stimuli and to omissions. While a reliable C1 effect was obtained for real visual stimuli (Standards and Deviants), Omissions did not elicit a C1 effect. Often it was argued that omission responses might not elicit short living early sensory ERPs as the C1 due to the temporal uncertainty associated with omissions. In the present study, we excluded this alternative account by specially marking the time point at which visual stimulation was to be expected: A background switch occurred simultaneously with the presentation of the grating stimulus. Thus, we think that we provided strong evidence in humans for the assumption that the neural mechanisms of early visual cortex activity for visual predictions are distinct from those of processing veridical stimuli (see: Klink et al., 2017 for non-human primate data; Keller & Mrsic-Flogel, 2018 for a mechanistic discussion). However, a lateralized and thus spatially specific omission response emerged later, that is at about 230 ms after the expected onset of the visual stimulus. First, this latency of an omission response in the present study concurs with previously observed onsets of omission responses (Ford et al., 1976; Klinke et al., 1968; Simson et al., 1976). Since in contrast to most of the previous studies we had employed lateralized visual stimuli we were able to test whether visual predictions are spatial specific that is, lateralized. In fact, they were. Here it has to be noticed that the ERPs in Omission trials comprised earlier deflections too. However, these were likely elicited by the background switch. Our design did not allow dissociating background switch related neural responses from spatially unspecific omission responses. The lateralized omission response observed in the present study supports the idea that omission responses preserve feature-specific information about the expected stimulus (Demarchi et al., 2019) and thus collaborates previous fMRI studies (Kok et al., 2014; Muckli et al., 2015). The new findings add that feature-specific response are restricted to late (>200 ms) time epochs and might be associated with a (negative) error signal in visual cortex. Thus, we concluded that visual prediction effects in visual cortex are stimulus specific, but the timing of crossmodally induced top-down activation does not mirror the timing of visual bottom-up activation and thus the neural mechanisms of bottom-up and top-down driven neural activity in early visual cortex are distinct.

If visual predictions elicit lateralized neural responses not before 230 ms in the absence of sensory-driven activity, the question arises of whether top-down effects might modulate stimulus-driven activity at an early point in time. In fact, Kok et al. (2016) found that while top-down activity predominantly modulated deeper layers, bottom-up activity seemed to elicit activity in all cortical layers. Comparing ERPs to stimuli that mismatched vs. matched visual predictions, we found no difference in the C1 time range. This finding is consistent with a large body of literature which found no evidence of top-down control during the first cortical response of visual processing (Alilović et al., 2019; Baumgartner et al., 2018; Di Russo et al., 2003; Di Russo et al., 2012; Roelfsema et al., 1998; Supèr et al., 2001). For example, Alilović et al. (2019) manipulated spatial visual expectations and spatial attention simultaneously by presenting a predictive word cue at the beginning of each trial (left/right/neutral) and a color cue indicating the side participants had to attend, respectively. In line with our results, they did not observe a C1 modulation related neither to prediction nor to attention. Taken together our results in the C1 time range indicate that the initial stages of visual processing might be independent of top-down control. To investigate further when in the visual pathway visual predictions modulate neural activity, we analyzed ERPs after the C1 time range. ERPs to Deviants compared to Standards started to differ after around 140 ms post stimulus presentation that is in the N1 time epoch (stimulus specific Mismatch effect). The spatially specific Mismatch effect started to differ for the two visual locations with a latency of about 170 ms. We observed a more negative going potential over the contralateral hemisphere. The here observed mismatch effects are reminiscent of a vMMN (Sulykos & Czigler, 2011). The vMMN response has been interpreted as reflecting an error signal to stimuli that violated visual expectations (for a review see: Stefanics et al., 2014). This error signal was localized to extrastriate visual cortex by Kimura et al. (2010). Thus, we consider that the spatially specific mismatch response of the present study similarly reflects an error signal associated with extrastriate cortex.

Recently, Keller and Mrsic-Flogel (2018) proposed that error signals might be generated by two partially independent neural populations in order to take into account that predictions can be violated in at least two different ways: sensory input can exceed (positive error processing) or fall below the predicted input (negative error processing). According to the proposed additive model by Keller and Mrsic-Flogel (2018) we defined three signals, namely the *Visual predictive signal*, the *Negative error signal* and the *Positive error signal* (for definitions see: Methods and Material). We observed a *Visual predictive signal* with a lateralized topography. Consistent with other neurophysiological studies investigating predictive processing in vision (Alilović et al., 2019; Lasaponara et al., 2017) that reported early effects in the P1 time epoch and audition this signal emerged early (Bendixen et al., 2009; Todorovic et al., 2011; Wacongne et al., 2011). The *Visual predictive signal* for BR vs. TL started to differ after around 70 ms after stimulus onset that corresponds to the early time epoch of the P1. However, this finding is in contrary to our results for Omission effects, which did not start as early as 230 ms after stimulus onset. A recent study used ultra-high field fMRI to more precisely unravel the detailed nature of omission responses to expected grating stimuli of different orientations (Aitken et al., 2020). Although, cortico-cortical feedback connections predominantly target the deep layers 5/6 and the superficial layer 1 (Harris & Mrsic-Flogel, 2013; Rockland & Pandya, 1979), the authors observed a feature-specific omission response only in the deep layers of V1. The authors proposed that feedback signals in the deep and superficial layers have distinct functions based on their connectivity pattern within a cortical column. Within the cortical column, the authors attributed a driving function to layers 5/6, whereas they assumed that feedback signals in layer 1 have only have a modulatory function. During omission trials, there is no bottom-up sensory signal to be modulated and might explain why the authors observed activation only in the deep layers (driving function) but not in the superficial layers (modulatory function). In line with their interpretation, previous findings observed feedback activation restricted to the deep layers in the absence of bottom-up sensory input, but activation in both deep and superficial layers when bottom-up input was present (Kok et al., 2016). This might explain why the latencies of the *Visual predictive signal* and the Omission effect were different. In the present study, the modulatory effect of the superficial layer would only be present in the *Visual predictive signal* since in the Omissions no bottom-up sensory input is given. These present results add to the layer specific brain imaging data the timing of top-down control: early modulatory effects if bottom-up sensory signals are present and later driving effects in the absence of bottom-up sensory signals.

Concerning error processing both defined error signals, namely the *Negative* and the *Positive error signal* were lateralized but had differential latencies. The *Negative error signal* started around 140 ms but already terminated after 260 ms, whereas the *Positive error signal* started around 300 ms and lasted until the end of the analysis window. Error processing seemed to modulate striate and extrastriate areas, but negative error processing seemed to lead positive error processing. These findings support the assumptions of Keller and Mrsic-Flogel (2018), who proposed two partially independent neural populations generating the negative and positive error signal, respectively. The Mismatch effects and the *Negative error signal* had similar latencies, speaking in favor of similar processes. The subsequent *Positive error signal* might indicate additional information processing and a revision of the internal model. However, it could also be speculated that at the onset of the expected stimulus, attention is relocated to the expected ‘empty’ location enabling negative error processing. Positive error processing is enabled only after redirecting attention to the unexpected location. The time needed to redirect attention could potentially explain why positive error processing followed negative error processing in the present study.

Analyzing the period prior to the background-switch (before the onset of the grating stimulus) revealed that ERPs differed for TL and BR visual expectations. The difference was most prominent at frontal electrodes and showed a relative negativity contralateral to the expected location of the grating stimulus. Similar pre-stimulus frontal ERPs have been observed for the control of spatial attention (e.g. anterior directing attention negativity, see: van Velzen & Eimer, 2003). Furthermore, pre-stimulus alpha power over posterior regions decreased contralateral to the expected location of the visual stimulus. This finding has been widely interpreted as reflecting top-down processes as spatial visual predictions (Alilović et al., 2019; Mayer et al., 2015; Rohenkohl & Nobre, 2011) and spatial visual attention (Foxe & Snyder, 2011; Sauseng et al., 2005; Worden et al., 2000). Recently, Alilović et al. (2019) observed a similar alpha-power lateralization depending on spatial visual predictions. Importantly, pre-background switch effects in the time and frequency domain did not emerge in the unimodal runs (Auditory and Visual only trials) in which expectation were not established yet, suggesting that they reflect genuine processes of top-down control.

Since our experimental manipulation involved spatial visual predictions, we must consider that it additionally elicited attentional processes related to endogenous spatial attention. With respect to attentional cueing, some previous studies have reported attentional modulations as early as during the C1 interval (Kelly et al., 2008; Rauss et al., 2012; Rauss et al., 2009), although this finding has repeatedly been refuted (Alilović et al., 2019; Baumgartner et al., 2018; Di Russo et al., 2003; Di Russo et al., 2012). A more robust finding is that attentional cueing results in a subsequent enhancement of P1, which has been reported to start as early as 70 ms (Mangun et al., 2001; Martinez et al., 1999; Martınez et al., 2001). Between the two conditions in which an attentional effect would have been most prominent (Standards vs. Deviants, similar to the valid vs. invalid contrast used typically in spatial attention studies), we observed no significant difference in the time range of the C1 nor the P1 component. Notably, Standards and Deviants started to differ 140 ms after the onset of the grating stimulus, but showed an opposite effect with an increased neural response to Deviants instead to Standards. In summary, we can rule out the possibility that the observed prediction effects can be solely explained by spatial attention.

The finding that visual predictions do not effect the initial but later activation of primary visual cortex sheds light on the time course by which top-down control modulates visual processing, that is, generating spatially specific error signals if the prediction and the actual visual input do not match, either because of an unexpected or a missing visual input. Future work building on these findings may be able to reveal the neural circuits underlying those different types of error signals.

Chapter III: The Extent of Endogenous and Exogenous Spatial Attention Effects on Oscillatory Activity

1. Introduction

Perception can be considered the outcome of integrating bottom-up and top-down communicated neural signals (Bullier, 2001; Meyer, 2012; Park & Friston, 2013). Bottom-up communication transmits new sensory information from the external world into the brain. Top-down communication, on the other hand, represents prior knowledge that reflects assumptions and inferences about the world (Friston, 2005; Lee & Mumford, 2003; Summerfield & Lange, 2014). However, how exactly these information streams are conveyed and successfully integrated is still under debate: within cortical areas of only a few cubic millimeters, segregated information has to be properly integrated without being altered; between cortical areas, information must travel across centimeters from the sending to the receiving area, whilst remaining intact. A growing body of literature supports the idea that reliable communication is established via synchronized oscillatory activity within specific frequency bands (Fries, 2005, 2015; Wang et al., 2016). It has been proposed that lower frequencies (alpha-/ beta-band) subserve intra-areal and top-down communication, as well as inhibition; whereas higher frequencies (gamma-frequency) index local as well as bottom-up communication (Bastos et al., 2015; Chao et al., 2022; Michalareas et al., 2016). This proposal is anatomically plausible: feedback connections predominantly target the superficial layers of the cortex and exert gamma-band synchronization, whereas feedforward connections mostly project to deep layers and show alpha- and beta-band synchronization (Bastos et al., 2015; Buffalo et al., 2011; van Kerkoerle et al., 2014).

A commonly used paradigm to investigate top-down and bottom-up communication is the spatial attention paradigm also known as the Posner paradigm (Posner, 1980). In this paradigm, goal-directed, voluntary or endogenous attention is manipulated to investigate top-down processes and stimulus-driven, involuntary or exogenous attention is utilized to investigate bottom-up processing, respectively (Corbetta & Shulman, 2002). Endogenous attention relates to our ability to voluntarily allocate attention on particular information to reach a specific goal. It takes at least 200 ms to deploy, and can be sustained until task completion. Exogenous attention on the other hand refers to an involuntary shift of attention to a sudden or salient stimulation. It is transient, and develops and decays quickly, peaking already around 100 ms after stimulation (Carrasco, 2011; Wright & Ward, 2008). Even though endogenous and exogenous cueing show some common behavioral and perceptional effects, most studies support the view (e.g. due to different temporal properties) that both types rely on independent but partially overlapping mechanisms that compete for resources of the same capacity-limited attention system (Chica et al., 2013).

Previous studies that investigated how oscillatory activity is related to attention mostly deployed endogenous attention. They reported that alpha power decreases contralateral to the attended side while on the ipsilateral side, alpha power increases (Okazaki et al., 2014; Worden et al., 2000; Zumer et al., 2014). This alpha power modulation has been widely interpreted as an intended top-down controlled release or confinement of inhibition and has been linked to improved behavioral performance. Increased alpha modulation has been reported to reduce both reaction times (Gould et al., 2011; Kelly et al., 2009) and distractor inference (Okazaki et al., 2014), as well as to increase detection and discrimination performance (Thut et al., 2006; van Dijk et al., 2008). As opposed to the direction of alpha lateralization, gamma power increases contralateral to the attended side (Fries et al., 2001; Müller et al., 2000) and is positively correlated with task performance (Hoogenboom et al., 2010; Siegel et al., 2008). These observations were interpreted as reflecting enhanced sensory processing of attended visual stimulation, and thus enhanced bottom-up information transmission. Alpha- and gamma-modulation might be closely related, as alpha power seems to control gamma power (Herring et al., 2019; Popov et al., 2017; Siegel et al., 2008). In a recent study, Herring et al. (2019) used tACS in the alpha range over the occipital cortex while recording MEG. They not only found that alpha tACS rhythmically suppressed visually induced gamma oscillations, but also that the degree of gamma suppression was negatively correlated with the decrease in performance in a visual detection task. These findings lead the authors to the conclusion that low frequency oscillations as such within the alpha range might gate top-down information, whereas bottom-up sensory processing is transmitted via high frequency oscillations such as gamma.

However, only the effects of endogenous attention on oscillatory activity in the gamma-band have been assessed so far. To our knowledge, no previous study has yet investigated whether exogenous attention also modulates neural activity in the gamma-band indicative of increased attentional selection. Since the frequency range of the gamma-band widely overlaps with biological (e.g. muscle noise) and other artifacts (e.g. line noise), and the spectral power of brain activity logarithmically decreases with increasing frequency, it is challenging to receive a sufficient signal-to-noise ratio in electrophysiological recordings. To increase the signal strength over visual areas, one experimental method is to present dynamic grating stimuli. In MEG recordings for example, they reliably induced a band-limited gamma response over the visual cortex (Hoogenboom et al., 2006; Muthukumaraswamy & Singh, 2013). However, the signal-to-noise ratio of the visually induced gamma response in EEG remains of poor quality (Muthukumaraswamy & Singh, 2013; Orekhova et al., 2015). In the present study, we tailored dynamic grating stimuli with optimal stimulus size (Jia et al., 2013), eccentricity (van Pelt & Fries, 2013), spatial frequency (Adjamian et al., 2004), and velocity (Orekhova et al., 2015), allowing us to record a reliable band-limited gamma responses in an EEG study. MEG studies investigating the impact of visual spatial attention on visually induced gamma responses consistently reported increased amplitudes over the occipital cortex contralateral to the attended hemisphere (Bauer et al., 2012; Magazzini & Singh, 2018; Marshall, O'Shea et al., 2015; Marshall, Bergmann, & Jensen, 2015; Siegel et al., 2008). However, these studies investigated solely the effects of endogenous attention.

While the temporal resolution of time frequency analysis is always a compromise between temporal and spectral resolution, the analysis of ERPs provides a resolution of milliseconds and therefore allows investigating the timing of attentional effects much more sufficiently. Both endogenous and exogenous attentional effects are observed as early as 70 ms after stimulus onset within the time range of the P1 (Di Russo et al., 2003; Hopfinger & Mangun, 1998, 2001; Mangun et al., 2001; Mangun et al., 1997). Valid cues increase the P1 amplitude compared to invalid cues. This is widely interpreted in terms of a sensory gain control mechanism resulting in enhanced processing of the validly cued stimuli (Mangun & Hillyard, 1991). The subsequent N1 component was also found to be modulated, thus only by endogenous attention and under specific task conditions. Valid cues, when compared to invalid ones, elicit increased amplitudes contralateral to the target stimulus, but only for difficult discrimination tasks (Hopfinger & West, 2006; Mangun & Hillyard, 1991; Vogel & Luck, 2000). The P300 component, on the other hand, which is associated with higher processing and related to working memory and decision making, is in turn affected by both endogenous and exogenous attention (Hopfinger & Mangun, 1998, 2001; Hopfinger & West, 2006). Valid cues elicit higher P300 amplitudes compared to invalid cues, indicating that the target location is treated as more relevant than the uncued location. Although the isolated effects of endogenous and exogenous attention on sensory processing are well studied, it is not clear how their effects interact and jointly affect neural activity. It is assumed that endogenous and exogenous attention rely on partially distinct neural systems: one dorsal fronto-parietal network, which mainly subserved endogenous orienting, and a more ventrally located fronto-parietal network, which mainly serves faster exogenous orienting (Chica et al., 2013; Funes et al., 2005; Wang et al., 2010). Despite this possible distinction, their effects could as likely interact on various stages of sensory processing (Müller & Rabbitt, 1989).

Although, alpha- and gamma-band might be closely related and their interaction might play a key role in spatial attention (Womelsdorf & Fries, 2007), research that investigated the interaction of endogenous and exogenous attention mainly reported behavioral and ERP findings and lacks oscillatory findings (Carrasco, 2011). For example, Hopfinger and West (2006) used a double-cue paradigm to simultaneously modulate spatial endogenous and exogenous attention while recording ERPs. In line with behavioral findings, that reported independent beneficial behavioral effects for valid endogenous and exogenous cueing (Berger et al., 2005; Grubb et al., 2015; Landry et al., 2021; Natale et al., 2009), endogenous and exogenous attention dominated different stages of sensory procesing. While exogenous attention dominated early processing stages (late phase of P1), endogenous attention dominated later higher order processing (P300). Nonetheless, in between these stages, both attention types interacted: whereas endogenous attention enhanced the N1 amplitude, exogenous attention modulated the latency of the endogenous N1 effect. The authors concluded that endogenous and exogenous attention depend on two partially independent but interacting systems.

In the current study, we implemented a new spatial attention paradigm. We presented the aforementioned bilateral dynamic grating stimuli to elicit a band-limited continuous response within the gamma range. Simultaneously, we manipulated goal-directed (endogenous) and stimulus-driven (exogenous) attention to investigate effects of top-down and bottom-up communication in visual areas, as well as their integration. In the past, arrows were typically used to direct attention to either the left or the right visual field. However, after finding that arrows partially also deploy exogenous attention (Stevens et al., 2008), more abstract cues as e.g. letters or color cues are used to ensure that solely endogenous attention is modulated. Therefore, we controlled spatial endogenous attention by presenting either directional (85%) or neutral (15%) letter cues at the beginning of each trial. With a high likelihood (82.35 %), the directional cues predicted whether the next target was presented on the left (‘L’) or the right side (‘R’). Consequently, in 17.65% the target was presented on the opposite side. The neutral cues (‘N’) did not possess any predictive value. Thus, endogenous cues could be either valid, invalid, or neutral to the target location. During each trial, we presented flashing frames around the dynamic gratings, either around one stimulus at a time or around both stimuli. These flashing frames served as spatial exogenous cues and were either congruent, incongruent or neutral (both frames flashing at the same time) to the target location. By analyzing the time frequency spectra of the recorded EEG, we were able to investigate the effects of top-down and bottom-up communication on alpha-band and gamma-band power. Additional analyses of ERPs allowed us to have a better insight of the time course of attentional effects and their interaction.

We hypothesize that directional endogenous attentional cues evoke lateralized alpha responses, whereas directional exogenous attentional cues evoke lateralized gamma responses of opposite polarity. Gamma lateralization, furthermore, is expected to be a function of alpha lateralization. In addition, we expected that the degree of alpha- and gamma-band modulation would correlate with behavioral effects. Since we utilized a difficult discrimination task, we expect not only increased P1 and P300 amplitudes when comparing valid and invalid as well as congruently and incongruently cued targets, but also increased N1 amplitudes when comparing valid and invalid cued targets, respectively. The simultaneous manipulation of endogenous and exogenous attention allows us to draw conclusions not only about the time point of top-down and bottom-up information, but also about the degree of their integration.

2. Methods and Materials

2.1 Subjects

Thirty-five participants were recruited from the University of Hamburg. They had an average age of 23.9 years (range: 19 to 39 years, SD = 3.9, 23 females, 4 left-handed). All participants were students and reported normal or corrected-to-normal vision, normal hearing and no history of psychiatric or neurological disorders. The Local Ethics board of the Faculty of Psychology and Movement Sciences, University of Hamburg, Germany had approved the study (No. 2019_221). All participants gave informed consent and received course credits or money for compensation.

2.2 Stimuli and Apparatus

Stimuli were generated using the Psychophysics Toolbox for MATLAB (Brainard, 1997; Kleiner et al., 2007) and presented with a 22.5’’ VIEWpixx LCD monitor with a refresh-rate of 120 Hz. All stimuli were presented against a black background. The fixation point consisted of a blurred circle using a Gaussian function with a diameter of 0.5° visual angle presented at the center of the screen. The visual stimulus consisted of an annular grating with a spatial frequency of 3 cycles/degree presented at full contrast covering a square with a side length of 8° visual angle (Figure 18). The grating stimulus was dynamic and the annular grating expanded with a velocity of 1.3 degree/second, and was bilaterally presented, with the outer edge being 0.5° visual angle far away from the fixation point. The center of both dynamic grating stimuli were covered by a grey circle with a diameter of 2° visual angle. As the target stimulus, we briefly presented the letter C in the center of these circles, on either the left or the right side. It subtended a visual angle of 0.9° and 45° tilted to either the right or the left. We introduced the grey circles and presented the target on top of it, to control the contrast between the target and its background reliably, and thereby keeping the difficulty of the task consistent. As endogenous attentional cues, we presented letters (L, R, N) at the center of the screen on top of the fixation point subtending a visual angle of 0.9°. Exogenous attentional cues were white frames with a width of 12° and thickness of 2° visual angle that were briefly presented around the grating stimuli. Exogenous cues were presented either around both dynamic grating stimuli or just around one at a time.

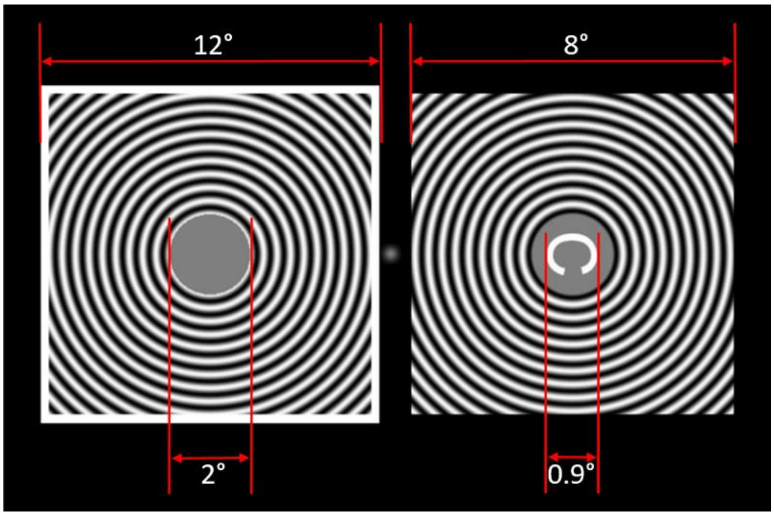

Figure 18. Grating stimuli, exogenous cue and target stimulus used in the experiment. The grating stimuli were always presented bilaterally. The target stimulus were tilted 90° either to the right or to the left. In this example, it is tilted to the right. The target stimulus was presented middle of either the left or the right grating stimulus. Frames around the grating stimulus served as exogenous cues. They were presented around the grating stimuli, either one a time or around both. In this example, the exogenous cue is incongruent to the target.

2.3 Design

All trials started with the presentation of the fixation point for 1000 ms, which remained visible the whole time (Figure 19). During that period, we controlled central fixation via an eye tracker. The next trials started only if fixation remained on the fixation point for at least 1000 ms. On top of the fixation point, the endogenous attentional cue was presented for 100 ms (the letter L, R or N). In 85% of the trials a directional cue was presented (L or R), in the remaining 15% a neutral non-directional cue (N) was presented. In 82.35% of trials, the directional cues were valid, meaning that the subsequent target was presented on the cued side. In 17.65%, the directional cues were invalid meaning that the target was presented on the non-cued side. Neutral endogenous cues were not predictable: in half of the trials, the target was presented on the left and in the other half on the right side. Thus, in each trial the endogenous cue could be valid, invalid or neutral. Afterwards the fixation point was presented alone for additional 500 ms. Then, the dynamic grating stimuli were presented bilaterally for 650 ms, followed by the exogenous cue was flashed for 50 ms. The exogenous cue consisted of white frames, flashed with equal probability either around the left, the right or around both dynamic grating stimuli (33.33%). Thus, exogenous attentional cues could be congruent, incongruent or neutral to the presentation side of the subsequent target. For a summary of all conditions, see Table 3. Before the target was presented for 33 ms, the dynamic grating stimuli were presented alone for additional 50 ms. Subsequently, the dynamic grating stimuli were presented alone for 500 ms. Upon stimulus extinction, the fixation point was presented for additional 467 ms. Starting with the onset of a target, participants had 1000 ms to respond via a Buddy Button (AbleNet, Inc., Minneapolis, United States of America) with their dominant hand. Participants' task was to discriminate whether the presented letter C was opened up to the top or bottom. They should only respond to one configuration (target vs. non-target trials). The configuration to which they should react was counterbalanced across participants. After this response time window, participants received feedback whether their response was correct. After a correct response, the background remained black, whereas after an incorrect response the background briefly brightened up for 42 ms. Participants task was to press a button when the target letter was presented in one of the two possible configurations. For example, the participant should only respond when the target was opened up to the top. Thus, if a target was presented that was opened up to the bottom; participants should withhold their response. To which configuration participants were asked to respond was counterbalanced. Each trial ended with a random ITI, ranging between 0 ms and 500 ms (uniform distribution, 100 ms steps).

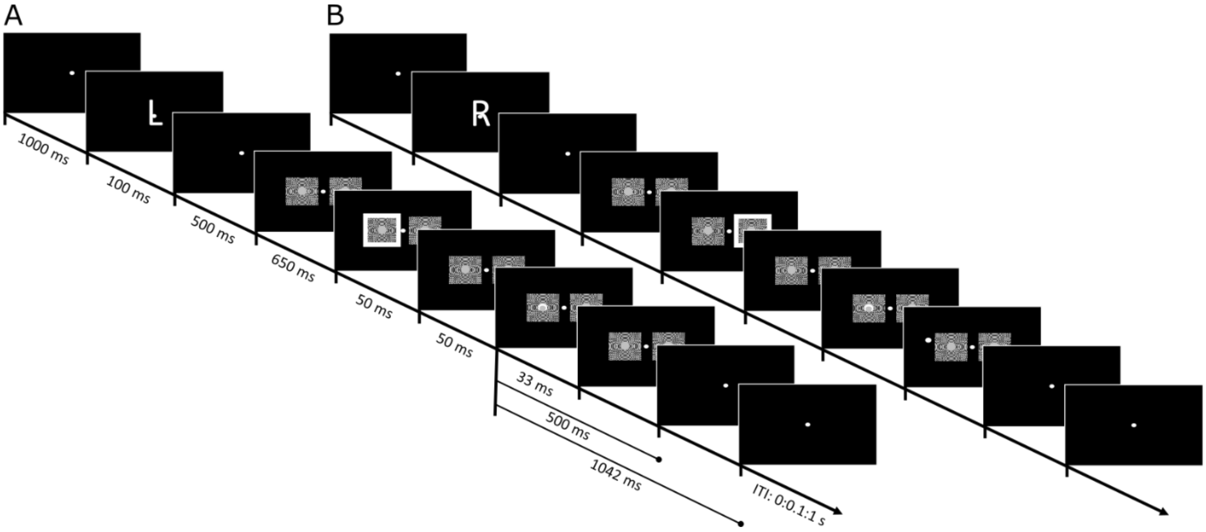

Figure 19. Study design and trial structure. (A) Trial structure of a valid/congruent trial. Valid i.e. endogenous cue and congruent i.e. exogenous cue correspond to subsequent target presentation on the cued side. (B) Trial structure of an invalid/incongruent trial. Invalid i.e. endogenous cue and incongruent i.e. exogenous cue correspond to subsequent target presentation on the uncued side. For a high-resolution display, see Figure 18.

To ensure that the difficulty of the discrimination task was equally high for all participants, we deployed an adaptive psychometric method called QUEST, as implemented in the Psychophysics Toolbox for MATLAB. By adjusting the contrast of the target, we targeted for a performance of 82%. We started the QUEST procedure with an estimated average contrast value of .15 Michelson contrast (SD = .05), a beta of 3.5, a delta of 0.02, a gamma of .5, a range of 2 and a grain of .001. Each trial of the QUEST procedure started with the presentation of the fixation point for 1000 ms. During that period, we controlled for fixation via an eye tracker as described above. Subsequently, the dynamic grating stimuli were bilaterally presented. The presentation time was randomized, ranging between 500 and 800 ms (uniform distribution, 50 ms steps). The target was presented for 33 ms (4 frames) in either the center of the left or the right grating stimulus. We deployed a two-alternative forced choice task. Participants had to indicate via a button-press with their dominant hand, whether the C was opened up to the top (45° tilted to the left) or the bottom (45° tilted to the right), independent of presentation side. Participants were told to respond as fast and as accurate as possible. After target extinction, the grating stimuli were presented for additional 500 ms. The next trial started either directly after a random ITI chosen from a uniform distribution ranging between 0 ms and 500 ms in 100 ms steps or after participants responded. The correctness of the response determined the next target contrast. A correct response lead to a contrast decrease, whereas a false response lead to a contrast increase. After 100 trials, the current contrast value was used for the subsequent experiment. Contrast values had an average of 0.14 Weber contrast (*SD* = 0.09) and ranged between 0.05 and 0.61.

Table 3
Probabilities of conditions in percentage

		Endogenous cueing					
		Valid		Invalid		Neutral	
		Left	Right	Left	Right		
Exogenous cueing	Congruent	11.66	11.66	2.5	2.5	5	5
	Incongruent	11.66	11.66	2.5	2.5	5	5
	Neutral	11.66	11.66	2.5	2.5	5	5

2.4 Procedure

Participants were seated in a dimly lit room 60 cm away from the screen. The experimental session always started with the individual contrast adaptation of the target consisting of 100 trials. Before starting with the actual experimental blocks, participants completed 36 exercise trials. The experiment consisted of 15 blocks, each containing 96 trials, resulting in 1440 trials. Trials were fully randomized.

2.5 EEG recording and Preprocessing

The electroencephalogram (EEG) was recorded from 74 Ag/AgCl electrodes positioned according to the 10-10 system (Acharya et al., 2016) and mounted in an elastic cap (EASYCAP GmbH, Herrsching, Germany), with location AFz serving as ground and the left earlobe as reference. The EEG signal was recorded at a sampling rate of 1000 Hz with a BrainAmp DC amplifier (Brain Products GmbH, Gilching, Germany) with a hardware bandpass filter with a passband of 0.0167 to 250 Hz. The electrode impedances were kept below 10kΩ.

Offline EEG data were processed using EEGLAB toolbox 2022.0 and the FieldTrip toolbox version 20210121 for Matlab version R2020a. After high-pass filtering the data at 0.1 Hz (6 dB cut off at 0.05 Hz, 0.1 Hz transition bandwidth) the data was epoched from -1.5 to +1.5 s according to the onset of the grating stimuli. To ensure that only trials were analyzed that stimulated participants' periphery, we rejected trials in which participants' gaze deviated from the fixation point more than 3° visual angle to the left or right. Afterwards the data was visually inspected and epochs containing biological artifacts, such as muscle artifacts or massive blinks, and electrode drifts were rejected. Before correcting for typical biological (blink, eye movement, muscle, heart) and other artifacts (line noise) using the ICA, as implemented by EEGLAB *runica* function (Lee et al., 1999), EEG data was baselined by subtracting the average activity of the whole epoch (-1500 ms to 1500 ms) from each time point. To identify components representing artifacts, we employed the ICLabel classifier (Pion-Tonachini et al., 2019). For each component, the classifier estimates the probability that it captures brain activity or activity related to artifacts. Components were removed if the probability exceeded 0.8 for one of the following artifact categories: eye, muscle, heart and line noise. On average 11.29 components were removed per participant (SD = 6.2899). As a last step EEG data were average-referenced.

2.6 Behavioral analysis

Behavioral performance was assessed by two different measurements: percentage correct and reaction time (RT). Percentage correct was defined as the percentage of correct responses divided by the absolute number of trials. For the analysis of RTs, we only included correct responses. RTs faster than 200 ms or exceeding two SDs of participants' individual RTs were excluded from the analysis. To investigate whether endogenous and exogenous spatial cues affect behavior, we conducted a two-way ANOVA for each of the two measurements, with the factors endogenous cueing (valid/invalid/neutral) and exogenous cueing (congruent/incongruent/neutral) condition.

2.7 Time-frequency analysis

Spectral analysis was computed using the Fieldtrip toolbox (Oostenveld et al., 2011) and customized MATLAB scripts using a Fast Fourier Transformation (FFT). For frequencies from 4 up to 30 Hz, a sliding window single-taper analysis was performed (Hanning taper, 300 ms window length zero padded, frequency resolution 1 Hz, 15 ms step size). For frequencies > 24 Hz, a multitaper approach was used. In this approach the window length (T) and bandwidth (W) were a function of frequency (F). Setting T to 8 cycles per window and W to 0.25 frequency smoothing, resulted in a bandwidth product of $(T/F)(W*F) = 2$ and number of tapers $K = 2TW\text{-}1= 3$. Since, T and W were a function of F, this resulted in decreasing temporal smoothing and increasing bandwidth for increasing F. Alpha-band activity was defined as 8-12 Hz. Since we were interested in the modulation of the strong sustained band-limited response, known to be produced by the dynamic grating stimuli (Hoogenboom et al., 2006; Muthukumaraswamy & Singh, 2013), gamma-band activity was defined accordingly as 50-74 Hz (Figure 20). We analyzed two time windows. The first one ranged from -500 to 650 ms according to the onset of the dynamic grating stimuli (called "post-endogenous epoch" in the following). The second analysis window ranged from 750 to 1250 ms according to the onset of the dynamic grating stimuli, or from 0 to 500 ms according to the onset of the exogenous spatial cues, respectively (called "post-exogenous epoch" in the following). All cluster-based permutation tests (Maris & Oostenveld, 2007) were run as implemented in the Fieldtrip toolbox.

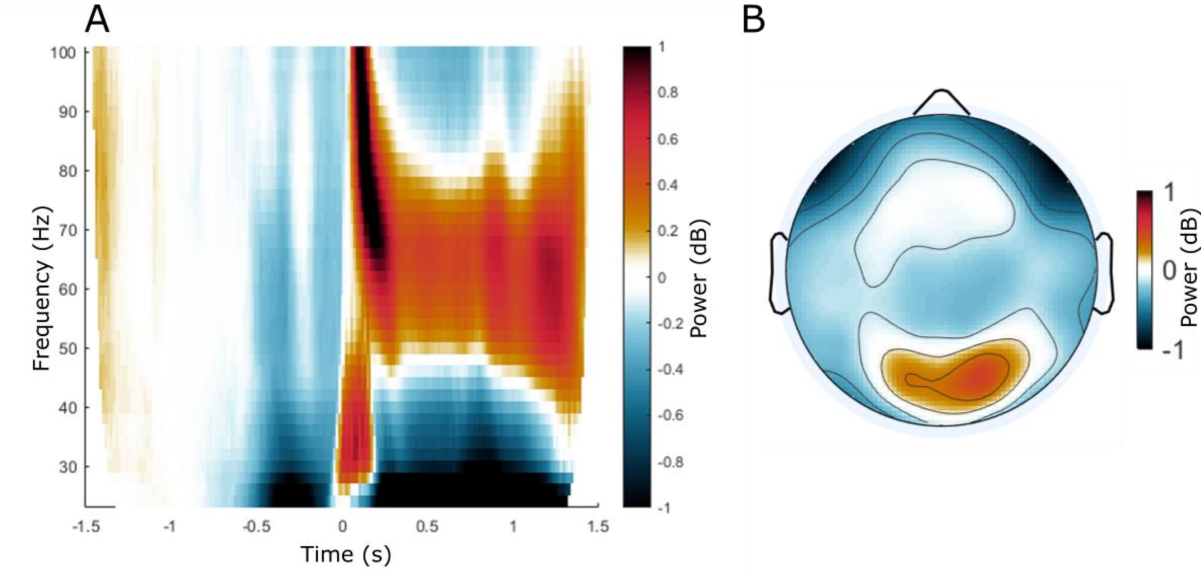

Figure 20. Grand average of the gamma reponse over all trials and the for neutral endogenous and neutral exogenous cueing condition. Time window for baseline correction: -1250 to 750 ms. (A) Time-frequency spectrum of the gamma response over all trials. Time zero is the onset of the dynamic grating stimuli. (B) Topographic representation of the grand average gamma reponse in the neutral endogenous and neutral exogenous cueing conditino between 50 to 74 Hz and 300 to 900 ms after the onset of the dynamic grating stimuli.

2.7.1 Determination of individual gamma-peak frequency

The band-limited gamma responses evoked by dynamic grating stimuli are highly varying across participants (Hoogenboom et al 2006, Swettenham et al. 2009). Since the frequency range of gamma-band activity overlaps widely with biological (e.g. muscle noise) and other artifacts (e.g. line noise), we identified individual gamma-peak frequencies to increase the signal-to-noise-ratio. To determine the individual gamma-peak frequency, spectral power values (24 to 100 Hz) were baselined to the average power per frequency from -1250 to -750 ms according to the onset of the dynamic stimuli. Subsequently, spectral power values were averaged over all trials and over an epoch ranging from 300 to 900 ms according to the onset of the dynamic grating stimuli. We selected this epoch, because it was free from the evoked immediate gamma response and comprised a clean period of the band-limited sustained gamma response. We deployed the find_peaks function implemented in MATLAB to detect local peaks in 13 occipital channels (Poz, Oz, Iz, PO4, O2, O10, PO8, PO10, PO3, O1, O9, PO7, PO9) between 40 to 90 Hz. Peaks were accepted for a minimum peak width of 2 Hz (estimated with the reference line positioned at one-half the peak height), a minimum peak prominence of 0.25 Hz and a minimum peak distance of 5 Hz. The individual gamma peak frequency and peak half-width per subject across the electrode cluster were defined as the average peak frequency and half-width of the detected peaks, respectively. Individual gamma power was calculated by averaging for each participant the power values at the gamma-peak frequency +/- one half-width across the 13 occipital channels.

2.7.2 Time-frequency comparisons

Since the sustained gamma response produced by the dynamic grating stimuli had no symmetrical topography but was stronger over the right hemisphere (see Figure 22B), we did not compare ipsi- versus contralateral, since remapping the electrode positions of one condition (swapping the data for left and right side electrodes) would have led to artificial differences. Thus, to remain consistent we compared left vs. right cueing conditions, not only for analysis of the gamma-band and individual gamma power but also for the alpha-band power. We analyzed alpha-band, gamma-band and individual gamma power in two time windows. The first ranged from -500 to 650 ms to the onset of the dynamic grating stimuli (called “post-endogenous epoch” in the following). The second analysis window was 500 ms long and started with the presentation of the target stimulus that is 50 ms after the offset of the exogenous cue and 1250 ms after the offset of the endogenous cue (called “post-exogenous epoch” in the following). For the post-exogenous epoch time point zero is the onset of the target stimulus. All cluster-based permutation tests (Maris & Oostenveld, 2007) were run as implemented in the Fieldtrip toolbox and included all scalp electrodes.

2.7.2.1 Post-endogenous epoch

Since in the post-endogenous epoch the exogenous attentional cues were not presented yet, oscillatory activity for the three endogenous cueing conditions (left, right and neutral) was averaged over the exogenous cueing conditions (congruent, incongruent, neutral).

2.7.2.1.1 Isolated effect of endogenous spatial cueing on task irrelevant stimulus processing

To investigate the effect of endogenous spatial attention on neural processing of task irrelevant stimuli, in the present study the dynamic grating stimuli, we compared alpha-band, gamma-band and individual gamma power in the leftward and rightward endogenous cueing conditions. One cluster-based permutation tests for each frequency range (alpha, gamma and individual gamma power) over the whole epoch and the whole electrode montage was run (left vs. right).

2.7.2.2 Post-exogenous epoch

For the analysis in the post-exogenous epoch, we first compared trials in which participants had to respond with trials in which they should not respond (non-target trials) with a cluster-based permutation test, separately for each frequency range of interest. If target and non-target trials were not significantly different, it would allow us to double the amount of data that could be included into the analysis.

2.7.2.2.1 Isolated effect of endogenous spatial cueing on target processing

To examine the effect of endogenous spatial attention on oscillatory activity, we compared alpha-band, gamma-band and individual gamma power for valid and invalid endogenously cued trials, separate for left and right presented targets. To exclude any effects due to directional exogenous cueing, only trials that presented neutral exogenous cues were analyzed. Two separate cluster-based permutation tests for each frequency range (alpha, gamma and individual gamma power) were run over the complete post-exogenous epoch and all channels.

2.7.2.2.2 Isolated effect of exogenous spatial cueing on target processing

To investigate the effect of exogenous spatial attention on oscillatory activity, we compared alpha-band, gamma-band and individual gamma power for congruent and incongruent exogenously cued trials, separate for left and right targets. To exclude possible effects due to directional endogenous cueing, we only analyzed trials that presented neutral endogenous cues. Two separate cluster-based permutation tests for each frequency range (alpha, gamma and individual gamma power) were run over the complete epoch and the whole electrode montage.

2.7.2.2.3 Effect of joint spatial endogenous and exogenous attentional shift

To investigate the effects of joint spatial endogenous and exogenous attentional shift, we compared conditions in which endogenous and exogenous cues directed attention to the identical visual field. We ran three separate cluster-based permutation test comparing left and right validly and congruently cued targets for alpha-band, gamma-band and gamma peak power. Three additional cluster-based permutation tests were run for the comparison of oscillatory activity for right and left targets that were cued invalidly and incongruently. To investigate possible differences (e.g. effects of reorientation of attention) we ran three additional cluster-based permutation tests to compare the difference for left vs. right target presentation in valid/congruent trials with the difference for right vs. left target presentation in invalid/incongruent trials.

2.7.3 Post-hoc cluster-based permutation test

To investigate whether gamma power was modulated by target presentation, we ran a post-hoc cluster-based permutation test over all frequencies and all channels over the whole epoch. We compared left target presentation with right target presentation, independent of the cueing condition. Subsequently, we extracted the gamma power values from possible significant clusters for each participant. With the obtained values, we ran a 3-way ANOVA with the factors side of target presentation (left/right), endogenous cueing (valid/invalid/neutral) and exogenous cueing (congruent/incongruent/neutral) to examine whether gamma power is modulated by endogenous and exogenous cueing.

2.7.4 Post-hoc analysis of the relation of behavioral and neural measurements

To relate the behavioral effects with the findings in the oscillatory activity, we ran three Pearson's correlations. We calculated the endogenous and exogenous behavioral effect separately, since the factors endogenous and exogenous cueing did not interact for the behavioral measurements. The endogenous behavioral effect was defined as the difference in reaction time for invalid and valid cued trials. The exogenous behavioral effect was defined as the difference in reaction time for incongruent and congruent cued trials. Positive values reflect that subjects reacted faster in valid/congruent trials, whereas negative values reflect that subjects were faster in the invalid/incongruent trials. We derived alpha and gamma power values for each participant from significant positive and negative clusters, respectively, in the post-endogenous epoch from the comparison of left vs. right endogenously cued trials to correlate those with the endogenous behavioral effect. In the post-exogenous epoch, we derived gamma power values from the positive cluster that resulted from the comparison of congruent vs. incongruent cued trials for right targets to correlate those with the exogenous behavioral effect.

2.8 ERP Analysis

ERP data were analyzed using the Fieldtrip toolbox (Oostenveld et al., 2011) and customized MATLAB scripts. As in the time-frequency analyses, we analyzed two time windows. The first ranged from 0 to 650 ms to the onset of the dynamic grating stimuli (called "post-endogenous epoch" in the following). The second analysis window ranged from 750 to 1250 ms according to the onset of the dynamic grating stimuli, or from 0 to 500 ms according to the onset of the exogenous spatial cues, respectively (called "post-exogenous epoch" in the following). For the post-exogenous time point zero is the onset of the target stimulus. All cluster-based permutation tests (Maris & Oostenveld, 2007) were run as implemented in the Fieldtrip toolbox and included all scalp electrodes. We defined positive and negative clusters according to the polarity of the difference waves.

2.8.1 Post-endogenous epoch

Since there was no exogenous cue presented yet, we averaged epochs according to the presentation of the endogenous cue, resulting in three conditions: left, right and neutral. Resulting epochs were baseline corrected to the average activity between -100 to 0 ms, according to the onset of the dynamic grating stimuli.

2.8.1.1 Isolated effect of endogenous spatial cueing on task irrelevant stimulus processing

In the first analysis window, we compared ERPs to left and right endogenous spatial cues to investigate whether endogenous attention modulates the processing of the task irrelevant dynamic grating stimuli spatially specific. Therefore we ran a cluster-based permutation tests over the 650 ms post-endogenous epoch (left vs. right).

2.8.2 Post-exogenous epoch

In this analysis window, epochs were baseline corrected to the average activity between -100 to 0 ms, according to the onset of target stimuli. Only trials to which participants should not respond were analyzed, which were free of manual responses, and thus, motor-related activity.

2.8.2.1 Isolated effect of endogenous spatial cueing on target processing

In the post-exogenous epoch, we compared valid and invalid endogenously cued trials separate for left and right target presentation, to examine the effect of spatial endogenous attention on target processing. To eliminate the effect of spatial exogenous attention only trials that presented neutral exogenous cues were analyzed. Two separate cluster-based permutation tests (left target: valid/neutral vs. invalid/neutral, right target: valid/neutral vs. invalid/ neutral) were run over the 500 ms epoch.

2.8.2.2 Isolated effect of exogenous spatial cueing on target processing

For the following analysis, we attempted to exclude the possibility that observed effects can be solely explained by the strong evoked response to the exogenous cues (bright blinking frames around the dynamic grating stimuli). Therefore, we compared ERPs to left and right target presentation, separately for congruent and incongruent exogenously cued trials. Only trials that presented neutral endogenous cues were analyzed. Subsequently, to eliminate stimulus-driven activity due to the presentation of the exogenous spatial cues we compared these two difference ERPs. The congruency effect was defined as the following:

$$\begin{gathered}\textit{Congruency effect} = \\ (\textit{ERP}(\textit{neutral/congruent left}) - \textit{ERP}(\textit{neutral/congruent right})) - \\ (\textit{ERP}(\textit{neutral/incongruent left}) - \textit{ERP}(\textit{neutral/incongruent right}))\ (6)\end{gathered}$$

Possible effects cannot be solely attributed to stimulus-driven activity evoked by the exogenous cues, but comprise exogenous attentional effects and effects due to attentional reorienting.

2.8.2.3. Effect of joint spatial endogenous and exogenous spatial attention

In this analysis, we had to tackle the same problem that the exogenous spatial cues evoked strong ERPs. We used the same approach. First, we compared ERPs to left and right non-targets, separately for valid/congruent and invalid/incongruent trials. Subsequently, we compared the difference ERPs to exclude stimulus-driven activity evoked by the exogenous spatial cues. The effect of joint attentional cues was defined as the following:

Joint effect =

(ERP(valid/congruent left) – ERP(valid/congruent right)) – (ERP(invalid/incongruent left) – (ERP(invalid/incongruent right)) (7)

Thereby, possible effects cannot be fully explained by stimulus-driven activity evoked by the spatial exogenous cues, but encompass endogenous and exogenous attentional effects, as well as attentional reorienting.

2.8.2.4 Difference in reorienting

To examine whether ERPs to target presentation differ if only exogenous attention or exogenous and endogenous attention is jointly directed to different sides, we compared the *Congruency* and the *Joint effect*. Difference in reorienting was defined as the following:

Difference reorienting = Congruency effect – Joint effect (8)

Possible difference can be attributed to the difference between neural processing when solely exogenous attention is directed or exogenous and endogenous jointly.

3. Results

3.1 Behavioral results

We analyzed reaction time in milliseconds, proportion of correct answers and d-prime (d') scores to investigate whether the spatial endogenous and the spatial exogenous attention modulated target processing.

3.1.1 Reaction Time

Running a two-way ANOVA with the factors endogenous and exogenous cueing revealed significant effects of both main factors (Figure 21; endogenous cueing: $F(2,68) = 15.20$, $p < .001$; exogenous cueing: $F(2,68) = 32.81$, $p < .001$) but no significant interaction ($F(4,136) = 0.97$, $p = .427$). Planned post-hoc pairwise comparisons revealed that for endogenous cueing participants were faster in the valid ($t(34) = 6.44$, $p < .001$) and neutral ($t(34) = 6.28$, $p < .001$) compared to the invalid condition (Table 4). Reaction times did not differ for the valid and the neutral condition ($t(34) = 0.62$, $p = .54$). For exogenous cueing, planned post-hoc pairwise comparison showed that participants were faster when exogenous cues were valid, compared to invalid ($t(34) = 10.63$, $p < .001$) and neutral cues ($t(34) = 6.85$, $p < .001$). Furthermore, reaction times were faster for neutral compared to invalid cues ($t(34) = 3.23$, $p = .003$).

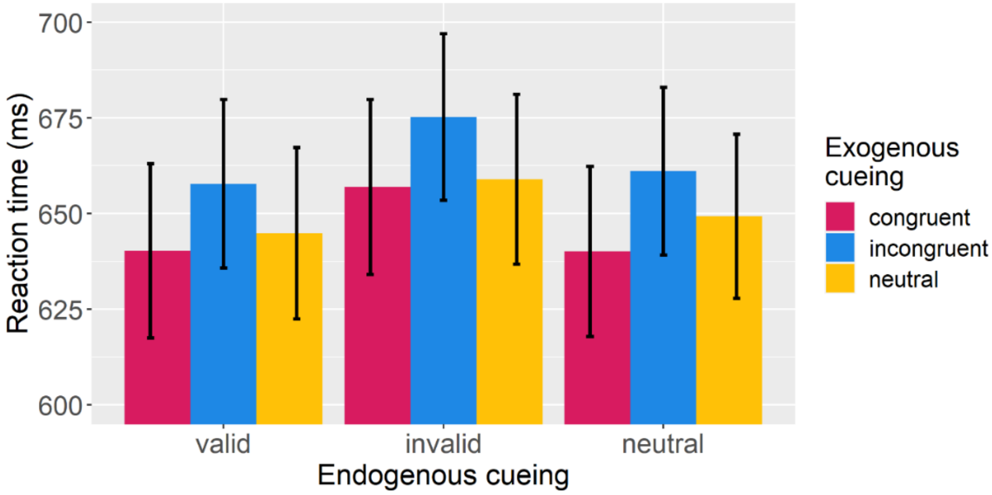

Figure 21. Mean response times in each condition. Error bars represent the standard error

Table 4

Mean reaction times and standard deviations for all conditions

		Endogenous cueing					
		Valid		*Invalid*		*Neutral*	
		M	*SD*	*M*	*SD*	*M*	*SD*
Exogenous cueing	*Congruent*	*640*	*135*	*657*	*135*	*640*	*132*
	Incongruent	*658*	*130*	*675*	*129*	*661*	*130*
	Neutral	*645*	*132*	*659*	*131*	*649*	*127*

3.1.2 Percentage correct

A two-way ANOVA with the factors validity of endogenous and congruency of exogenous cues showed significant effects of both main factors (Figure 22, endogenous cueing: *F*(2,68) = 5.78, *p* = .004; exogenous cueing: *F*(2,68) = 3.30, *p* = .043). The interaction of both factors was not significant (*F*(4,136) = 2.12, *p* = .082). Planned post-hoc comparisons revealed that percentage of correct responses did not differ for valid and neutral endogenous cues (*t*(34) = 0.62, *p* = .194, Table 5). However, participants gave more correct responses for valid (*t*(34) = 6.44, *p* = .017) and neutral endogenous cues (*t*(34) = 6.28, *p* < .001) compared to invalid endogenous cues. For exogenous cueing, planned post-hoc comparisons showed that only for valid and invalid exogenous cues, the amount of correct responses did significantly differ (*t*(34) = 2.52, *p* = .017). Participants gave more correct responses for valid than for invalid exogenous cues. Percentage of correct responses for neutral exogenous cues were not different to valid (*t*(34) = 0.79, *p* = .434) as well as to invalid exogenous cues (*t*(34) = 1.90, *p* = .067).

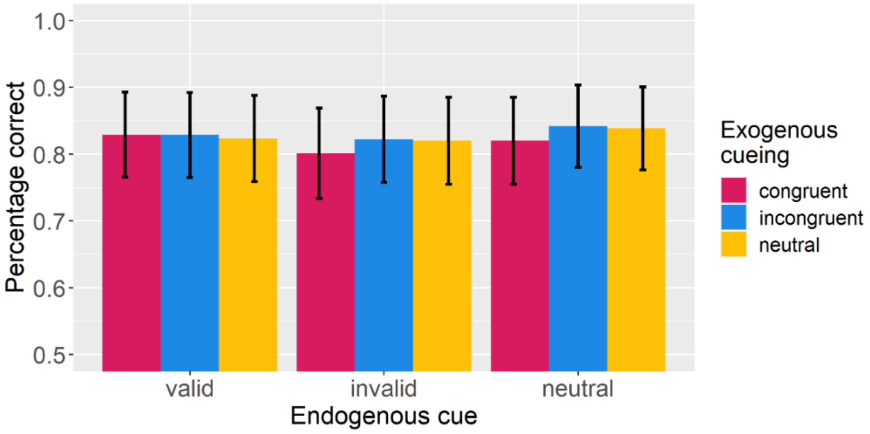

Figure 22. Mean percentage correct responses in each condition. Error bars represent the standard error.

Table 5

Mean percentage correct responses and standard deviations for all conditions

		Endogenous cueing					
		Valid		*Invalid*		*Neutral*	
		M	*SD*	*M*	*SD*	*M*	*SD*
Exogenous cueing	*Congruent*	*0.83*	*0.38*	*0.80*	*0.40*	*0.82*	*0.38*
	Incongruent	*0.83*	*0.38*	*0.82*	*0.38*	*0.84*	*0.36*
	Neutral	*0.82*	*0.38*	*0.82*	*0.38*	*0.84*	*0.37*

3.2 Time-frequency analysis

To investigate whether endogenous and exogenous spatial cueing modulates alpha (8 to 12 Hz), gamma (50 to 74 Hz) and individual gamma power, respectively, we analyzed alpha and gamma oscillatory activity in two different time windows. The first analyzed epoch ranged from -500 to 650 ms according to the onset of the dynamic grating stimuli. The window started at the offset of the endogenous cues. From -500 to 0 ms, only the fixation point was presented. Point zero is the onset of the dynamic grating stimuli (called 'post-endogenous epoch' in the following). During this period, only endogenous cueing affected neural activity, since the exogenous cues were not presented yet. The second window started with the onset of the target stimuli, that is 1250 ms after the onset of the endogenous cue and 100 ms after the onset of the exogenous cue, respectively (called 'post-exogenous epoch' in the following). During this second time window, we were able to investigate the isolated effects of endogenous and exogenous cueing by analyzing the trials in which exogenous or endogenous cues were neutral, respectively. Furthermore, we were able to investigate the combined effects of endogenous and exogenous cueing, since both cue types were presented.

3.2.1 Individual gamma peak frequency

Induced and evoked gamma responses to dynamic visual stimuli are highly varying in frequency across subjects (Hoogenboom et al 2006, Swettenham et al. 2009). To reach a better signal to noise ratio, we first defined individual gamma peak frequencies. Afterwards, we investigated the effect of endogenous and exogenous cueing on individual gamma frequency power. For 23 out of 35 subjects, an individual gamma peak was detected (Figure 23). Average peak frequency was 64.43 Hz (*SD* = 5.96) and average half-peak width was 11.57 Hz (*SD* = 2.02). The following analyses of gamma power at the individual peak frequency comprised the datasets of those 23 participants. We calculated individual gamma power as the average power at their individual gamma peak frequency +/- a half-peak width.

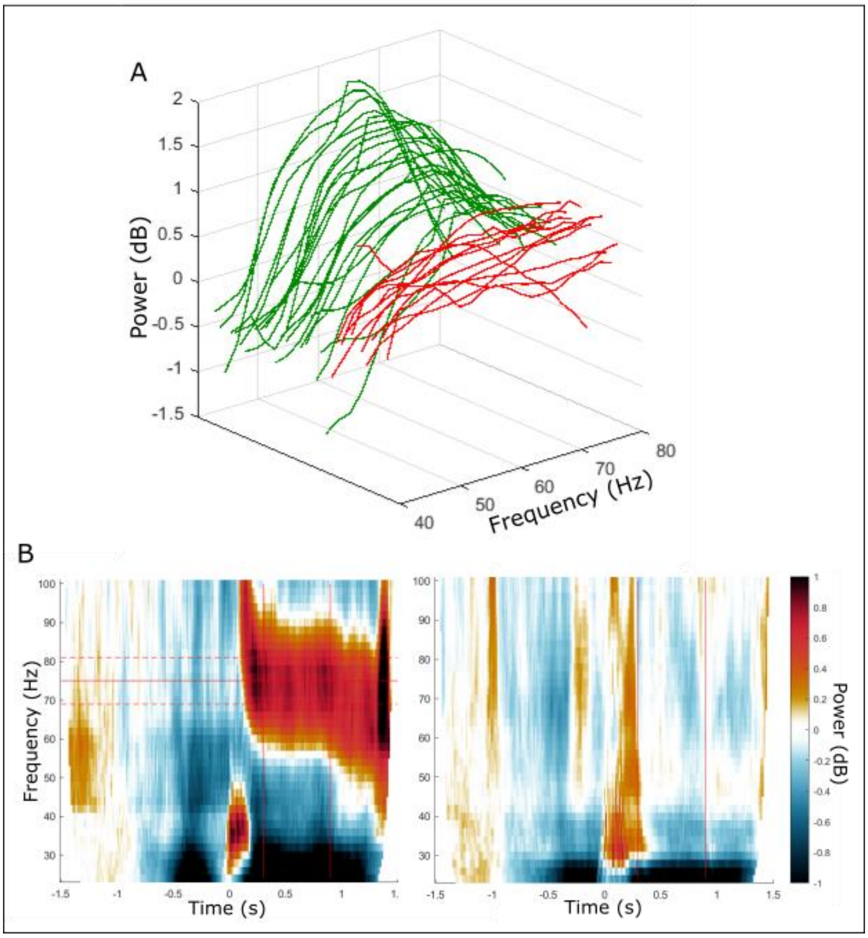

Figure 23. Gamma-peak frequency estimation. (A) Each line represents the average power spectrum of one participant. Power values were averaged over a time period from 300 to 900 ms after the onset of the dynamic grating stimuli and over 13 occipital channels. For 23 (green) participants a gamma peak was detected. For the remaining 12 (red) no peak was detected. (B) Time-frequency spectra examples for one participant for who a gamma peak was obtained (left) and for one for who no peak was obtained (right). Time zero is the onset of the dynamic grating stimuli. Red vertical lines show the time window over which power values were averaged. The red horizontal line marks the estimated individual gamma peak frequency. The red dashed lines mark the individual peak frequency +/- one individual one-half the peak width.

3.2.2 Post-endogenous epoch

To investigate the isolated effect of endogenous spatial cueing, we first analyzed a time window in which only endogenous cues were presented. If alpha oscillatory activity subserves top-down communication, we would expect that alpha power would decrease contralateral and increase ipsilateral to the attended side. Furthermore, if alpha lateralization is controlling gamma lateralization, we would expect that gamma power will be modulated in the opposite direction, that is increasing contralateral and decreasing ipsilateral to the attended side

3.2.2.1 Alpha power decreased contralateral to the endogenously cued side

To investigate whether endogenous spatial cues modulate alpha power in a spatially specific manner, we compared alpha power for left and right endogenous cues. For the comparison of left and right endogenous cued trials, alpha power showed a stronger decrease that is first visible as a positivity over central, and then posterior regions, over the left hemisphere (indicating a relative decrease in alpha power contralateral to the attended side), to then progress also to the right hemisphere. This effect started around -160 and ended after approximately 520 ms (positive cluster: from -165 to 360 ms, p = .022, Figure 24A and C) according to the onset of the dynamic stimuli.

3.2.2.2 Gamma power increased contralateral to the endogenously cued side

To investigate whether the effect of endogenous cueing on gamma power modulation is spatially specific, we compared gamma power for left and right endogenously cued trials. Gamma power increased for right cued trials over posterior regions, that was visible first as a negativity over the left hemisphere (indicating a relative increase in gamma power contralateral to the attended side), to then progress also over the right hemisphere. This effect started around -100 ms and ended after 220 ms (negative cluster: from -105 to 120 ms, p = .024, Figure 24B and D) according to the onset of the dynamic stimuli.

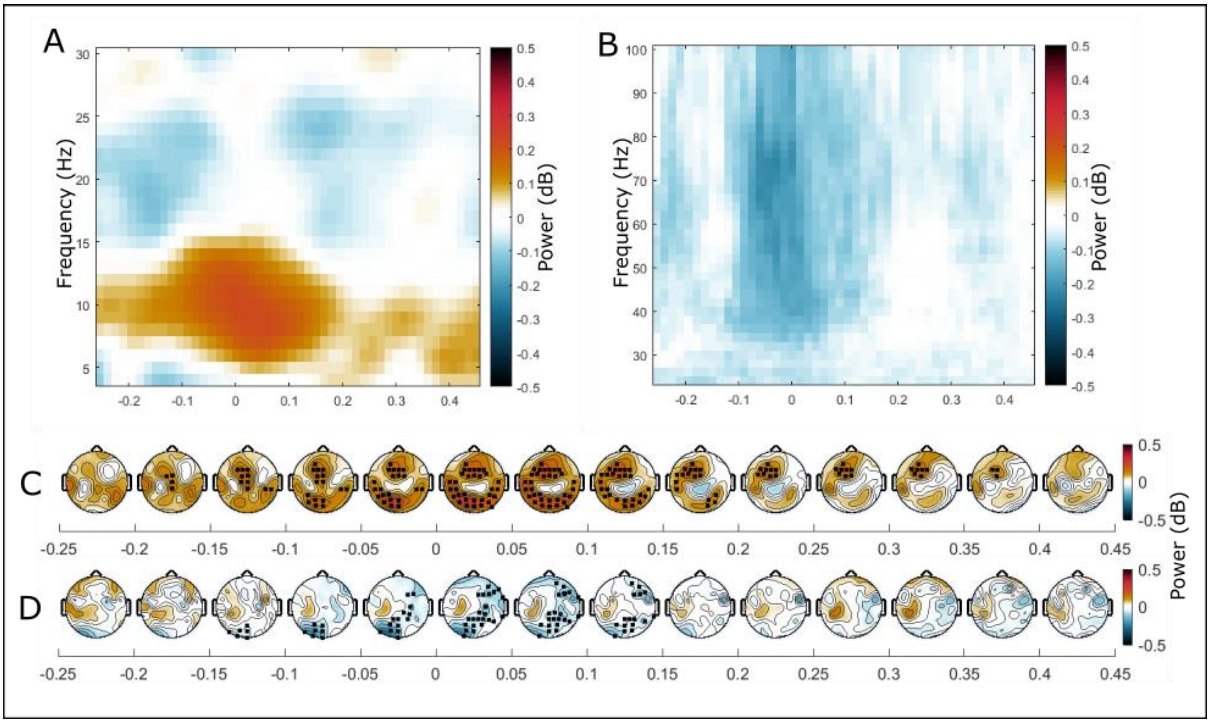

Figure 24. Effect of endogenous spatial cueing on alpha-band (8 to 12 Hz) and gamma-band (50 to 74 Hz) power. Time zero is the onset of the dynamic grating stimuli occurring 500 ms after endogenous cue appearance. (A) Time frequency chart of the change in alpha power averaged over seven posterior electrodes (POz, PO3, Oz, O1, Iz, O9, PO9). Displayed is the difference left minus right endogenous cueing condition. Power is displayed in dB values with respect to a baseline period between –1.25 to -0.75 s before the onset of the dynamic grating stimuli. (B) Time frequency chart of the change in gamma power averaged over seven posterior electrodes (POz, PO3, Oz, O1, Iz, O9, PO9). Displayed is the difference left minus right endogenous cueing condition. Power is displayed in dB values with respect to a baseline period between –1.25 to -0.75 s before the onset of the dynamic grating stimuli. (C, D) Stars in the topographies indicate electrodes that survived tests for multiple comparisons (p < .05). (C) Average EEG topographies of alpha power across participants of the effect of left vs. right endogenous cueing condition. (D) Average EEG topographies of gamma power across participants of the effect of left vs. right endogenous cueing condition.

3.2.2.3 Individual gamma peak frequency was not modulated by endogenous attention

The comparison between left and right endogenous cues (first positive cluster: $p = .657$, first negative cluster: $p = .072$) showed no significant difference gamma power at the individual gamma peak frequency (Figure 25).

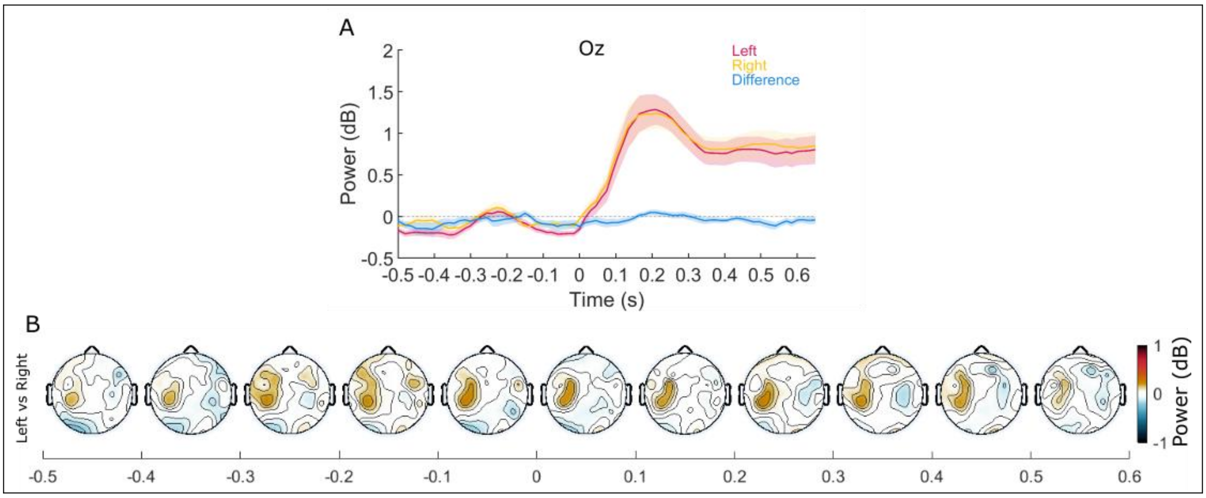

Figure 25. Effect of endogenous spatial cueing on individual gamma power. Time zero is the onset of the dynamic grating stimuli occurring 500 ms after endogenous cue appearance. (A) Grand-averaged of individual gamma power over time to left (red) and right (yellow) endogenous cues, and the difference left minus right (blue) endogenous cueing condition at electrode Oz. Power is displayed in dB values with respect to a baseline period between –1.25 to -0.75 s before the onset of the dynamic grating stimuli. Error bands represent the standard error of the mean. (B) Average EEG topographies of individual gamma power across participants of the effect of left vs. right endogenous cueing condition.

3.2.3 Post-exogenous epoch

To investigate the effect of endogenous and the effect of exogenous cueing in isolation, as well as their interaction on alpha and gamma oscillations, we analyzed a second epoch. This epoch ranged from 0 to 500 ms according to the onset of the target stimulus (1250 ms after the offset of the endogenous cue and 50 ms after the offset of the exogenous cue). As for the post-endogenous epoch, we would expect that alpha power decreases contralateral and increases ispsilateral to the attended side. Furthermore, we would expect the opposite effect on gamma power, that is, increasing power contralateral and decreasing power ispilateral to the attended side.

3.2.3.1 Alpha and gamma power did not differ for target and non-target trials

Since, alpha power (no positive cluster was detected, first negative cluster: *p* = .063) and gamma power (first positive cluster: *p* = .059, first negative cluster: *p* = .355) were not significantly different for target and non-target trials (Figure B.1), we pooled target and non-target trials together (for a detailed description see: Methods).

3.2.3.2 Isolated effect of spatial endogenous attention on target processing

To investigate the isolated effect of spatial endogenous attention, only trials that presented neutral exogenous cues (both frames flashed) were included in the analysis to eliminate any potential effects of spatial exogenous attention.

3.2.3.2.1 Alpha power related to target processing was not modulated by endogenous attention

To examine the effect of the spatial endogenous attention, we compared valid and invalid endogenous cues separately for left and right targets. If alpha power lateralization indicates top-down spatial orienting, we would expect stronger alpha modulation in valid compared to invalid trials. However, alpha power was not significantly different for valid compared to invalid endogenously cued trials, neither for left (first positive cluster: $p = .568$, no negative cluster was detected, Figure 26A) nor for right targets (no positive cluster was detected, first negative cluster: $p = .052$, Figure 26B)

3.2.3.2.2 Gamma power related to target processing was also not modulated by endogenous attention

In line with the results in the alpha-band, we found no significant differences in gamma power when comparing valid and invalid endogenously cued trials either for left (first positive cluster: $p = .519$, first negative cluster: $p = .514$, Figure 27A) or for right targets (first positive cluster: $p = .111$, no negative cluster was detected, Figure 27B).

3.2.3.2.3 Individual gamma peak frequency related to target processing was not modulated by endogenous attention

Similar to the analysis of gamma range (54 to 70 Hz), we found no significant difference when comparing valid and invalid endogenously cued trials, neither for left (first positive cluster: $p = .456$, first negative cluster: $p = .672$, Figure 28A and C) nor for right targets (first positive cluster: $p = .370$, first negative cluster: $p = .673$, Figure 28B and D).

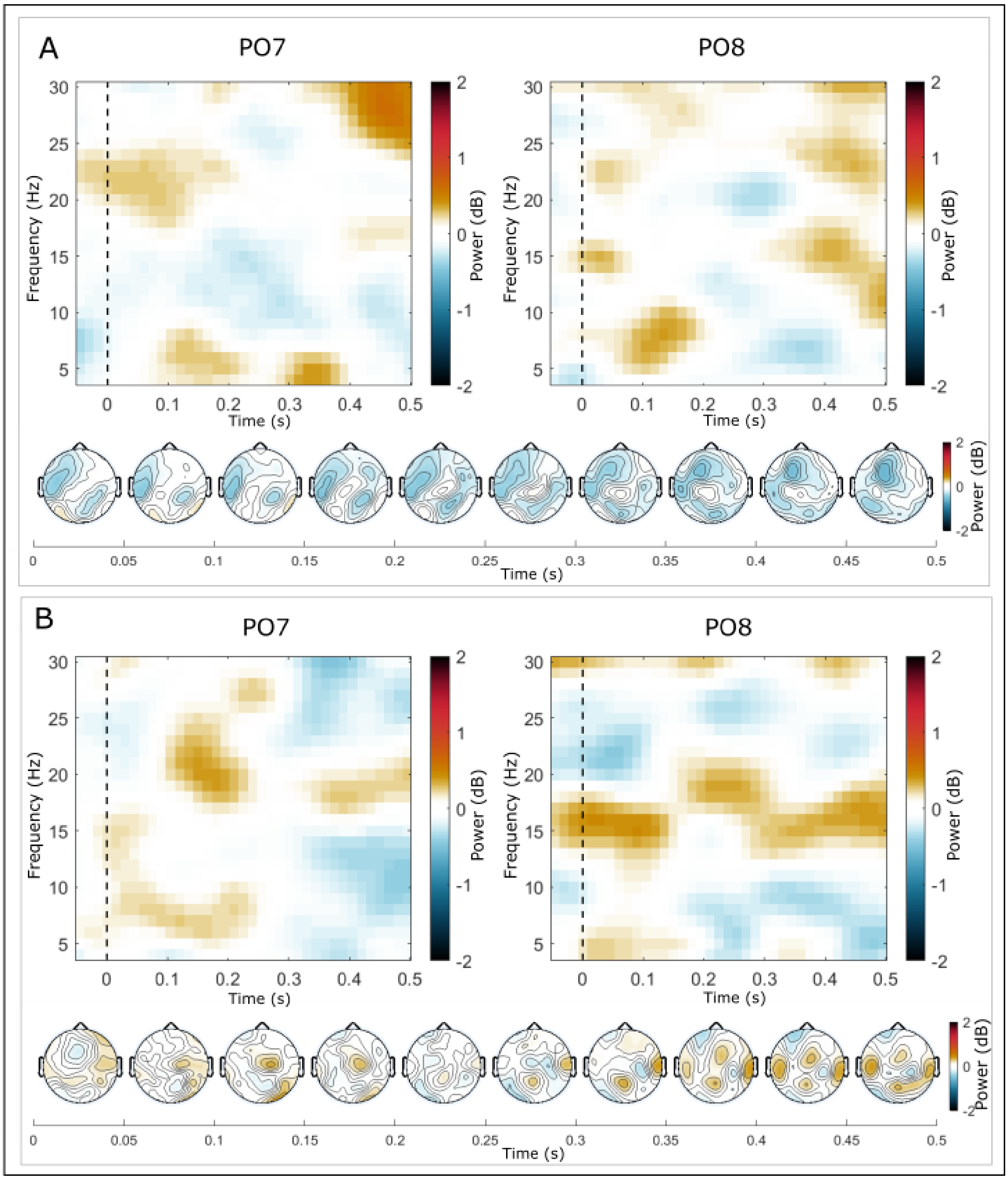

Figure 26. Effect of endogenous spatial cueing on alpha-band (8 to 12 Hz) power during left and right target processing. Time point zero represents the onset of the target. (A) Results for left target presentation. First row: Time frequency charts of the change in alpha power at electrode PO7 (left) and PO8 (right). Displayed is the difference valid minus invalid endogenous cueing condition. Power is displayed in dB values with respect to a baseline period between –1.25 to -0.75 s before the onset of the dynamic grating stimuli. Second row: Average EEG topographies of alpha power across participants of the effect of valid vs. invalid endogenous cueing condition. (B) Results for right target presentation. First row: Time frequency chart of the change in alpha power at electrode PO7 (left) and PO8 (right). Displayed is the difference valid minus invalid endogenous cueing condition. Power is displayed in dB values with respect to a baseline period between –1.25 to -0.75 s before the onset of the dynamic grating stimuli. Second row: Average EEG topographies of alpha power across participants of the effect of valid vs. invalid endogenous cueing condition.

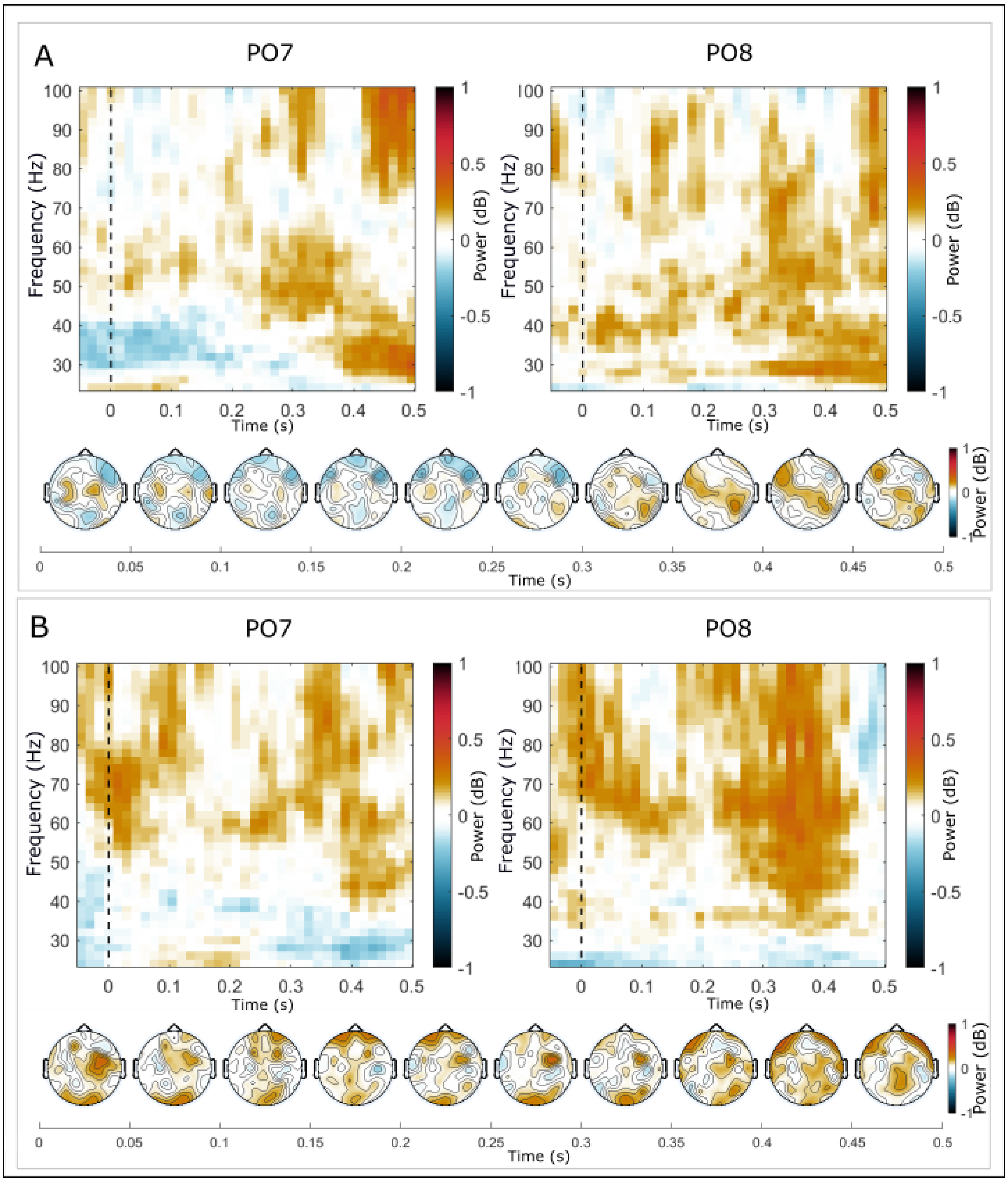

Figure 27. Effect of endogenous spatial cueing on gamma-band (50 to 74 Hz) power during left and right target processing. Time point zero represents the onset of the target. (A) Results for left target presentation. First row: Time frequency chart s of the change in gamma power at electrode PO7 (left) and PO8 (right). Displayed is the difference valid minus invalid endogenous cueing condition. Power is displayed in dB values with respect to a baseline period between –1.25 to -0.75 s before the onset of the dynamic grating stimuli. Second row: Average EEG topographies of gamma power across participants of the effect of valid vs. invalid endogenous cueing condition. (B) Results for right target presentation. First row: Time frequency chart s of the change in gamma power at electrode PO7 (left) and PO8 (right). Displayed is the difference valid minus invalid endogenous cueing condition. Power is displayed in dB values with respect to a baseline period between –1.25 to -0.75 s before the onset of the dynamic grating stimuli. Second row: Average EEG topographies of gamma power across participants of the effect of valid vs. invalid endogenous cueing condition.

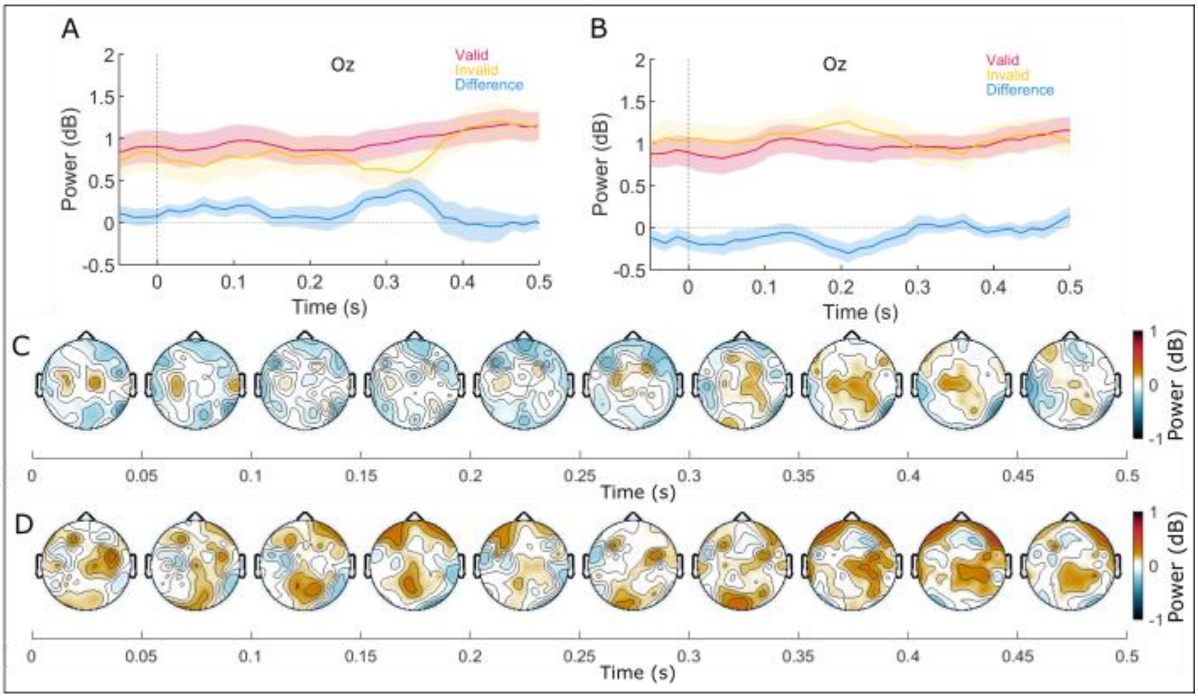

Figure 28. Effect of endogenous spatial cueing on individual gamma power during left and right target processing. Time point zero represents the onset of the target. (A,C) Results for left target presentation. (B,D) Results for right target presentation. (A) Grand-averages of individual gamma power over time during target processing on the left side for valid (red) and invalid (yellow) endogenous cues, and the difference valid minus invalid (blue) endogenous cueing condition at electrode Oz. Power is displayed in dB values with respect to a baseline period between –1.25 to -0.75 s before the onset of the dynamic grating stimuli. (B) Grand-averages of individual gamma power over time during target processing on the left side for valid (red) and invalid (yellow) endogenous cues, and the difference valid minus invalid (blue) endogenous cueing condition at electrode Oz. Power is displayed in dB values with respect to a baseline period between –1.25 to -0.75 s before the onset of the dynamic grating stimuli. (C) Average EEG topographies of individual gamma power across participants of the effect of valid vs. invalid endogenous cueing condition for left targets. (D) Average EEG topographies of individual gamma power across participants of the effect of valid vs. invalid endogenous cueing condition for right targets.

3.2.3.3 Isolated effect of spatial exogenous attention on target processing

To investigate the isolated effect of spatial exogenous attention, we analyzed only trials that presented neutral endogenous cues. We analyzed alpha, gamma and individual gamma-peak frequency power in a time window from 0 to 500 ms according to the onset of the target stimuli, that is, 50 ms after the offset of the exogenous cue.

3.2.3.3.1 Alpha power related to left target processing decreases contralateral to the attended side

We compared trials in which the exogenous cue was congruent with trials in which the exogenous cue was incongruent, to examine whether exogenous spatial cueing modulates alpha power, separately for left and right targets. For left targets, alpha power was significantly lower for congruent vs. incongruent exogenous cueing over posterior regions contralateral to the target, starting around 160 ms after the onset of the target stimuli, and lasting till the end of the analysis window (negative cluster: from 165 to 500 ms, *p* = .030, Figure 29A). For left targets, alpha power decreased contralateral to the attended side. However, for right targets, we found no significant difference (first positive cluster: *p* = .067, no negative cluster was detected, Figure 29B).

3.2.3.3.2 Gamma power related to right targets processing increases contralateral to the attended side

To investigate the effect of spatial exogenous attention on bottom-up communication, we compared gamma power for congruent and incongruent trials, separately for left and right targets. We found no significant cluster for left targets (first positive cluster: *p* = .362, no negative cluster was detected, Figure 30A). However, when comparing congruent and incongruent trials for right targets, we found a significant difference over posterior central regions starting at time point 0 ms, and lasting for approximately 240 ms (positive cluster: from 0 to 240 ms, *p* = .047, Figure 30B) according to the onset of the target. For targets presented on the right side, gamma power increased contralateral to the attended side.

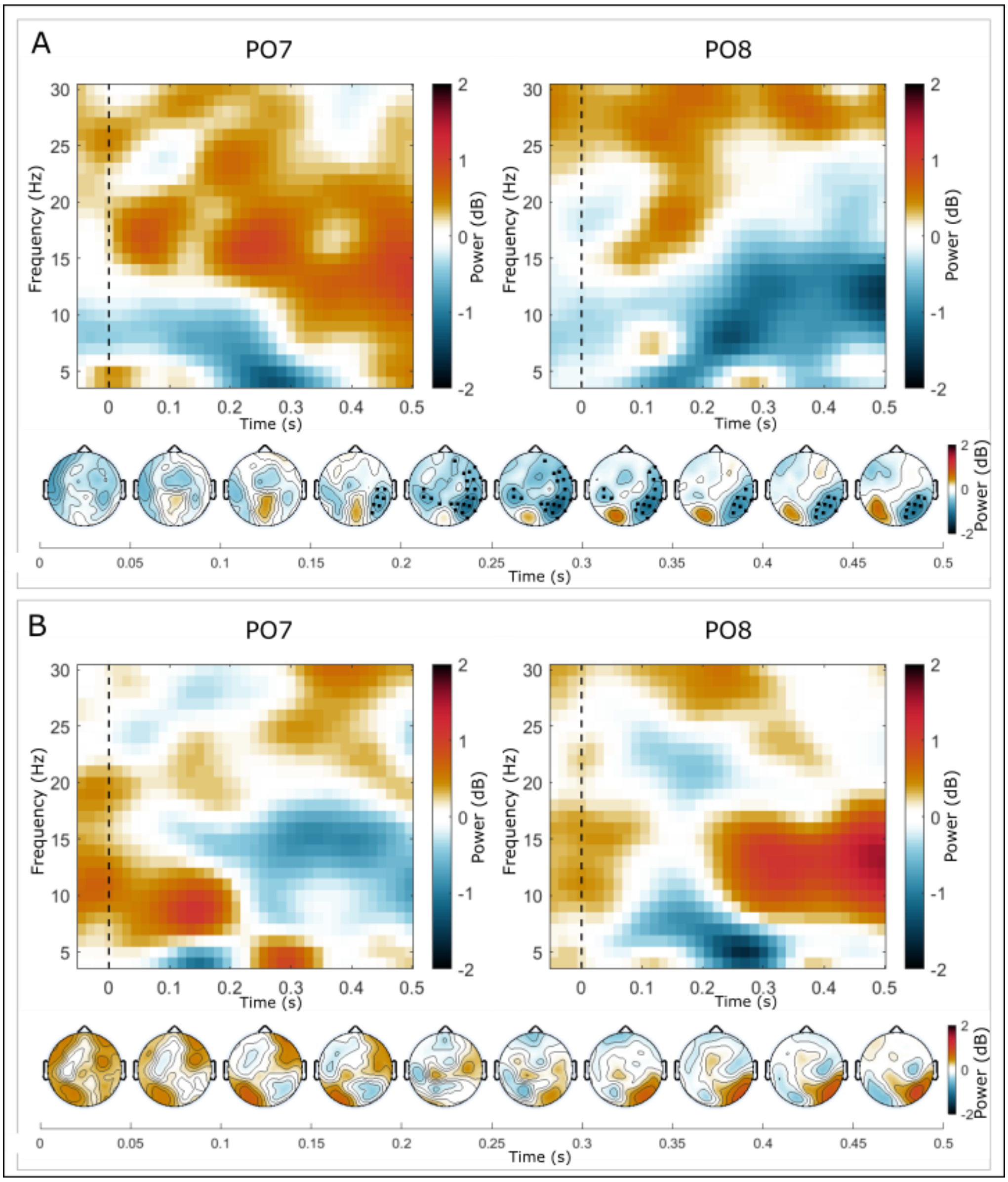

Figure 29. Effect of spatial exogenous cueing on alpha-band (8 to 12 Hz) power during left and right target processing. Time point zero represents the onset of the target. (A) Results for left target presentation. First row: Time frequency chart s of the change in alpha power at electrode PO7 (left) and PO8 (right). Displayed is the difference congruent minus incongruent exogenous cueing. Power is displayed in dB values with respect to a baseline period between –1.25 to -0.75 s before the onset of the dynamic grating stimuli. Second row: Average EEG topographies of alpha power across participants of the effect of congruent vs. incongruent exogenous cueing condition. Stars in the topographies indicate electrodes that survived tests for multiple comparisons (p < .05). (B) Results for right target presentation. First row: Time frequency chart s of the change in alpha power at electrode PO7 (left) and PO8 (right). Displayed is the difference congruent minus incongruent exogenous cueing condition. Power is displayed in dB values with respect to a baseline period between –1.25 to -0.75 s before the onset of the dynamic grating stimuli. Second row: Average EEG topographies of alpha power across participants of the effect of congruent vs. incongruent exogenous cueing condition. Stars in the topographies indicate electrodes that survived tests for multiple comparisons (p < .05).

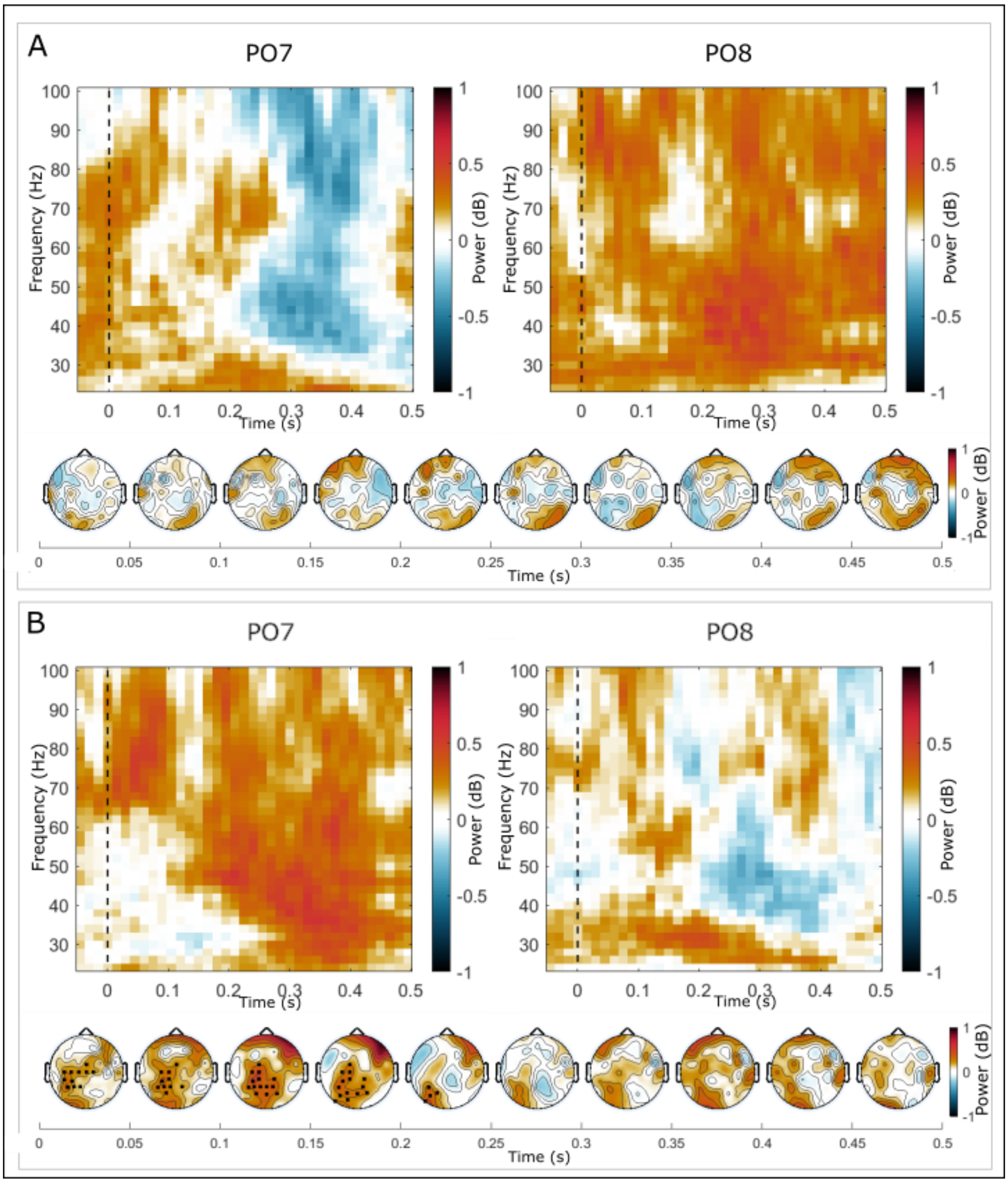

Figure 30. Effect of spatial exogenous cueing on gamma-band (50 to 74 Hz) power during left and right target processing. Time point zero represents the onset of the target. (A) Results for left target presentation. First row: Time frequency chart s of the change in gamma power at electrode PO7 (left) and PO8 (right). Displayed is the difference congruent minus incongruent exogenous cueing. Power is displayed in dB values with respect to a baseline period between –1.25 to -0.75 s before the onset of the dynamic grating stimuli. Second row: Average EEG topographies of gamma power across participants of the effect of congruent vs. incongruent exogenous cueing condition. Stars in the topographies indicate electrodes that survived tests for multiple comparisons (p < .05). (B) Results for right target presentation. First row: Time frequency chart s of the change in gamma power at electrode PO7 (left) and PO8 (right). Displayed is the difference congruent minus incongruent exogenous cueing condition. Power is displayed in dB values with respect to a baseline period between –1.25 to -0.75 s before the onset of the dynamic grating stimuli. Second row: Average EEG topographies of gamma power across participants of the effect of congruent vs. incongruent exogenous cueing condition. Stars in the topographies indicate electrodes that survived tests for multiple comparisons (p < .05).

3.2.3.3.3 Individual gamma peak power related to left target processing increased contralateral to the attended side

To examine the isolated effect of spatial exogenous attention on bottom-up communication, we compared individual gamma power for congruent and incongruent trials separately for left and right targets. For left targets, we found a significant cluster over posterior regions contralateral to the target, starting after around 240 ms after the onset of the target stimulus, and lasting for approximately 220 ms (positive cluster: from 240 to 465 ms, *p* = .027, Figure 31A and C). Gamma power increase contralateral to the attended side. However, we found no significant difference when comparing congruent and incongruent cueing for right targets (first positive cluster: *p* = .142, first negative cluster: *p* = .684, Figure 31B and D).

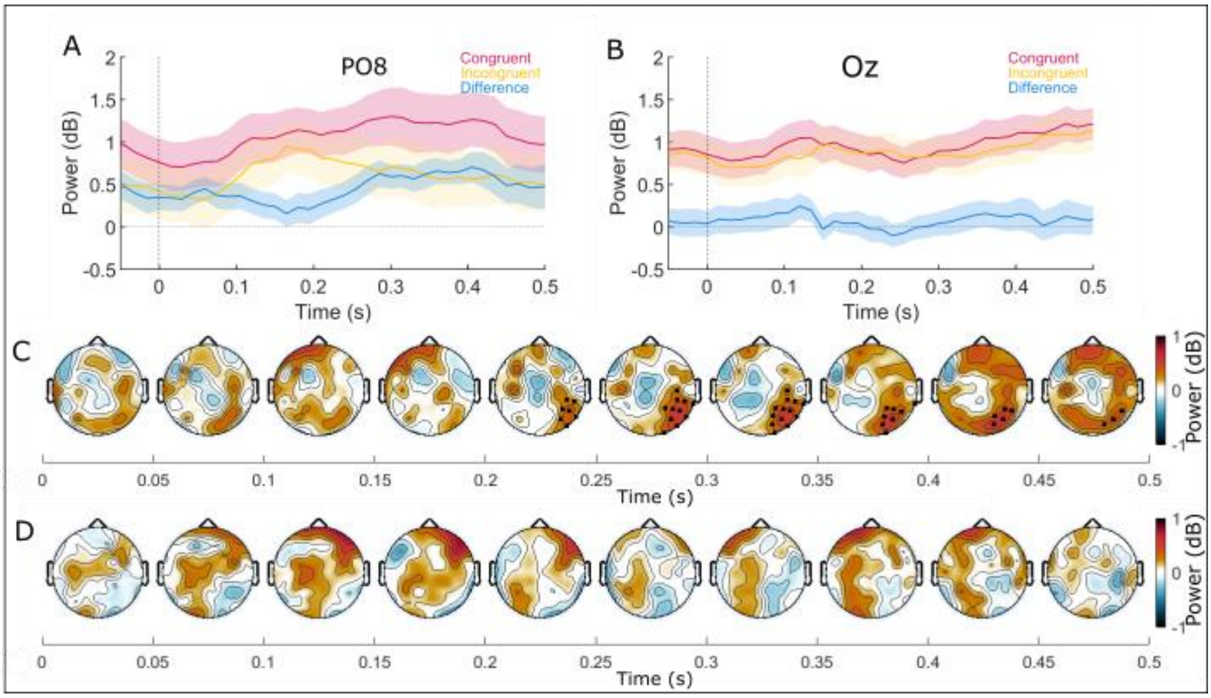

Figure 31. Effect of exogenous spatial cueing on individual gamma power during left and right target processing. Time point zero represents the onset of the target. (A,C) Results for left target presentation. (B,D) Results for right target presentation. (*Caption continues on following page*)

(*Continued from Figure 31 on preceding page)* (A) Grand-averages of individual gamma power over time during target processing on the left side for congruent (red) and incongruent (yellow) exogenous cues, and the difference congruent minus incongruent (blue) exogenous cueing condition at electrode PO8. Power is displayed in dB values with respect to a baseline period between –1.25 to -0.75 s before the onset of the dynamic grating stimuli. (B) Grand-averages of individual gamma power over time during target processing on the left side for congruent (red) and incongruent (yellow) endogenous cues, and the difference congruent minus incongruent (blue) exogenous cueing condition at electrode Oz. Power is displayed in dB values with respect to a baseline period between –1.25 to -0.75 s before the onset of the dynamic grating stimuli. (C) Average EEG topographies of individual gamma power across participants of the effect of congruent vs. incongruent exogenous cueing condition to left targets. Stars in the topographies indicate electrodes that survived tests for multiple comparisons (p < .05). (D) Average EEG topographies of individual gamma power across participants of the effect of congruent vs. incongruent endogenous cueing condition to right targets.

3.2.3.4 Effect of joint spatial endogenous and exogenous attentional shift

To investigate whether we find any effect of spatial orienting on neural oscillatory activity if the effects of endogenous and exogenous spatial orientation add up, we compared oscillatory activity to left and right target presentation in conditions in which the strongest spatial orientation difference was expected: Valid endogenously and congruent exogenously cued trials, and invalid endogenously and incongruent exogenously cued trials. If spatial orientation modulates alpha and gamma power, we would expect that the best combination would modulate oscillatory activity to a stronger degree than the worst combination.

3.2.3.4.1 Alpha modulation reflected redirection of attention

When comparing alpha power to valid/congruent (V/C) cued left and right target presentation, we found a significant negative cluster over the right posterior hemisphere starting around 150 ms after the onset of the target stimulus, and lasting till the end of the analysis window (negative cluster: from 150 to 500 ms, $p = .033$, Figure 32). When comparing invalid/incongruent (I/I) cued left and right targets, we found a significant positive cluster over the right posterior hemisphere, starting around 60 ms after the onset of the target stimulus, and lasting till the end of the analysis window (positive cluster: from 60 to 500 ms, $p = .012$). Over the epoch, the cluster changed topography, and was over the left posterior hemisphere at the end of the analysis window. When comparing these two differences to investigate whether V/C and I/I cueing conditions modulate alpha power differently, we found a negative cluster over the posterior right hemisphere, starting around 70 ms after the onset of the target stimulus, and lasting for approximately 200 ms (negative cluster: 75 to 285 ms, *p* = .030). It seemed like that during this period in the I/I combination, alpha power was stronger on the contralateral compared to the ipsilateral side, the opposite to the alpha lateralization of the V/C combination, fitting to the direction attention was shifted to. In the I/I combination, alpha lateralization changed to the opposite polarity, with decreased alpha power on the contralateral compared to the ipsilateral side.

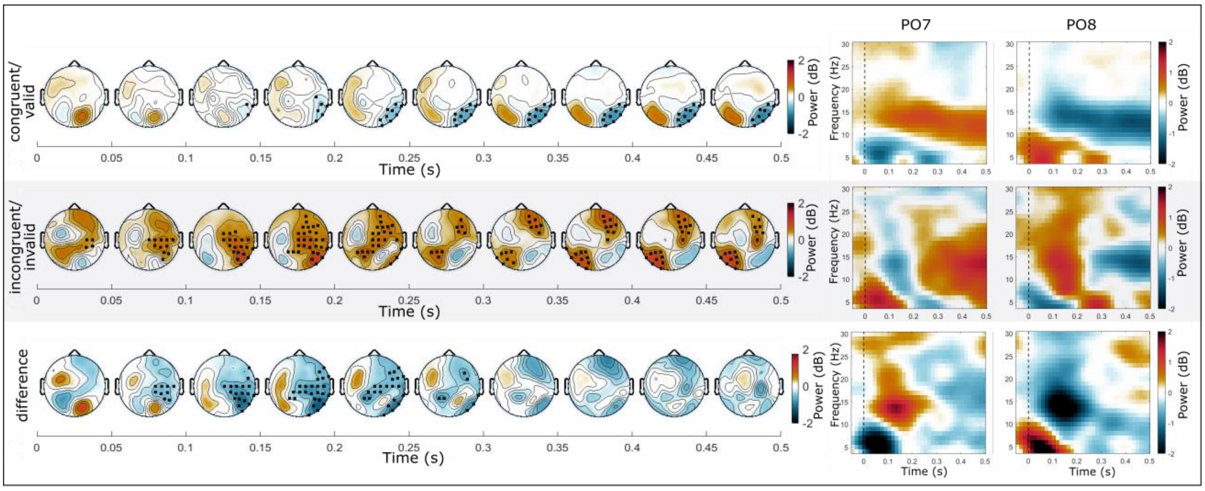

Figure 32. Effect of joint spatial endogenous and exogenous attentional shift on alpha-band (8 to 12 Hz) power. Time point zero represents the onset of the target. Time frequency charts of the change in alpha power at electrode PO7 (left) and PO8 (right). Power is displayed in dB values with respect to a baseline period between –1.25 to -0.75 s before the onset of the dynamic grating stimuli. Stars in the topographies indicate electrodes that survived tests for multiple comparisons (p < .05). First row: Average EEG topographies and time frequency charts of alpha power across participants of the effect of valid/congruent cueing condition. Displayed is the difference valid/congruent cued left target minis valid/congruent right target. Second row: Average EEG topographies and time frequency charts of alpha power across participants of the effect of invalid/incongruent cueing condition. Displayed is the difference invalid/incongruent cued right target minus invalid/incongruent left target. Third row: Average EEG topographies and time frequency charts of alpha power across participants of the effect of valid/congruent vs. invalid/incongruent cueing condition.

3.2.3.4.2 Gamma power is modulated by joint attentional shifts if attention is directed to the incorrect hemifield

We found no significant difference in gamma power for valid/congruent (V/C) cued left and right targets (first positive cluster: *p* = .360, first negative cluster: *p* = .126, Figure 33).

However, when comparing invalid/incongruent (I/I) cued left and right target, we found a significant positive cluster over the left frontal hemisphere, starting after around 10 ms after the onset of the target stimulus, and lasting for approximately 270 ms (positive cluster: from 15 to 285 ms, p = .030). However, comparing these two differences, we found no significant difference (no positive cluster was detected, first negative cluster: p = .095).

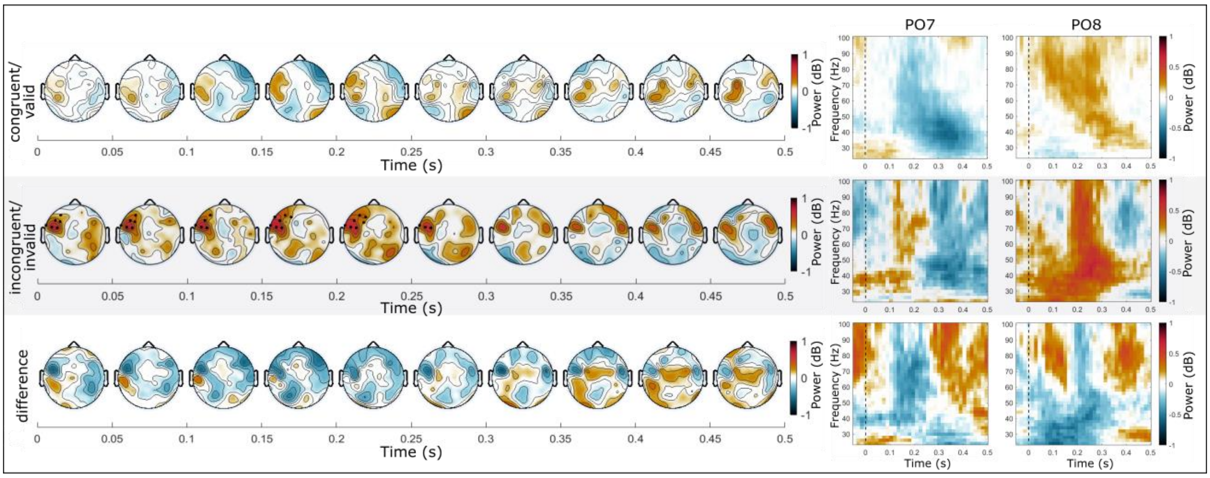

Figure 33. Effect of joint spatial endogenous and exogenous attentional shift on gamma-band (50 to 74 Hz) power. Time point zero represents the onset of the target. Time frequency charts of the change in gamma power at electrode PO7 (left) and PO8 (right). Power is displayed in dB values with respect to a baseline period between –1.25 to -0.75 s before the onset of the dynamic grating stimuli. Stars in the topographies indicate electrodes that survived tests for multiple comparisons (p < .05). First row: Average EEG topographies and time frequency charts of gamma power across participants of the effect of valid/congruent cueing condition. Displayed is the difference valid/congruent cued left target minis valid/congruent right target. Second row: Average EEG topographies and time frequency charts of gamma power across participants of the effect of invalid/incongruent cueing condition. Displayed is the difference invalid/incongruent cued right target minus invalid/incongruent left target. Third row: Average EEG topographies and time frequency charts of gamma power across participants of the effect of valid/congruent vs. invalid/incongruent cueing condition.

3.2.3.4.3 Individual gamma peak frequency is modulated by joint attentional shifts, if attention is directed to the correct hemifield

When comparing valid/congruent (V/C) trials for left and right targets, we found a significant negative cluster over the left posterior hemisphere, starting around 30 ms after the onset of the target stimulus, and lasting for approximately 360 ms (negative cluster: 30 to 390 ms, p = .018, Figure 34). However, when comparing left and right targets for invalid/incongruent (I/I) trials, we found no significant difference (first positive cluster:

p = .144, first negative cluster: *p* = .472). Furthermore, we found no significant difference when comparing the differences of V/C and I/I trials (first positive cluster: *p* = .543, first negative cluster: *p* = .233).

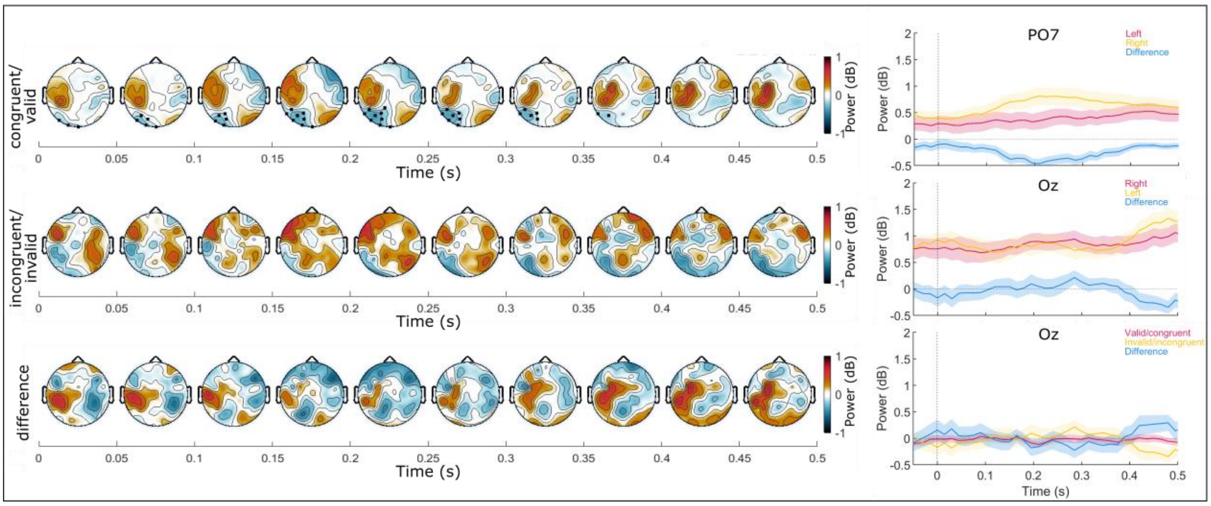

Figure 34. Effect of joint spatial endogenous and exogenous attentional shift on individual gamma power. Time point 750 ms represents the onset of the target. Grand-averages of individual gamma power change over time at electrode PO7 or Oz. Power is displayed in dB values with respect to a baseline period between –1.25 to -0.75 s before the onset of the dynamic grating stimuli. Stars in the topographies indicate electrodes that survived tests for multiple comparisons (p < .05). First row: Average EEG topographies and time frequency charts of individual gamma power across participants of the effect of valid/congruent cueing condition. Displayed is the difference valid/congruent cued left target minis valid/congruent right target. Second row: Average EEG topographies and time frequency charts of individual gamma power across participants of the effect of invalid/incongruent cueing condition. Displayed is the difference invalid/incongruent cued right target minus invalid/incongruent left target. Third row: Average EEG topographies and time frequency charts of individual gamma power across participants of the effect of valid/congruent vs. invalid/incongruent cueing condition.

3.3 Gamma power increases contralateral for congruent compared to incongruent exogenously cued targets

We conducted a post-hoc cluster-based permutation test over all electrodes and frequencies ranging from 30 to 90 Hz comparing left vs. right target trials. We found a significant cluster (Figure 35) starting around 180 after the onset of the target stimulus, and lasting for approximately 170 ms over the left hemisphere, ranging over the whole frequency range from 30 to 90 Hz (negative cluster: from 180 to 450 ms, *p* = .041). We derived the gamma power values from this cluster, and conducted a within-subjects 3-way ANOVA with the factors target side (left/right), endogenous cue (valid/invalid/neutral) and exogenous cue (congruent/incongruent/neutral) to investigate the effect of endogenous and exogenous attention on gamma power. There was a significant main effect of target (*F*(1,34) = 4.95, *p* = .033), an interaction of target and endogenous cueing (*F*(2,68) = 4.82, *p* = .011) and a three-way interaction of all three factors (*F*(4,136) = 3.61, *p* = .008, Figure 36). We calculated two separate ANOVAs for left and right target presentation to disentangle the effects. The ANOVA for left targets showed no significant effects (all *F*(4,136) < 1.81, all *p* > .131). However, for right targets, there was a significant main effect of endogenous cueing (*F*(2,68) = 5.41, *p* = .007) and a significant interaction (Greenhaus-Geiser corrected for sphericity: *F*(3.12,106.22) = 3.45, *p* = .018). To disentangle further the interaction effects, we conducted three additional ANOVAs with the factor exogenous cueing, one for each factor level of the factor endogenous cueing. There was no significant effect of exogenous cueing on gamma power for valid (*F*(2,68) = .047, *p* = .628) and invalid endogenous cues (*F*(2,68) = .97, *p* = .383). However, when comparing gamma power in the neutral endogenous cued trials, we observed a trend (*F*(2,68) = 3.06, *p* = .053). Post-hoc comparison using paired t-tests showed a trend (*t*(34) = 1.77, *p* = .085) that the mean gamma power in the incongruent condition (*M* = -0.13, *SD* = 0.84) was lower than in the congruent condition (*M* = 0.14, *SD* = 0.95). However, the neutral condition (*M* = 0.05, *SD* = 0.87) was not different from either the congruent (*t*(34) = 0.96, *p* = .343) or to the incongruent condition (*t*(34) = 0.96, *p* = .343).

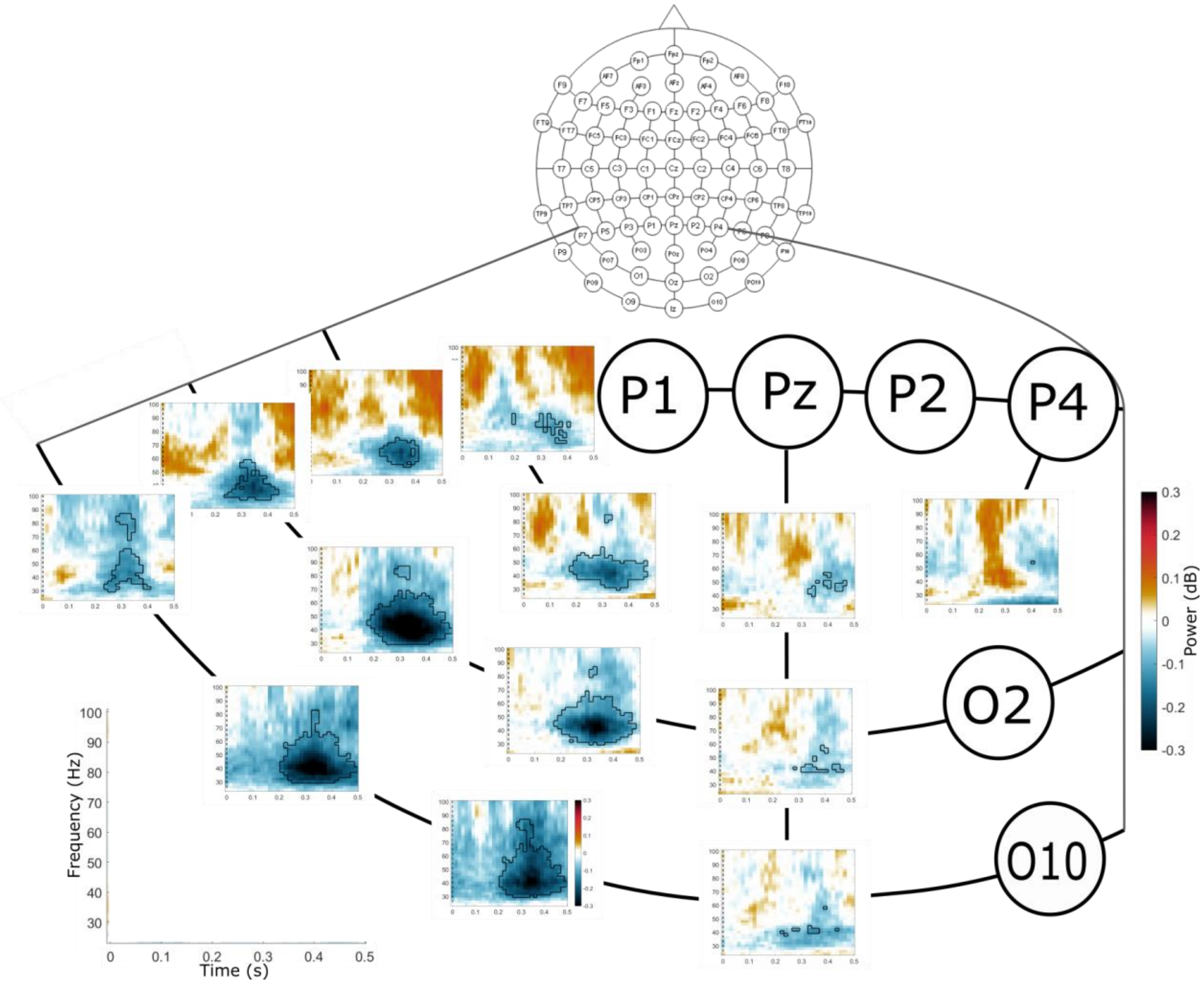

Figure 35. Effect of target side on gamma power. Time point zero represents the onset of the target. Time frequency charts of the change in gamma power at the electrodes, which were comprised in the negative cluster. Power is displayed in dB values with respect to a baseline period between –1.25 to -.75 s before the onset of the dynamic grating stimuli. Masks in the time frequency charts indicate time points and frequencies that survived tests for multiple comparisons (p < .05).

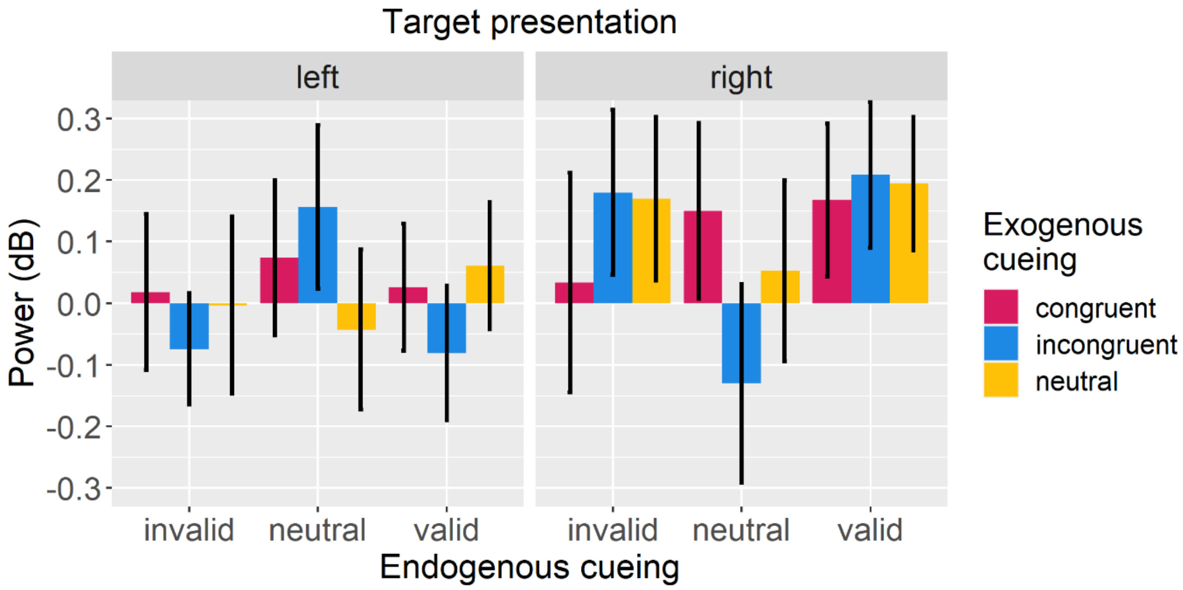

Figure 36. Grand-average gamma power for each condition and target side derived from the significant negative cluster over the left hemisphere. Error bars represent the standard error.

3.4 Relation of behavioral and neural measurements

To examine whether the neural effects are related to the behavioral ones, we correlated alpha and gamma power derived from significant clusters, respectively, with either the endogenous or the exogenous behavioral effect.

3.4.1 Alpha and gamma modulation is not related to the endogenous behavioral effect

First, we correlated the difference alpha power values derived from the significant positive cluster from the comparison of left and right endogenously cued trials in the post-endogenous epoch, described above in section *Alpha power decreased contralateral to the endogenously cued side* (Figure 24A). The observed negative correlation was not significant (*R*(33) = -.25, *p* = .14, Figure 37A). Furthermore, we correlated the difference values in gamma power derived from the significant negative cluster resulting from the same comparison in the post-endogenous epoch. The observed negative correlation was also not significant (*R*(33) = -.13, *p* = .46, Figure 37B).

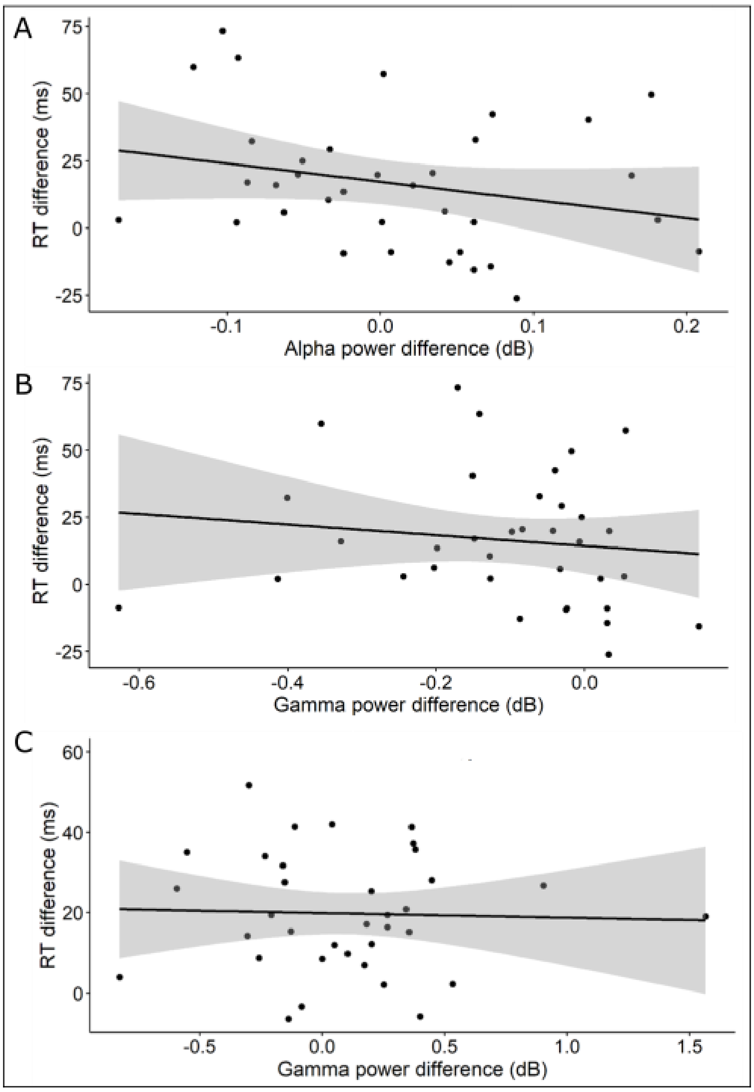

Figure 37. Correlations between behavioral and neural effects. (A) Interindividual differences in post-endogenous alpha-band (8 to 12 Hz) power did not correlate with the behaviorally observed endogenous effect (RT(valid trials) minus RT(invalid trials)). (B) Interindividual differences in post-endogenous gamma-band (50 to 74 Hz) power did not correlate with the behaviorally observed endogenous effect (RT(valid trials) minus RT(invalid trials)). (C) Interindividual differences in post-exogenous gamma-band (50 to 74 Hz) power did not correlate with the behaviorally observed exogenous effect (RT(congruent trials) minus RT(incongruent trials)).

3.4.2 Gamma power modulation is not related to the exogenous behavioral effect

We correlated the difference values in gamma power derived from the significant positive cluster when comparing isolated exogenous cueing effects for right targets with the exogenous behavioral effect described above in section *Gamma power related to right targets processing increases contralateral to the attended side* (Figure 30B). The observed negative correlation was not significant ($R(33) = .03$, $p = .85$, Figure 37C).

3.5 Event-related potentials

To investigate whether spatial endogenous and exogenous attention modulate neural activity during the anticipation and processing of target stimuli, we analyzed ERPs in two different time windows. The first analysis window encompassed the presentation of the dynamic grating stimuli after the presentation of the endogenous cue, but before the presentation of the exogenous cue (0 to 650 ms to the onset of the dynamic stimuli). Therefore, all identified ERP effects to the irrelevant dynamic stimuli during that period can be attributed exclusively to the effect of spatial endogenous cueing in anticipation of a target. The second analysis window started with the presentation of the target, and lasted for 500 ms (1250 ms after the offset of the endogenous and 50 ms after the offset of the exogenous cue). This period encompasses the effects of spatial endogenous as well as spatial exogenous attention on target processing, and possible interactions of both effects.

3.5.1 Post-endogenous epoch

To investigate whether directional endogenous spatial cues modulate neural processing spatially specifically, we contrasted ERPs to left and right cued trials. ERPs to left and right cued trials started to differ starting around 100 ms after stimulus onset (first positive cluster: 101 from to 188 ms, $p = .05$; second positive cluster: from 275 to 462 ms, $p = .016$; third positive cluster: from 494 to 650 ms, $p = .017$; negative cluster: from 106 to 650 ms, $p = .002$, Figure 38).

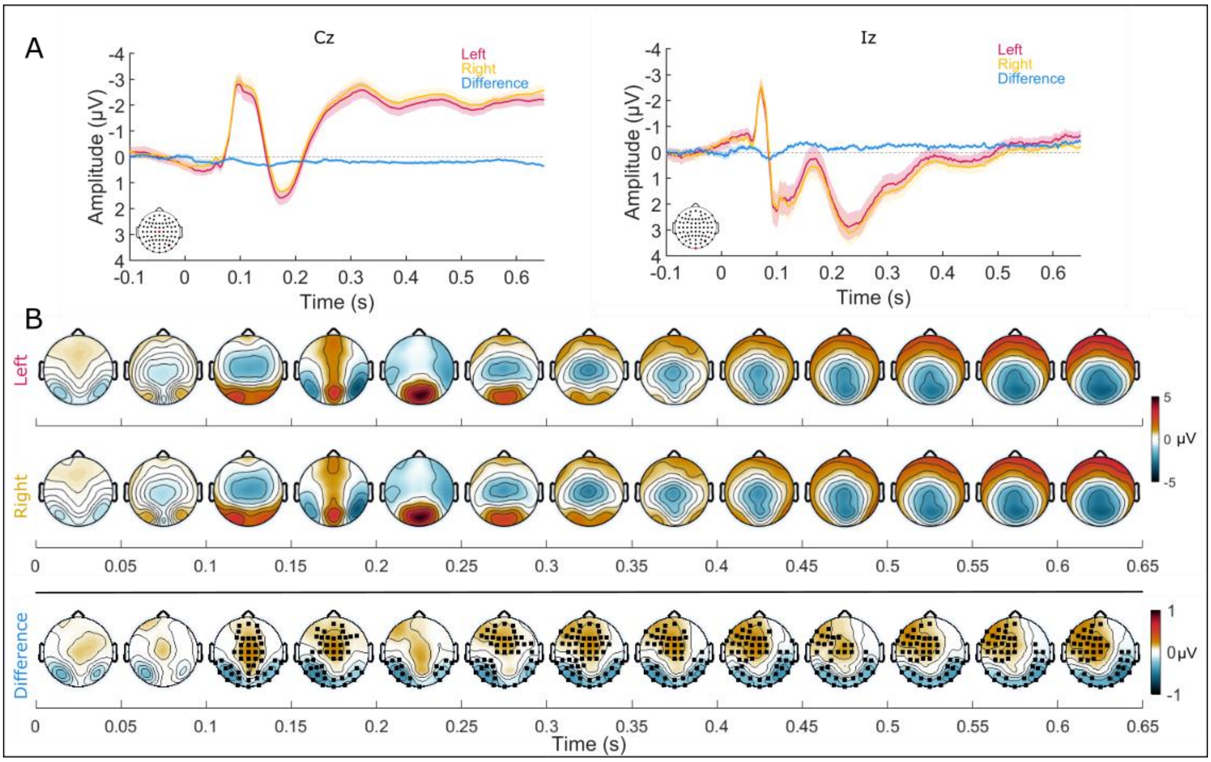

Figure 38. Grand averages of the ERPs for left and right endogenous cueing condition in the post-endogenous epoch. (A) ERPs to left (red), right (yellow) endogenous cues and the difference ERP (blue) derived by subtracting ERPs to right from ERPs to left endogenous cues at electrode Cz (left) and Iz (right) (see red marked electrodes in the schematic drawing of the electrode montage). Error bands represent the standard error of the mean. Time zero is the moment of the dynamic grating stimuli. (B) ERP topographies to left (first row) and right (second row) endogenous cues as well as the difference ERP (ERP(left) minus ERP(right); last row) for the post-endogenous epoch 0 to 650 ms in 50 ms steps. Dots on the ERP topography in the last row indicate electrodes that survived tests for multiple comparisons (p < .05).

3.5.2 Post-exogenous cue epoch

In order to investigate the effects of spatial endogenous and exogenous cues in isolation, and their interaction, on stimulus processing, we compared ERPs to different combinations of endogenous and exogenous spatial cues. Only trials in which non-targets were presented were included in the analysis.

3.5.2.1 Isolated effect of spatial endogenous attention

To investigate the effects of spatial endogenous attention on stimulus processing we compared ERPs to valid and invalid endogenously cued trials, separately for left and right targets. Only trials that presented neutral exogenous cues were included. Neither for left (first positive cluster: *p* = .066, first negative cluster: *p* = .060, Figure 39) nor for right targets (first positive cluster: *p* = .126, first negative cluster: *p* = .060, Figure B.2) showed a difference in ERPs when comparing validly and invalidly cued trials.

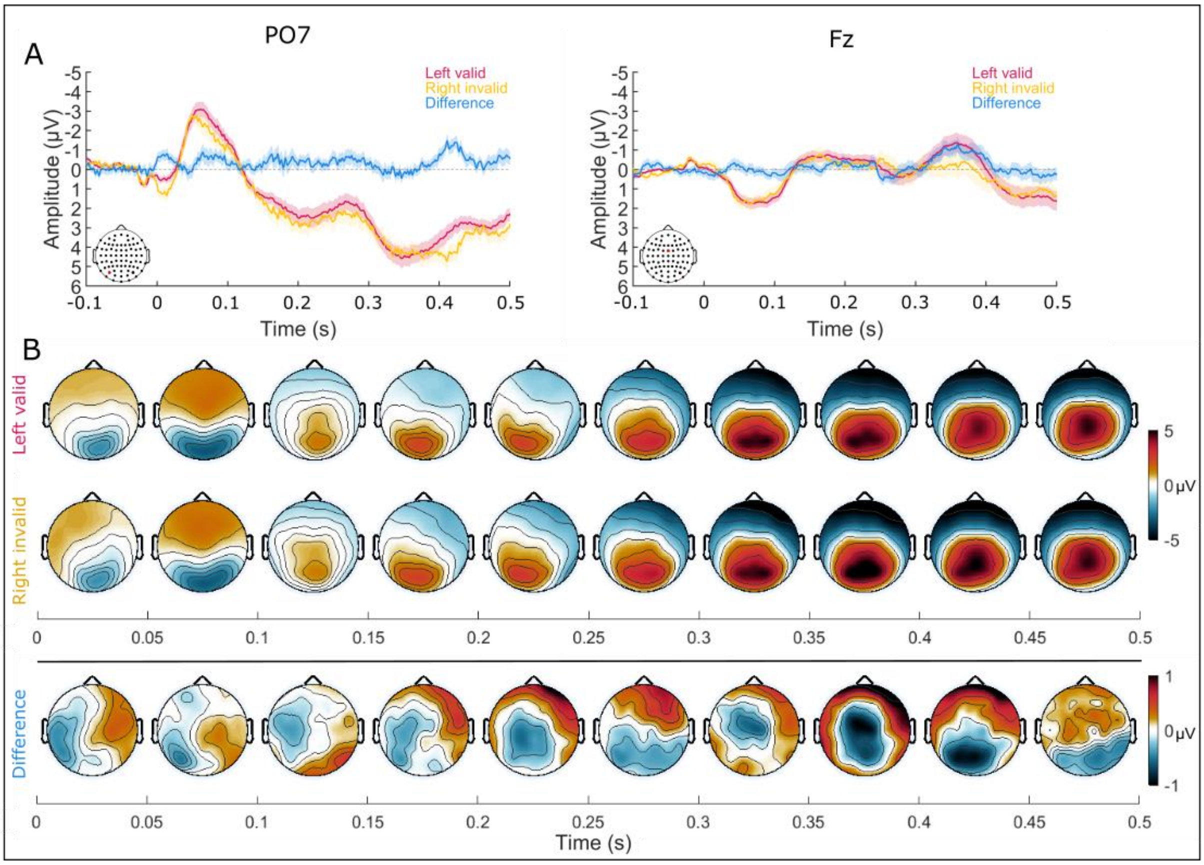

Figure 39. Grand averages of the ERPs for valid and invalid endogenously cued leftward targets. (A) ERPs to left valid (red), right invalid (yellow) endogenous cues and the difference ERP (blue) derived by subtracting ERPs to right invalid from ERPs to left valid endogenous cues at electrode PO7 (left) and Fz (right) (see red marked electrodes in the schematic drawing of the electrode montage). Error bands represent the standard error of the mean. At time point zero, the target stimulus was presented. (B) ERP topographies to left valid (first row) and right invalid (second row) endogenous cues as well as the difference ERP (ERP(left valid) minus ERP(right invalid); last row) for the post-exogenous epoch 0 to 500 ms in 50 ms steps. Dots on the ERP topography in the last row indicate electrodes that survived tests for multiple comparisons (p < .05).

3.5.2.2 Isolated effect of spatial exogenous attention

In order to investigate the effect of spatial exogenous attention, we compared ERPs to trials that presented congruent and incongruent exogenous cues, but only neutral endogenous cues. First, we compared ERPs for left and right targets that were congruently cued and for right and left targets that were incongruently cued. Afterwards, to eliminate stimulus-driven activity due to the presentation of the exogenous cues, we calculated the *Congruency effect* (Equation 1) by subtracted these two difference ERPs (for a detailed description see: Methods).

ERPs to trials that presented congruent exogenous cues to the left and the right started to differ directly with the onset of the target stimulus (first positive cluster: from 27 to146 ms, $p = .008$; second positive cluster: from 125 to 288 ms, $p < .001$; negative cluster: from 4 to 347 ms, $p < .001$, Figure 40) and showed a lateralized difference potential with a negative potential over the right hemisphere. Effects before the onset of the target are exclusively related to stimulus driven activity elicited by the frames flashing around the dynamic stimuli. Subsequently, ERPs to trials that presented incongruent exogenous cues to either the left or the right started to differ after around 20 ms after the onset of the target stimulus (first positive cluster: from 35 to 175 ms, $p < .001$; second positive cluster: from 184 to 405 ms, $p < .001$; first negative cluster: from 20 to 175 ms, $p < .001$; second negative cluster: from 183 to 389 ms, $p < .001$, Figure 41). At first, the difference potential was lateralized in the same direction as the congruent one, with a negative potential over the right hemisphere. Starting from approximately, 150 ms the lateralization switched in that way that the more negative potential was now over the left hemisphere.

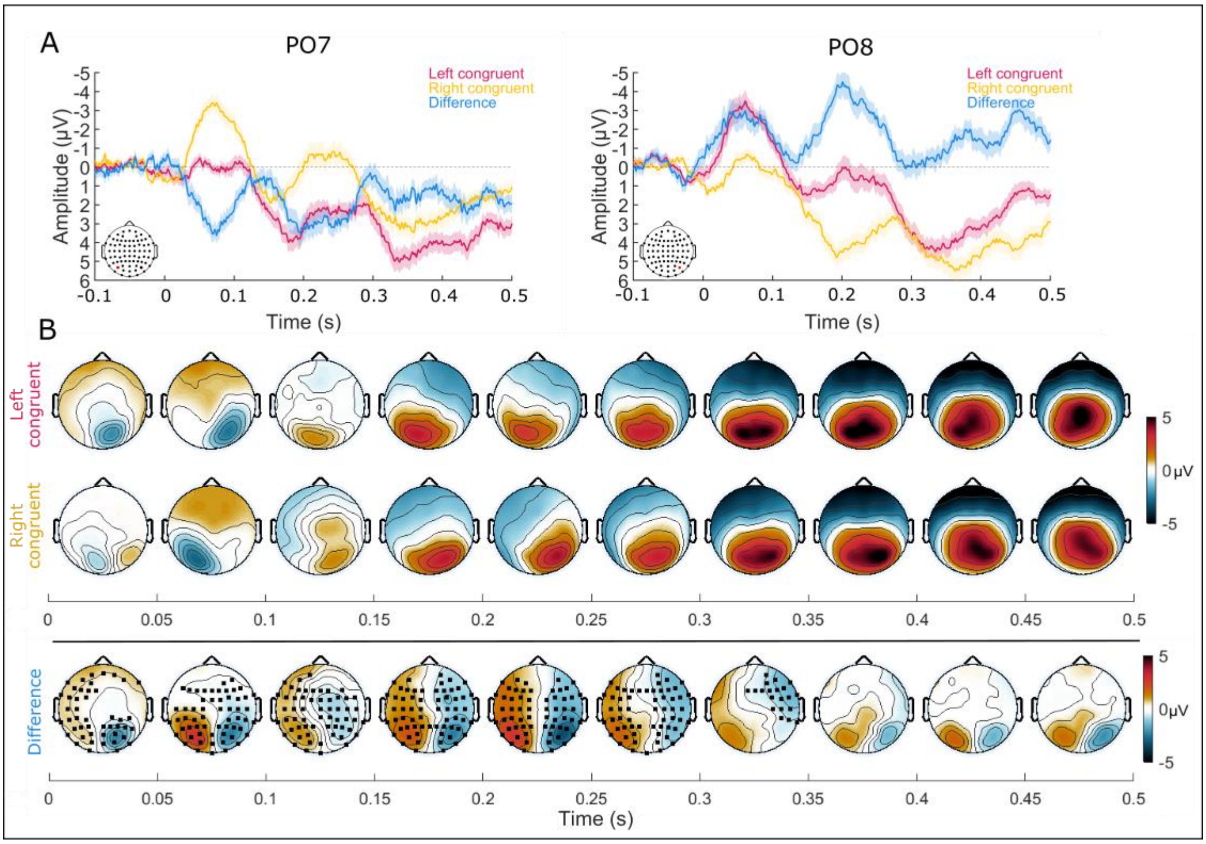

Figure 40. Grand averages of the ERPs for congruent exogenously cued targets. (A) ERPs to left congruent (red), right congruent (yellow) exogenous cues and the difference ERP (blue) derived by subtracting ERPs to right congruent from ERPs to left congruent exogenous cues at electrode PO7 (left) and Fz (right) (see red marked electrodes in the schematic drawing of the electrode montage). Error bands represent the standard error of the mean. At time point zero, the target stimulus was presented. (B) ERP topographies to left congruent (first row) and right congruent (second row) exogenous cues as well as the difference ERP (ERP(left congruent) minus ERP(right congruent); last row) for the post-exogenous epoch 0 to 500 ms in 50 ms steps. Dots on the ERP topography in the last row indicate electrodes that survived tests for multiple comparisons ($p < .05$).

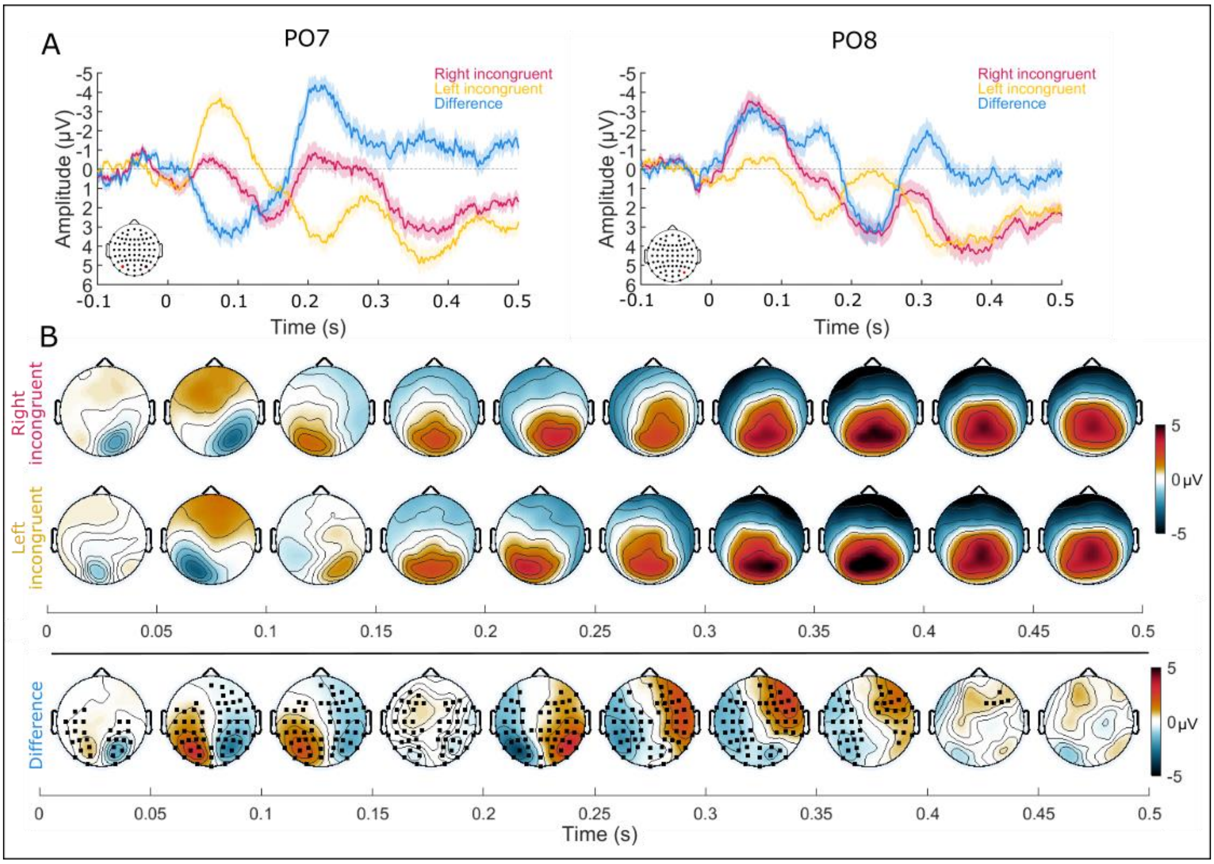

Figure 41. Grand averages of the ERPs for incongruent exogenously cued targets. (A) ERPs to right incongruent (red), left in congruent (yellow) endogenous cues and the difference ERP (blue) derived by subtracting ERPs to left incongruent from ERPs to right incongruent exogenous cues at electrode PO7 (left) and PO8 (right) (see red marked electrodes in the schematic drawing of the electrode montage). Error bands represent the standard error of the mean. At time zero, the target stimulus was presented. (B) ERP topographies to right incongruent (first row) and left incongruent (second row) endogenous cues as well as the difference ERP (ERP(right incongruent) minus ERP(left incongruent); last row) for the post-exogenous epoch 0 to 500 ms in 50 ms steps. Dots on the ERP topography in the last row indicate electrodes that survived tests for multiple comparisons (p < .05).

To eliminate stimulus-driven activity elicited by the exogenous spatial cues, we compared the difference potentials of the congruent and incongruent exogenous cueing conditions. Difference potentials to congruent and incongruent exogenous cueing started to differ after around 170 ms from the onset of the target stimulus (positive cluster: from 170 to 385 ms, $p < .001$; negative cluster: from 174 to 396 ms, $p < .001$, Figure 42), and showed a lateralized topography with a negative potential over the right hemisphere.

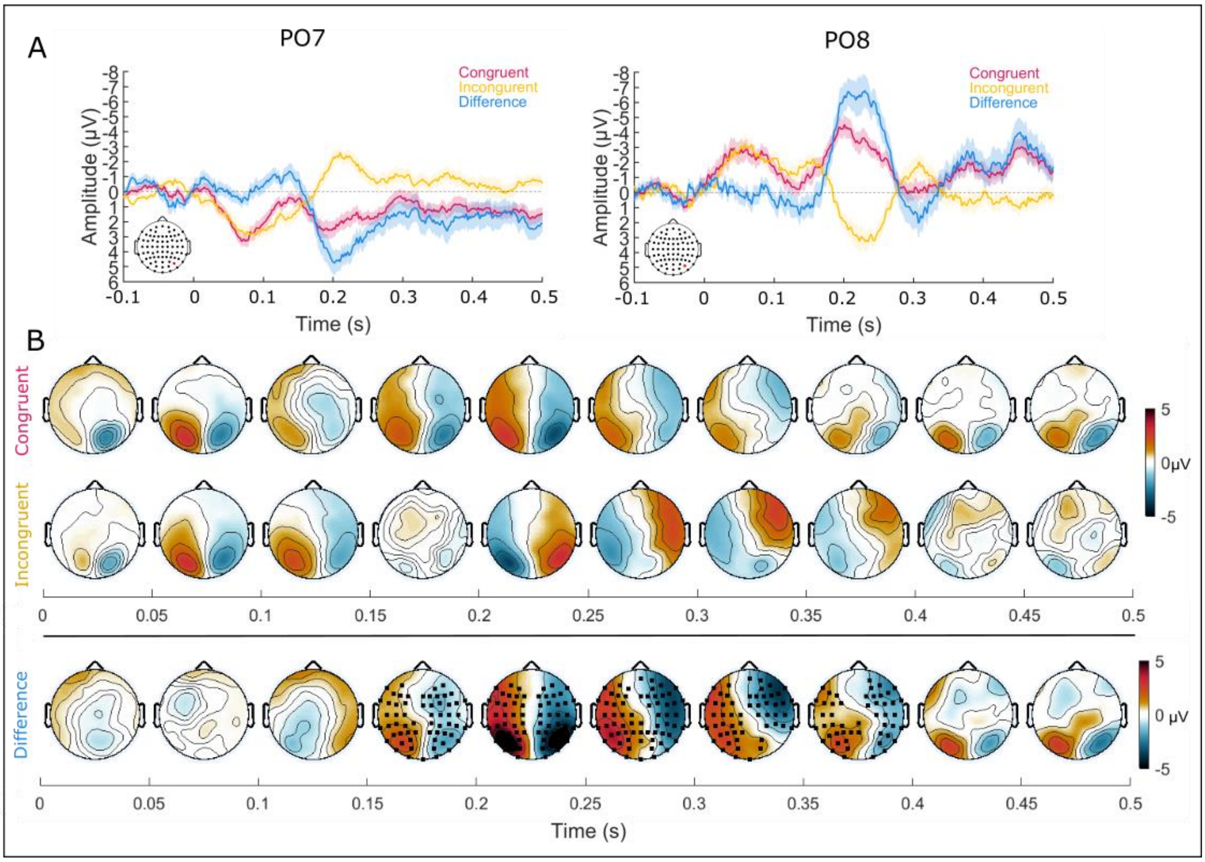

Figure 42. Grand averages of the ERPs for congruent and incongruent exogenously cued targets. (A) Difference ERP to congruent (red), incongruent (yellow) exogenously cued targets and the difference ERP (blue) derived by subtracting the difference ERPs to incongruent cued targets from the difference ERPs to right congruent exogenous cued targets at electrode PO7 (left) and PO8 (right) (see red marked electrodes in the schematic drawing of the electrode montage). Error bands represent the standard error of the mean. At time point zero, the target stimulus was presented. (B) Difference ERP topographies to congruent (first row) and incongruent (second row) exogenously cued targets as well as the difference ERP (ERP(congruent) minus ERP(incongruent); last row) for the post-exogenous epoch 0 to 500 ms in 50 ms steps. Dots on the ERP topography in the last row indicate electrodes that survived tests for multiple comparisons ($p < .05$).

3.5.2.3 Effect of joint spatial endogenous and exogenous spatial attention

To investigate whether we find any effect of spatial orienting on ERPs if the effects of endogenous and exogenous spatial orientation add up, we compared left and right target presentation in conditions in which the strongest spatial orientation differences were expected: Valid endogenously and congruent exogenously cued trials, and invalid endogenously and incongruent exogenously cued trials. To eliminate neural activity related to stimulus-driven activity from the exogenous cues, we calculated the *Joint effect* (Equation 2) by subtracting the invalid/incongruent difference ERP from the valid/congruent difference ERP (for a detailed description see: Methods). If spatial orientation modulates ERP activity, we would expect that the condition with the most strongest effect on behavior would modulate neural activity to a stronger degree than the condition with the most impairing effect. For the comparison of valid/congruent cued trials for left and right targets, we found one positive cluster over the left hemisphere and one negative cluster over the right hemisphere starting directly after the onset of the target stimulus, and lasting until the end of the analysis window (positive cluster: from 23 to 500 ms, $p < .001$, negative cluster: from 3 to 500 ms, $p < .001$, Figure 43). For the comparison of left and right target presentation in invalid/incongruent cued trials, we found also a positive cluster over the left hemisphere and two negative clusters both over the right hemisphere (first positive cluster: from 33 to 178 ms, $p < .001$; second positive cluster: from 191 to 414 ms, $p < .001$; first negative cluster: from 21 to 175 ms, $p < .001$; second negative cluster: from 190 to 451 ms, $p < .001$, Figure 44).

The comparison of both difference potentials revealed one positive and one negative cluster, starting around 150 ms after the presentation of the target stimulus, and lasting for around 280 ms (positive cluster: from 150 to 437 ms, $p < .001$; negative cluster: 163 to 424 ms, $p < .001$, Figure 45).

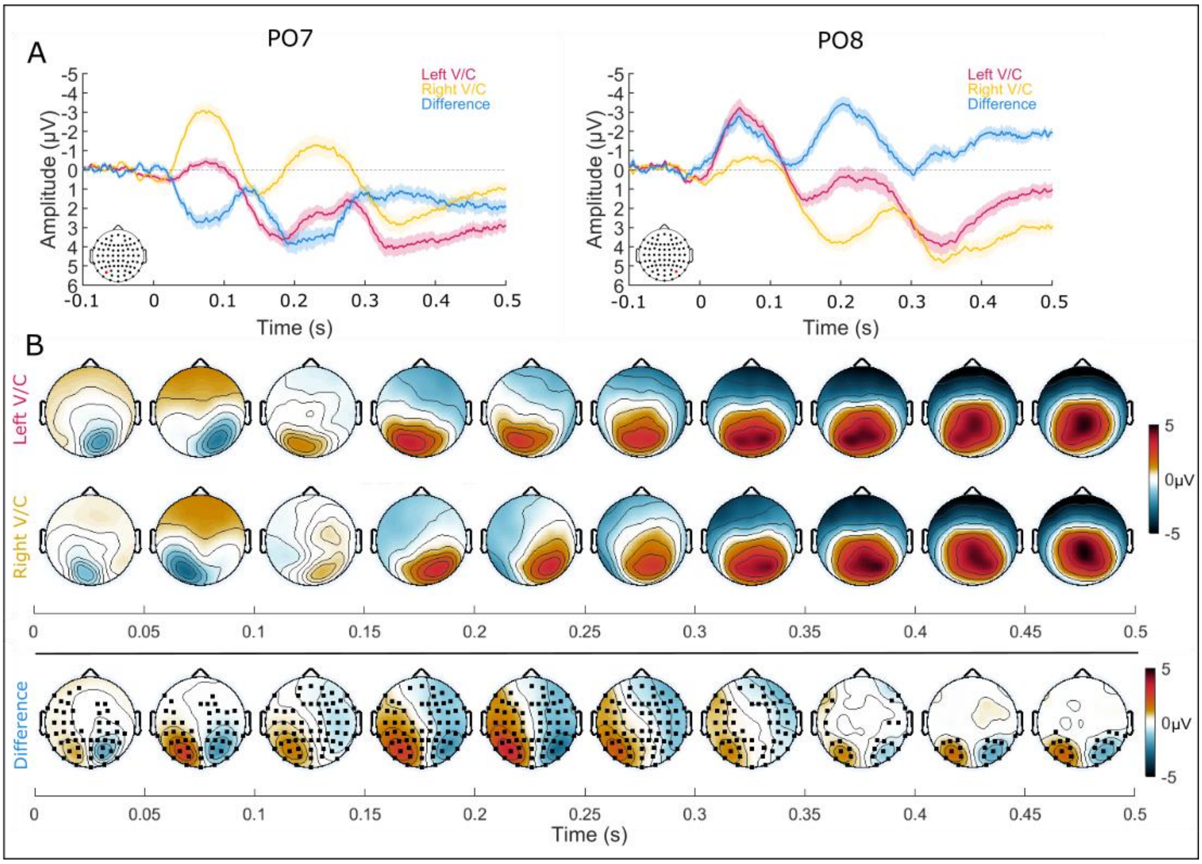

Figure 43. Grand averages of the ERPs for valid/congruent endogenously/exogenously cued targets. (A) ERPs to left valid/congruent (red, Left V/C), right valid/congruent (yellow, Right V/C) endogenous/exogenous cues and the difference ERP (blue) derived by subtracting ERPs to right valid/congruent from ERPs to left valid/congruent endogenous/exogenous cues at electrode PO7 (left) and PO8 (right) (see red marked electrodes in the schematic drawing of the electrode montage). Error bands represent the standard error of the mean. At time point zero, the target stimulus was presented. (B) ERP topographies to left valid/congruent (first row) and right valid/congruent (second row) endogenous/exogenous cues as well as the difference ERP (ERP(Left V/C) minus ERP(Right V/C); last row) for the post-exogenous epoch 0 to 500 ms in 50 ms steps. Dots on the ERP topography in the last row indicate electrodes that survived tests for multiple comparisons ($p < .05$).

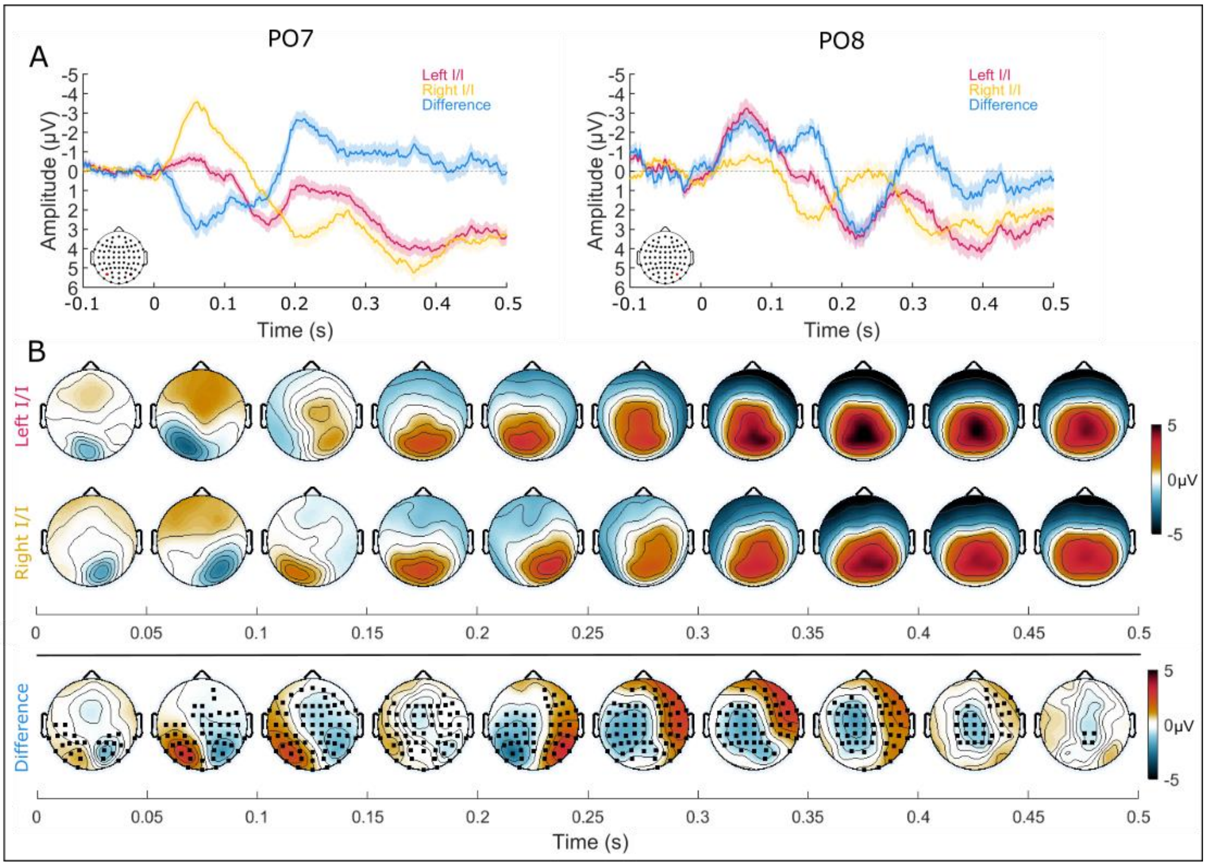

Figure 44. Grand averages of the ERPs for invalid/incongruent endogenously/exogenously cued targets. (A) ERPs to left invalid/incongruent (red, Left I/I), right invalid/incongruent (yellow, Right I/I) endogenous/exogenous cues and the difference ERP (blue) derived by subtracting ERPs to right invalid/incongruent from ERPs to left invalid/incongruent endogenous/exogenous cues at electrode PO7 (left) and PO8 (right) (see red marked electrodes in the schematic drawing of the electrode montage). Error bands represent the standard error of the mean. At time point zero, the target stimulus was presented. (B) ERP topographies to left invalid/incongruent (first row) and right invalid/incongruent (second row) endogenous/exogenous cues as well as the difference ERP (ERP(Left I/I) minus ERP(Right I/I); last row) for the post-exogenous epoch 0 to 500 ms in 50 ms steps. Dots on the ERP topography in the last row indicate electrodes that survived tests for multiple comparisons ($p < .05$).

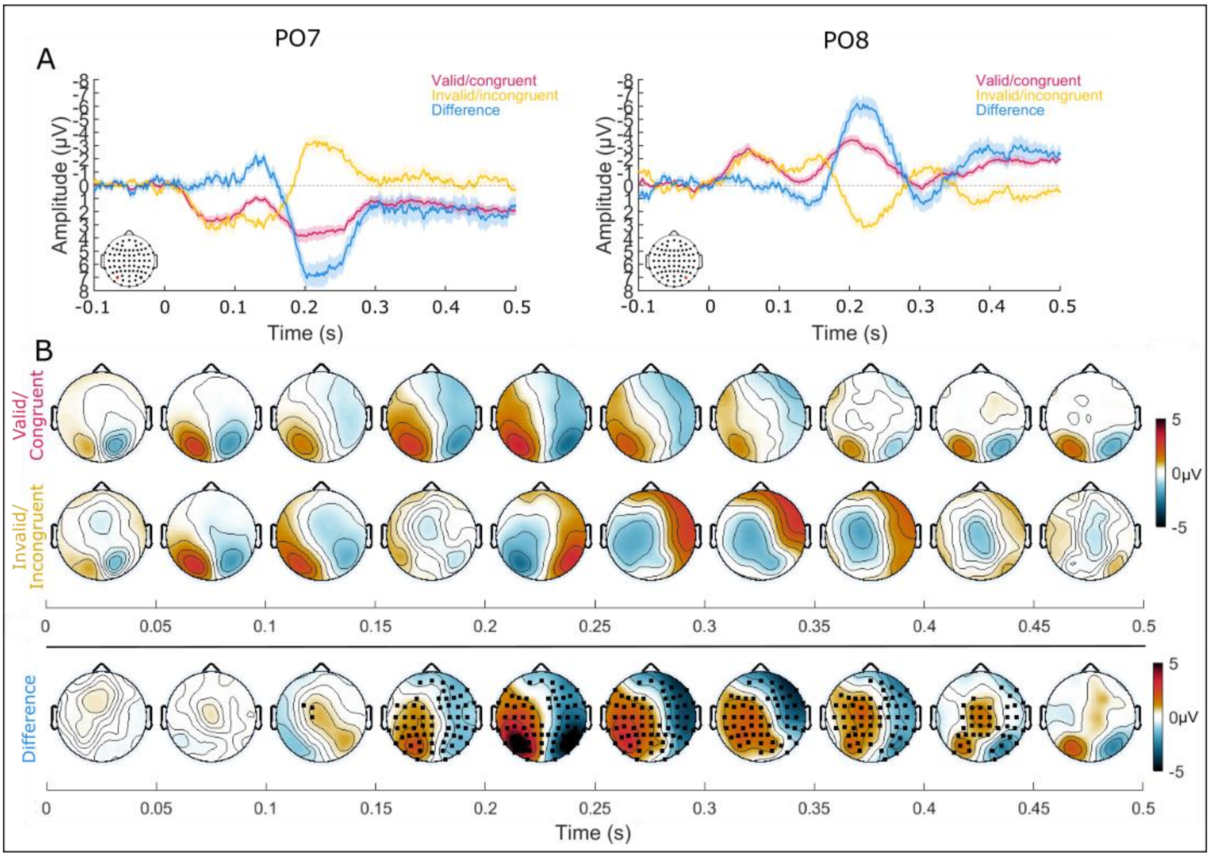

Figure 45. Grand averages of the ERPs for valid/congruent and invalid/incongruent endogenously/exogenously cued targets. (A) ERPs to invalid/incongruent (red, Valid/congruent), invalid/incongruent (yellow, Invalid/incongruent) endogenous/exogenous cues and the difference ERP (blue) derived by subtracting ERPs to invalid/incongruent from ERPs to invalid/incongruent endogenous/exogenous cues at electrode PO7 (left) and PO8 (right) (see red marked electrodes in the schematic drawing of the electrode montage). Error bands represent the standard error of the mean. At time point zero, the target stimulus was presented. (B) ERP topographies to invalid/incongruent (first row) and right invalid/incongruent (second row) endogenous/exogenous cues as well as the difference ERP (ERP(Valid/congruent) minus ERP(Invalid/incongruent); last row) for the post-exogenous epoch 0 to 500 ms steps. Dots on the ERP topography in the last row indicate electrodes that survived tests for multiple comparisons (p < .05).

3.5.2.4 Difference in reorienting of attention

To investigate whether the effect of exogenous spatial orienting differs from the effect of jointly oriented exogenous and endogenous attention on the same side, we compared the *Congruency* (Equation 6) with the *Joint effect* (Equation 7). However, the Congruency and the Joint effect did not differ (first positive cluster: p = .116, first negative cluster: p = .368, Figure 46). Difference ERPs to congruent and incongruent attention shift and to valid/congruent and invalid/incongruent attention shift did not differ from each other.

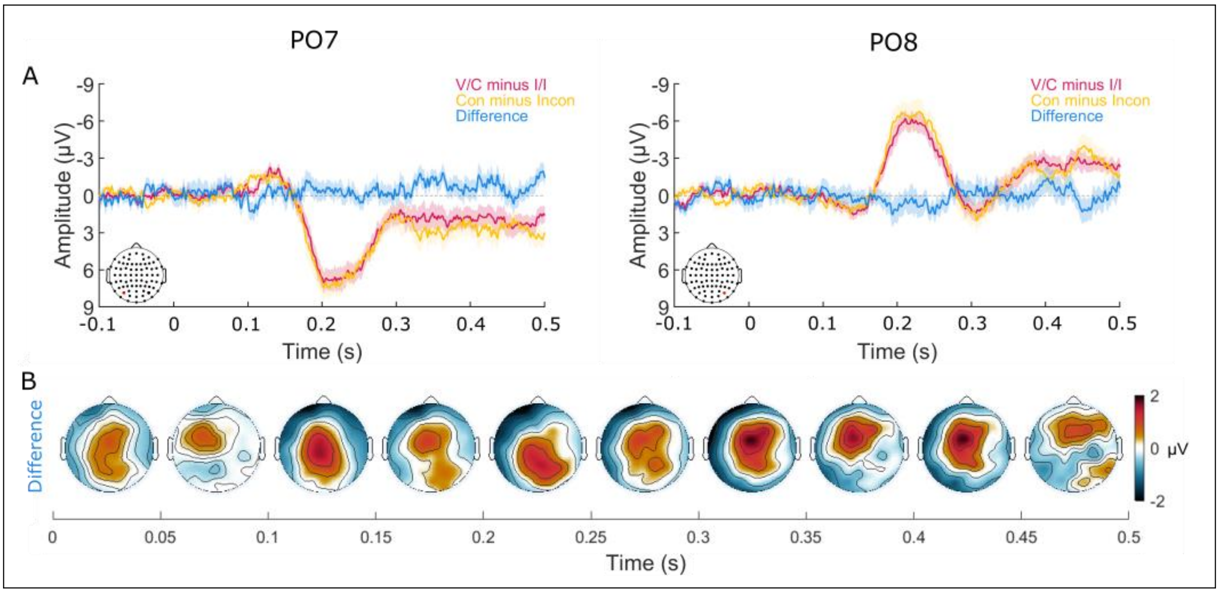

Figure 46. Grand averages of the Congruency and the Joint effect and their difference. (A) Difference ERPs to valid/congruent minus invalid/incongruent (red, V/C minus I/I), congruent minus incongruent (yellow, Con minus Incon) endogenous/exogenous cues and the difference ERP (blue) derived by subtracting the difference ERPs to congruent minus incongruent from ERPs to valid/congruent minus invalid/incongruent endogenous/exogenous cues at electrode PO7 (left) and PO8 (right) (see red marked electrodes in the schematic drawing of the electrode montage). Error bands represent the standard error of the mean. At time point zero, the target stimulus was presented. (B) Topographies of the difference ERP (ERP(Valid/congruent minus invalid/incongruent) minus ERP(congruent minus incongruent)) for the post-exogenous epoch 0 to 500 ms steps. Dots on the ERP topography in the last row indicate electrodes that survived tests for multiple comparisons (p < .05).

4. Discussion

In the present study, we used a spatial attention paradigm to investigate whether alpha and gamma power are reflecting top-down and bottom-up communication, respectively, as mapped onto endogenous and exogenous spatial attention. To record a sufficient gamma response, we presented bilateral dynamic grating stimuli, which are known to elicit a sustained band-limited response in the gamma range. At the beginning of each trial, we presented letter cues that served as directional (L/R) or undirectional (N) endogenous cues. Directional cues predicted the correct side of the next upcoming target with an 80% probability. Before target presentation, we flashed bright frames around the dynamic grating stimuli, either around both or around one at a time. These frames served as undirectional or directional exogenous cues. Exogenous cues had no predictive value. The presentation of bilateral dynamic grating stimuli resulted in a strong sustained band-limited response in the gamma range. In anticipation of visual stimulation, directional endogenous cues resulted in lateralized alpha and gamma responses in the hypothesized directions. However, after the onset of dynamic grating stimuli, these effects did not proceed over the whole period of stimulus presentation. Furthermore, endogenous cueing did not affect oscillatory activity after target presentation, neither in the alpha- nor in the gamma-band. The ERP results corresponded to the observations from oscillatory activity: Endogenous cueing modulated ERPs to the task irrelevant dynamic grating stimuli, but not to target presentation. Exogenous cueing effects resulted in lateralized alpha and gamma responses in the expected direction. However, these effects were not observed consistently across conditions. For an illustration of an extract of the present results, see appendix: Figure B.3. Even though behavioral results were in line with typical cueing effects, showing behavioral benefits for valid and congruent cueing and behavioral disadvantages for invalid and incongruent cueing respectively, findings in the electrophysiological and behavioral measurements were not correlated.

Prior to the onset of the dynamic stimuli, endogenous cues directing attention to the right side decreased alpha power contralateral to the attended side compared to cues that directed attention to the left side. In line with our hypothesis, this effect was accompanied by a contralateral increase in gamma power for rightward cueing compared to leftward cueing. In accordance with the present results, previous studies reported equivalent effects for alpha- and gamma-band activity during the anticipation of visual stimulation after endogenous cueing (Poch et al., 2014; Siegel et al., 2008). However, these studies not only reported contralateral effects, but also increased alpha-band and decreased gamma-band power ipsilateral to the attended side. It could be hypothesized that we did not find similar effects since it was reported that alpha lateralization needs at least 600 ms after cue offset to be detectable in EEG recordings (Worden et al., 2000). In the present study, the anticipation window was only 500 ms long.

This period might have been too short to detect effects that are more pronounced, and they might have been superimposed by the onset of the strong bilateral stimulation, eliciting a strong overall decrease of alpha activity. Furthermore, the studies by Poch et al. (2014) and Siegel et al. (2008) recorded MEG, that yields a better signal-to-noise ratio in contrast to the present study that utilized EEG. Moreover, the observed effects in alpha- and gamma-band power did not extend over the whole period of only bilateral dynamic grating presentation. In addition, no effect of directional endogenous cueing on oscillatory activity was observed during target processing, neither in the alpha nor in the gamma range, or at gamma peak frequency. In accordance with these results Siegel et al. (2008) also reported only effects of endogenous directional cues in primary and secondary visual areas on alpha and gamma activity during the anticipation phase, but not during stimulus presentation. One possible explanation could be that endogenous cues did not direct attention properly, and thus no modulation of alpha- and gamma-band activity was detected. However, the clear behavioral effects speak against this interpretation. Moreover, the present result is inconsistent with other studies that reported modulations of the stimulus induced gamma response by endogenous attention (Gruber et al., 1999; Koelewijn et al., 2013; Magazzini & Singh, 2018). For example, Magazzini and Singh (2018) reported that endogenous spatial attention increased the power of the stimulus induced gamma response contralateral to the attended side. However, they presented unilateral grating stimuli, which were task relevant. This methodological difference could explain the discrepancy with our results. Since, in the present study the dynamic stimuli and thus their spatial location were neither task-relevant, nor distracting from the current task, it might be hypothesized that the attentional focus was very narrow, and did not subtend the dynamic grating stimuli. The grating stimuli might have been processed automatically, without attentional modulation (Rees et al., 1997). Consequently, alpha desynchronization might have operated locally, and it did not affect the surrounding areas. To complete the task successfully, it was only necessary to pay attention to the center of the dynamic grating stimuli, more specifically the gray circles. The gray circles themselves were probably not sufficient to elicit a reliable sustained gamma response in the EEG, since they were small and static. Consistent with this interpretation, Busch et al. (2006) observed top-down effects on visually induced gamma power only when participants had to attend to the large surrounding grating (9° visual angle). When participants attended to small circular gratings (only 1.5° visual angle) which were presented on top of the large ones, these effects were not observed. The authors assumed that compared to the large stimuli, the number of neural assemblies activated by the small stimuli were not sufficient to detect top-down effects. Consequently, inhibition might had a local effect, which did not affect the visually induced gamma-band power in adjacent regions because attentional focus was limited to a small area in the visual field. Indeed, behavioral studies that investigated the properties of attentional focus reported that in the periphery, the size of attentional focus can be as small as only 1° visual angle (Intriligator & Cavanagh, 2001), which could correspond to local alpha effects limited to receptive fields corresponding to 1° visual angle. In line with this assumption, recent neurophysiological studies suggest that the neural mechanisms of visual spatial attention underlying alpha desynchronization are focal and topographically organized (Popov et al., 2019; Rihs et al., 2007) and that these processes occur in a relatively narrow profile (Hopf et al., 2006; Müller & Kleinschmidt, 2004). Moreover, the strong visual stimulation by the dynamic grating stimuli resulted in a very strong overall alpha decrease that was superimposed on the cueing effects, making it additionally difficult to detect potential small effects. In line with this interpretation, ERPs to attended and unattended targets did also not differ, even though ERP effects of endogenous spatial orienting are typically reported for the contralateral P1 and N1 component, reflecting the retinotopic organization of spatial attention (Di Russo et al., 2003; Hopfinger & Mangun, 1998, 2001; Mangun et al., 2001; Mangun et al., 1997). Thus, taken together, our findings speak in favor of the interpretation that during visual stimulation, attentional effects on oscillatory activtiy in the gamma-band were too small and localized to be picked up by the EEG.

When isolating the effect of directional exogenous cueing on oscillatory activity for target presentation, the direction of the observed effects were as expected. We observed increased gamma and gamma peak power, and decreased alpha power contralateral to the side of target presentation when comparing congruent with incongruent exogenous cueing conditions. However, the observed effects were not consistent over all conditions. For alpha power, we observed a contralateral decrease only for left targets. This finding is in line with other studies that reported alpha effects only for targets on the left side (Lasaponara et al., 2019; Thut et al., 2006). Thut et al. (2006) suggested that the hemispheric distribution of alpha activity might be attributed to a fundamental bias towards leftward attention (for a review see: Jewell & McCourt, 2000). This bias is closely linked to the overall dominance of the right hemisphere in controlling spatial attention. To our knowledge, the current study is the first that investigated effects of exogenous attention on oscillatory activity in the gamma-band. As discussed above, even though the direction of the observed effects were as predicted, they were not consistently found across conditions: An increase in power contralateral to the target side was observed in the gamma range only for right targets, and for gamma peak frequency, only for left targets. This inconsistency could result from the fact that it was potentially not the sustained band-limited gamma response that was modulated by spatial attention, but rather a lower gamma-band that partly overlapped with the range of the visually induced gamma response. In line with this interpretation, a post-hoc comparison of gamma power for left and right target presentation showed a significant cluster over the left hemisphere, most prominent in the range between 30 to 50 Hz, but including also frequencies up to 90 Hz (see Figure 35). As for the effect of endogenous cueing on the modulation of visually induced gamma responses discussed above, exogenous attention might have not affected gamma-band activity since alpha power modulation was restricted to local areas that did not include the adjacent areas stimulated by the dynamic grating stimuli. In conclusion, in the present study, directional exogenous cues modulated oscillatory activity in the gamma-band, but possibly not the visually induced gamma response. Future work is required to investigate whether exogenous attention modulates the stimulus induced band-limited gamma response when these stimuli and thus their location are task-relevant, or whether exogenous attentional orienting is capable of doing so at all. However, we must also consider a possible alternative explanation: that attentional effects during exogenous directional cues also reflect differences of bottom-up stimulus-driven activity, due to the presentation of the exogenous cues (flashed frames around the dynamic grating stimuli) acting as different input in itself. A potential solution would have been to measure the sensory-driven responses to exogenous cues without subsequent target presentation, to serve as a baseline. Since the experiment already lasted a total of six hours and participants were beginning to tire, we discarded this additional condition in favor of clean and reliable data. Nonetheless, since we observed attentional effects during the anticipation phase and isolated exogenous attentional effects on alpha-band power were limited to left targets, we can rule out the possibility that the observed effects can be explained solely by differences in stimulus presentation.

Even though we observed lateralized oscillatory activity in the alpha- and gamma-band in the expected directions, the results in both frequency bands were not consistently significant across conditions. Although both alpha- and gamma-band power were lateralized in the pre-stimulus phase, we would not have expected any modulation in the utilized gamma range at this time point, since we assessed stimulus induced gamma responses. The visual stimulation that induced the band-limited gamma response were not presented yet. Moreover, this observed effect of endogenous attention did not extend into the stimulation phase, and did not affect target processing. Thus, the present data do not suggest that activity in the alpha- and gamma-band were related, but rather that they did not interact. This assumption is also in line with our behavioral findings. Endogenous and exogenous spatial cueing modulated the behavioral outcomes independently from each other. For both attentional types, valid or congruent cues resulted in shorter reaction times and higher performances compared to invalid or incongruent cues. These findings are in line with a big body of literature that reported similar independent behavioral effects for endogenous and exogenous spatial cues (Berger et al., 2005; Grubb et al., 2015; Landry et al., 2021; Natale et al., 2009). The result that endogenous and exogenous behavioral effects are independent match our electrophysiological findings that oscillatory activity in the alpha- and gamma-band might not have interacted in this paradigm. Furthermore, subsequent post-hoc comparisons of gamma power values derived from the negative cluster that resulted from the comparison of left vs. right presented targets showed that gamma power in that cluster was only higher for neutral/congruent compared to neutral/incongruent trials. The other comparisons were not significant; also, no interaction was observed, speaking in favor of independent mechanisms. Taken together, our results indicate that endogenous and exogenous spatial attention, as well as reorienting, affected not only behavior but also oscillatory activity independently from each other. However, behavioral and electrophysiological findings were not related. As stated above, we assume that because the dynamic grating stimuli were not task-relevant and thus their location, they were automatically processed and did not require attentional modulation. In the present study, visually induced gamma responses may not be an appropriate means to investigate the neural mechanism underlying the behavioral effects. However, a recent MEG study that presented task-relevant stimuli - the participants executed a variant of the Simon task - did also fail to relate their behavioral and electrophysiological measures (van Es et al., 2020). Even though alpha- and gamma-band power showed the expected lateralization and were stronger for congruent compared to incongruent trials, variation in oscillatory activity was not related to reaction times or performance. Future work is needed to explore which tasks, stimuli and methods are appropriate to identify the neural mechanisms underlying the behavioral effects of attention.

The present paradigm was designed to investigate the effects of endogenous and exogenous attention on oscillatory neural activity. To reliably differentiate ERPs to the exogenous cue and to the target, which were presented in close proximity, interstimulus jittering or at least a baseline recording of the ERP to the exogenous cue is crucial (Chica et al., 2014). Due to the lack of jitter and baseline recordings, we were not able to examine exogenous cueing effects directly. As an exploratory analysis, we subtracted the ERPs to congruent and incongruent exogenous cues for left and right targets and examined their difference to have a proximity for exogenous attentional reorienting. We used the same approach to investigate reorienting of attention when exogenous and endogenous attention were jointly directed to one side. ERPs corresponding to exogenous reorientation of attention alone started to differ after approximately 170 ms after target onset. ERPs corresponding to the reorientation of attention when exogenous and endogenous attention were directed together to one side started to differ already after around 150 ms. However, when we directly compared these two effects did not significantly differ. Thus, the neural representation of attentional reorienting for exogenous attention alone, or exogenous attention jointly modulated together with endogenous attention, do not differ. These results suggest that endogenous and exogenous reorientation modulate neural activity independently from each other. In line with this assumption are the results by Natale et al. (2009) who used a double-cueing paradigm to investigate the fMRI correlates of visual spatial reorienting. They reported that neural activity in distinct circuits reflecting endogenous and exogenous reorienting was unaffected by the validity of the corresponding other cue. Taken together, our findings suggest that sequential endogenous and exogenous reorienting operate independently from one another.

To summarize, our selected stimulus parameters elicited a reliable band-limited response in the gamma range. In anticipation of visual stimulation, endogenous spatial attention resulted in lateralized alpha- and gamma-band responses. However, after target presentation, these effects were not observed anymore. This result might be considered surprising in contrast to the reliable behavioral effects showing costs and benefits due to valid or congruent and invalid or incongruent, endogenous and exogenous cues. In line with the lack of ERP effects, we assume that the inhibitory effects of alpha desynchronization, that were present in the anticipation phase, were local and did not spread into other regions, preventing the observation of consecutive effects. Furthermore, the absence of effects in the gamma range may also be because the dynamic grating stimuli and their location were not task-relevant and therefore were not affected by spatial attention. Taken together, as reflected not only by the present behavioral, but also by the electrophysiological results, endogenous attention reflecting top-down communication and exogenous attention reflecting bottom-up communication seemed to be independent of each other.

Chapter IV: General Discussion

In the present dissertation, two different approaches were used to investigate the neural mechanisms underlying top-down and bottom-up communication. The first approach aimed at investigating the temporal and spatial specificity of top-down and bottom-up signals, in the framework of predictive coding. In this framework, it is assumed that top-down predictions are sent upstream, and then compared to the actual sensory input, at each level of sensory processing. Only the residual is sent downstream, as a bottom-up error signal. A novel ERP omission paradigm was developed that made use of a visual ERP effect, namely the C1 effect, to investigate whether top-down predictions modulate the first cortical response of visual processing. The second approach aimed at investigating whether top-down and bottom-up information are transmitted via oscillatory activity in specific frequency bands, that is, the alpha- and gamma-band, respectively. A spatial cueing paradigm was used to simultaneously modulate top-down and bottom-up processing, which map onto endogenous and exogenous spatial attention, while recording EEG. This approach allowed us to investigate whether directional endogenous and exogenous cues result in spatial specific lateralized alpha and gamma responses and whether attentional effects in the oscillatory activity do, in fact, interact.

Results of the first study (Chapter II) showed that the first cortical response of visual processing, corresponding to the well-known C1 ERP, was indeed independent of top-down predictions. Unexpected stimulus omissions elicited a lateralized ERP response. Neural responses to unexpected omissions were frequently interpreted to reflect the pure top-down prediction signal. However, recent research emphasizes negative error processing, that is, the error signal to expected but missing sensory input, and challenges the assumption that omissions actually reflect only the top-down signal, suggesting that omissions might also reflect an additional negative error response. By using a subtraction approach, we isolated a newly defined *Visual predictive signal*, which showed an early effect starting around 70 ms after stimulus presentation. These top-down effects seemed to be spatially specific and occurred early, but did not show the same activation pattern as veridical stimuli. Mismatching sensory input elicited a spatially specific ERP response comparable with the vMMN. Furthermore, the isolated *Negative error signal* (missing sensory input) preceded the *Positive error signals* (sensory input that exceeds the expected one). Both signals were spatially specific, as they showed lateralized responses. Thus, bottom-up error signals emerged only after top-down predictions, but both preserved stimulus specific information.

Results of the spatial attention paradigm showed that directional endogenous cues resulted in lateralized alpha- and gamma-band activity in the anticipation of visual stimulation. However, during stimulation and target processing, endogenous attentional effects did not persist. Alpha- and gamma-band power in response to target presentation were not modulated by directional endogenous attention. Nevertheless, the null findings could be due to methodological limitations. The dynamic grating stimuli, which are known to elicit a band-limited response in the gamma range, were not task-relevant. Modulatory attentional effects were potentially limited to a small number of neural assemblies that responded to task-relevant information, and did not spread to surrounding areas processing the surrounding dynamic grating stimuli. The limited areas affected could have resulted in local effects, which were too small to be detected with EEG. Exogenous attentional cues modulated alpha- and gamma-band power, but not consistently across all conditions. In line with the behavioral results, endogenous and exogenous attentional effects also did not interact in the electrophysiological measurements.

Communication of bottom-up error signals

Predictive coding assumes that the mismatch between bottom-up sensory input and top-down prediction is sent feedforward as an error signal, to update future sensory predictions. Increased neural responses to sensory input that does not match the prediction, as compared to input which match the prediction, were interpreted as reflective of the error response (Alink et al., 2010; Den Ouden et al., 2008; Todorovic & Lange, 2012; Wacongne et al., 2011). In line with previous studies, we observed stimulus- and spatially-specific mismatch responses (Standard minus Deviant) that were comparable with the vMMN, an ERP component that was repeatedly associated with error processing (Stefanics et al., 2014). However, predictions can be violated in more than one way: Sensory input can be less than expected (negative error processing), but it can also be more than expected (positive error processing). Recently, Keller and Mrsic-Flogel (2018) provided a detailed description of the neural circuitry of negative and positive error processing at the cellular level. We defined two novel neural responses via a subtraction approach based on their description: the *Negative error signal* and the *Positive error signal*, which accounted for these two different types of prediction violation. The observed stimulus and spatially specific error signals mentioned above were comparable in latency and topography with the *Negative error signal*, suggesting that they reflect similar processes: the detection or underlying computations of missing sensory input. The *Positive error signal* followed the *Negative error signal* implying that positive error processing might take place only after attentional redirection. However, empirical work that differentiates between negative and positive error processing is still limited. A recent fMRI study presented faces and houses while recording activity from the fusiform face area (FFA) and the parahippocampal place area (PPA; Schliephake et al., 2021). They defined positive error processing as activity stemming from brain areas that preferentially processes the presented stimuli when it was not expected, e.g. FFA activity when a face was presented, but not expected. Negative error processing was defined as activity stemming from brain areas which do not preferentially process the presented stimuli, although the preferred stimuli was expected, e.g. FFA activity when a house was presented, but a face was expected. Their results revealed increased neural responses to expected vs. unexpected stimuli only within the non-preferred category, suggesting negative error processing. Schliephake et al. did not find evidence for positive error signals. However, during positive error processing, category specific regions showed increased coupling with the right inferior frontal gyrus (IFG). Research has shown that there is typically an increase in IFG activity in response to prediction errors, across various modalities (Chao et al., 2018; Trempler et al., 2020). Therefore, the authors interpret their findings as reflective of increased information flow from lower to higher areas, that subsequently led to a revision of the current internal model from which former sensory predictions are drawn. Taken these recent considerations into account, the present *Positive error signal* might represent these postulated signals which drive the update or revision of the internal model, respectively. Both the present thesis and the study by Schliephake et al. (2021) were not able to fully disentangle negative and positive error processing, since the presentation of mismatching stimuli potentially elicited both negative and positive error signals. In the present thesis, the Deviant condition comprised of missing stimulus which was expected (negative error), and additionally an unexpected stimulus which was presented (positive error). Similarly, in the study by Schliephake et al. (2021), presenting a house even though a face was expected might have elicited a negative error signal due to the missing face, and an additional positive error signal due to the presentation of the house. Furthermore, as mentioned above, the present omission condition might not only represent the top-down prediction, but also negative error processing, since a visual stimulus was expected but not presented. Thus, future empirical work is needed to disentangle the underlying neural mechanisms of negative and positive error signals in single conditions, making it easier to differentiate between positive and negative error effects. A possible solution could be to include two additional conditions: one in which no stimulus is expect to be presented (expected omission), and a corresponding condition in which a stimulus is nevertheless presented (unexpected stimulus). The expected omission should not lead to error processing. However, neural responses to the unexpected stimulus (no stimulus is expected, but presented) should reflect positive error processing. Contrasting the neural responses to these unexpected stimulus presentations with a condition in which the same stimulus was expected (stimulus is expected and presented, referred to as *Standards* in the present thesis), could potentially isolate positive error processing by subtracting any stimulus-driven related activity.

In addition to empirical work, there is a growing body of literature that uses computational models to study the neural mechanisms underlying negative and positive error processing (Chao et al., 2022; Hertäg & Clopath, 2022; Hertäg & Sprekeler, 2020; Koelewijn et al., 2013). Recent computational model studies demonstrated that the formation of negative and positive prediction error circuits as proposed by Rao and Ballard (1999) are biologically plausible (Hertäg & Clopath, 2022; Hertäg & Sprekeler, 2020). Furthermore, neural responses to locomotion in mouse V1 could be differentiated into neural assemblies, showing consistent response behavior associated with negative and positive error units (Jordan & Keller, 2020).

Taken together, in the present work, negative error processing emerged before positive error processing. Both error signals seemed to preserve stimulus specific information, since both signals were lateralized. However, positive error processing might additionally reflect a subsequent updating process. Thus, even though computational models demonstrated that the differentiation into negative and positive error units is biologically plausible, there remains a lack of empirical work in non-human animals as well as humans supporting this theoretical framework.

Communication of top-down predictions

The present dissertation showed that the first cortical response of visual processing is independent of top-down predictions. ERPs to unexpected omissions, as well as the defined *Visual predictive signal,* showed effects only after the first visual ERP, namely the C1 component. The C1 component is assumed to reflect predominantly neural activity stemming from V1 (Di Russo et al., 2002). Thus, consistent with prior work, the first cortical response seemed to be independent of top-down control during predictive processing. However, visual processing seemed to be modulated in a stimulus-specific manner to a later time point, since the *Visual predictive signal* was lateralized and started with a latency of 70 ms, that is, within the early time epoch of the P1. By contrast, lateralized ERPs to omissions in the top-left and bottom-right started to differ only after 230 ms. Thus, the question of what we can conclude from the differences found between the *Omission signal* and the *Visual predictive signal* still remains. Both signals should reflect top-down processing, but in two different contexts: in the absence or presence of bottom-up driven sensory activity respectively. One promising approach to better disentangle observed neural activity into top-down and bottom-up signals is high-resolution fMRI, which allows for differentiating the laminar profile of neural activity. One recent high-resolution fMRI study observed that during unexpected omissions, stimulus-specific neural activity was restricted to the deep layers of V1 (Aitken et al., 2020). The authors assumed that in the absence of bottom-up sensory input, the activation in the deep layers reflects top-down driving effects. In contrast, in the presence of bottom-up sensory input, Kok et al. (2016), also observed modulation of superficial layers using a similar study design, attributing it to additional modulatory top-down effects. The differences between the *Omission* and the *Visual predictive signal* in the present thesis could thus be explained by these findings: the *Omission signal* might only reflect the modulatory effects, but the *Visual predictive signal* might reflect both the modulatory and the driving effects. Furthermore, the present thesis adds the potential time course of driving and modulatory effects, as driving effects reflected by the *Visual predictive signals* might occur earlier as the modulatory effects reflected by the *Omission signal*. To sum up, after stimulus presentation, the first cortical response of visual processing remained independent of top-down control. Only after that first response, top-down predictions modulated visual processing, with the modulatory effect of incoming sensory information emerging first, followed by driving effects.

Although prior research assumed that the neural responses to unexpected omissions reflect the pure top-down signal, since it was assumed that no error signal would arise in the absence of bottom-up sensory input (Jiang et al., 2022; Wacongne et al., 2011), this view was recently challenged. Neural responses to omissions might not only reflect the prediction, but also an error signal, since the expected sensory input is missing (Chao et al., 2022; Keller & Mrsic-Flogel, 2018). Thus, the observed lateralized responses during omissions might not only reflect the top-down prediction, but also negative error processing, or a subsequent update of the internal model. When interpreting the timing of top-down predictions, the newly defined *Visual predictive signal* might be a more promising approach. Baseline measurements of the sensory-driven activity due to the presented visual grating stimuli were subtracted from the neural responses to the same stimuli, which fulfilled the sensory predictions later on in the experiment. However, it must be mentioned that a subtraction approach, as in the present thesis, might not be representative, since it assumes only additive interactions. It has been shown that non-linear predictive coding models can explain a wider range of empirical findings in comparison to purely linear models (Spratling, 2008). Thus, further research is needed to investigate the underlying neural mechanisms of omission responses. Furthermore, future work could examine whether non-linear approaches to isolating the prediction signal are more promising than a subtraction approach.

Recent work has shown that sensory predictions already modulate neural activity in the anticipation of expected input. For example, an MEG study by Kok et al. (2017) revealed that pre-stimulus neural activity exhibited a high degree of specificity, encoding predictable stimuli in the brain even before the actual stimulus was presented. Kok et al. (2017) interpret this specific pre-stimulus encoding as indicative of the brain engaging in anticipatory neural processing prior to sensory input. Furthermore, pre-stimulus activity also seemed to affect subsequent sensory processing: pre-stimulus alpha power and P1 amplitude were related (Samaha et al., 2016). Thus, it could be that top-down predictions already modulate neural activity during the expectation phase of an upcoming stimulus, and impacts subsequent sensory processing. Our findings are in line with this interpretation, as we observed lateralized alpha responses in anticipation of visual stimulation, reflecting the expected stimulus location. Top-down sensory predictions might already modulate sensory areas before stimulus onset by e.g. biasing baseline activity towards the expected stimulus (Alilović et al., 2019; de Lange et al., 2013). This modulatory pre-stimulus activity might be less specific than the modulation of stimulus-driven bottom-up activity. In Chapter III, pre-stimulus effects of lateralized oscillatory activity were reported for spatial endogenous attention. However, these effects did not persist during visual stimulation. Modulatory effects might have been restricted to a limited behaviorally relevant area, speaking in favor of pre-stimulus effects being rather broad, subtending a whole hemisphere. Subsequent effects during stimulation might be more restricted to areas that are coding for relevant, stimulus-specific input.

The present thesis contributed to our understanding of the well-known effects of top-down control of primary visual cortex, by establishing the time course of top-down predictions and bottom-up error signals. Taken together, our data and previous studies suggest that triggering predictions lead to changes in baseline activity, biasing neural responses to the preferred stimulus. These baseline changes seemed to emerge early, and to have some broad spatial specificity. The first cortical response of visual processing seemed to be independent of top-down influences. However, top-down predictions influenced subsequent early visual processing stages, potentially stemming from extrastriate areas. Negative error processing might be faster than positive error processing, however the observed differences in latencies might be due to methodological conditions, since positive error processing might have required attentional redirection. Future research is needed to further disentangle the underlying neural mechanisms of negative and positive error processing.

Measurement of alpha- and gamma-band activity

As discussed in Chapter III, the observed effects in the gamma-band likely did not reflect modulations of the visually induced gamma response. Below, I speculate on which neural mechanisms might underlie the observed effects. In the anticipation phase both, alpha- as well as gamma-band power were modulated in a stimulus specific manner, since both were lateralized. Alpha modulation in the present project could reflect preparatory activity as discussed above biasing baseline activity spatially in the direction of the preferred or expected stimulus. Changes in alpha activity are associated with intended top-down controlled release, or confinement of inhibition of neural assemblies (Okazaki et al., 2014; Worden et al., 2000; Zumer et al., 2014). Therefore, the observed gamma modulations might reflect the change in excitability of neural assemblies and local processing. This is in line with previous studies showing that oscillatory activity in the gamma-band and spiking activity in monkey V1 were correlated (e.g. Ray & Maunsell, 2011). With increasing gamma-band power, spiking activity increased. Thus, in line with previous work, decreased alpha-band power in the present thesis could reflect decreased local inhibition, resulting in increased local processing and spiking activity, as reflected by increased gamma-band power (Haegens et al., 2011; Ray & Maunsell, 2011; van Kerkoerle et al., 2014).

During stimulus presentation, gamma-band activity increased contralateral to the attended side. However, results were not consistent across conditions. The observed effects in the gamma range might not predominantly reflect changes in the visually induced gamma response, but in a slightly lower range, which was not related to the stimulus. Previous studies have reported that during visual stimulation, as well as during cognitive tasks, e.g. memory tasks, more than one frequency band in the gamma range was modulated, not only in primates, but also in humans (Koelewijn et al., 2013; Kucewicz et al., 2017; Murty et al., 2018). Furthermore, there are plenty of studies that showed activity in two differentiated frequency bands when examining gamma activity, however, did not explicitly report them (Hoogenboom et al., 2006; Muthukumaraswamy & Singh, 2013; Orekhova et al., 2015; Swettenham et al., 2009). Thus, the differentiation of neural oscillations in the gamma range into more than one broad frequency band seems to be a common observation. For example, consistent with the present interpretation, in a MEG study by Koelewijn et al. (2013), spatial attention did not modulate the visually induced gamma response in V1, but instead modulated a slightly different frequency range within the gamma-band. They defined a faster and a slower gamma response. The faster gamma response has been associated with more local processing, whereas the slower gamma range has been associated with reflecting properties of larger networks (Murty et al., 2018). Therefore, the observed modulation in the present thesis in a slightly lower gamma range might not reflect the local processing of the visual stimulation, but neural processes that expand onto a wider neural network. It could be hypothesized that this wider network is involved in attentional processes, as it has been shown that both endogenous and exogenous attention rely on widely distributed neural networks (Chica et al., 2013; Corbetta & Shulman, 2002; Funes et al., 2005). Future research is needed to further differentiate the different sub-bands included in the broadly defined gamma-band (> 30 Hz). In fact, two recent studies that recorded neural responses from cat V1 and primate early auditory cortex, respectively, reported at least three distinct gamma rhythms with different neural origins (Chao et al., 2018; Han et al., 2021), which potentially subserve the processing and transmission of different information.

Alternative functions of alpha- and gamma-band activity

The findings in the present thesis were not entirely consistent with the proposal that alpha solely subserves inhibitory processes and global computations, since e.g. alpha power in the anticipation of visual stimulation seemed to be modulated by endogenous spatial attention in a spatially specific way, but not during stimulus presentation. Previous studies have also reported findings that do not fit into the proposed inhibitory function of alpha oscillations (Mo et al., 2011; Samaha et al., 2016). For example Samaha et al. (2016) reported that prior knowledge about upcoming visual stimuli increased posterior alpha power prior to stimulus onset, speaking against an inhibitory function. Furthermore, the magnitude of pre-stimulus alpha modulation was positively correlated with the P1 amplitude across participants. They concluded that the observed alpha modulation might originate in regions where alpha does not play an inhibitory role. In line with this contrary finding, pre-stimulus alpha power in monkey inferotemporal cortex was positively instead of negatively correlated with visually induced gamma power (Mo et al., 2011). Furthermore, a very recent EEG study used a classical spatial cueing paradigm to investigate whether the direction in which alpha-band oscillations propagate might change the functional role of alpha (Alamia et al., 2023). During visual stimulation, alpha-band waves were propagating from occipital to frontal regions, reflecting visual processing. On the other hand, during the anticipation of the upcoming target and after cue off-set, respectively, alpha-band waves propagated in the opposite direction, that is, from front to back, potentially subserving top-down processing. The authors concluded that alpha-band waves could be involved in both distractor suppression and target enhancement, depending on the direction in which information is transmitted. Taken together, although it is widely accepted that alpha plays a major role in top-down processing and inhibitory control, new properties of oscillatory activity in the alpha-band additionally point to multiple functions.

Thus, further research is needed to get a better idea of the overall functional role of alpha oscillations, and their potential dependence on context and processing stage.

The role played by gamma-band activity in cognitive function is still under debate. It has been proposed that oscillatory activity in the gamma-band facilitates visual feature binding and communication between cortical areas (Bastos et al., 2015; Fries, 2009; Tallon-Baudry, 2009). However, some studies question this idea and the oscillatory nature of gamma-band activity (Chalk et al., 2010; Jia et al., 2011; Ray & Maunsell, 2010). For oscillatory activity in the gamma-band to transmit information across neural assemblies, it is important that the frequency range remains consistent enough to achieve sufficient temporal alignment. It is not yet clear whether the gamma rhythms that occur simultaneously in various neural assemblies during stimulus processing are stable and reliable enough to enable binding, communication, or joint coding (Jia et al., 2011; Ray & Maunsell, 2010). For example, Ray and Maunsell (2010) recorded neural activity from macaque V1, and observed that large stimuli with contrast variations across space generated gamma rhythms at significantly different frequencies within simultaneously recorded but different neural assemblies within 400 µm of each other. Hence, according to these findings, neural activity in the gamma-band might not be a suitable candidate for binding or communication due to temporal smearing, possibly hampering neural communication, at least in V1. Furthermore, in contrast to highly controlled experimental stimuli, natural stimuli are composed of even more complex features, which can vary over small spatial and temporal ranges, making binding and communication via consistent frequencies even less probable. Ray and Maunsell (2010) offer an alternative explanation: gamma rhythms might emerge as a resonant phenomenon due to the interplay between regional excitation and inhibition. Further work is required to determine which of both accounts holds true.

Sensory predictions and attention as common or distinct processes

In the present thesis, top-down and bottom-up communication were investigated using two different approaches: The manipulation of predictions and attention, more specifically of spatial visual predictions and covert spatial attention. However, it is still under debate whether predictions and attention are two independent mechanisms that can be investigated in isolation, or whether they are two integrative mechanisms, which are hard to disentangle. Since the initial proposals on the integration of attention within the predictive coding framework by Feldman and Friston (2010), there have been diverging perspectives on how prediction and attention interact to facilitate accurate perception. Prominent models present conflicting evidence regarding whether attention and prediction have opposing or interactive roles, whether attention promotes or suppresses predictive errors, and whether these processes are neurologically interconnected or distinct from each other (Garrido et al., 2018; Jiang et al., 2013; Kok, Rahnev et al., 2012; Smout et al., 2019; Summerfield & Egner, 2009). One proposal assumes that attention is weighting the sensory evidence, leading to increased error signals if the expected sensory input is attended vs. unattended (Friston, 2005; Rao, 2005). By contrast, another proposal suggests that the silencing effect of predictions (reduction of error signals) stands in contrast to the boosting effect of attention (attentional gain; for a review see: Summerfield & Egner, 2009).

In the present thesis, observed top-down effects in anticipation of upcoming visual stimulation were comparable across the two studies. In both studies (Chapter II and III), pre-stimulus alpha desynchronization was stronger over the left hemisphere when comparing left vs. right sensory predictions or spatial attention, respectively (Figure 17 and 24), corresponding to a stronger decrease over the contralateral hemisphere for rightward cueing or predictions. It should be noted that in the study of Chapter II, a significant difference in alpha power was also observed over the right hemisphere, reflecting stronger decrease in alpha power over the contralateral hemisphere for leftward predictions. The present findings and previous results (Alilović et al., 2019; Okazaki et al., 2014; Sauseng et al., 2005; Worden et al., 2000; Zumer et al., 2014) suggest that due to top-down signals, whether related to spatially specific sensory predictions or attention, alpha power decreases contralateral in anticipation of visual stimulation and potentially increases ipsilateral to the side of expected visual stimulation. However, even though similar effects of top-down processing in the pre-stimulus phase were observed in the present dissertation, these might have affected sensory processing in different ways. In Chapter II, the *Visual predictive signal* started to differ early for upper vs. lower visual stimulation (70 ms after stimulus onset). The *Visual predictive signal* resulted from the subtraction of the ERPs to the visual baseline measurements (Visual only) from the ERPs to Standards; in other words, ERPs to predicted visual input minus ERPs to visual input without any prediction. When we interpret our findings in terms of attentional effects, Standards were not only expected, but also attended. Therefore, the increased ERP responses to Standards compared to Visual only trials might have reflected the facilitation of sensory processing due to attention. When we follow this line of interpretation, visual input in the mismatch condition (Deviant) was not only unexpected, but also unattended. Accordingly, if our results could be solely explained by attention, we would have expected that Standards compared to Deviants show increased neural responses, reflecting a sensory gain-control mechanism due to attention. Moreover, we would have expected that this effect occurs early, since attentional effects are already observable in the early phase of the P1 component (Di Russo et al., 2002; Martinez et al., 1999). However, we did not observe an early effect when comparing Standards and Deviants. Furthermore, neural responses to unexpected visual input were actually increased compared to expected input, but only at a later time point. Indeed, the findings in the present thesis speak for an interpretation that the decrease due to predictions and the facilitation due to attention canceled each other out, resulting in similar neural responses during the early phase of visual processing. In Chapter III, endogenous spatial cues did modulate ERPs to task irrelevant bilateral stimulation: ERPs to rightward cueing were increased compared to leftward cueing. This effect was not lateralized, and seemed to be spatially unspecific. However, when examining target processing, spatial endogenous cueing did not affect neural activity - neither ERP responses nor oscillatory activity were modulated. The interpretation of the effects observed in Chapter III in terms of predictions may be difficult due to the methodological limitations mentioned above. Speculatively, observed modulations of neural responses were local and did not spread to surrounding areas, which prevented the observation of more clear effects. However, following the assumption that inhibitory effects of prediction and facilitating effects of attention might cancel each other, neural activity during target processing might reflect the result of these opposing effects, leading to null findings. However, a significant constraint in the existing literature and in the present dissertation is that prediction and attention are often assessed as overlapping factors, posing challenges in discerning whether they truly operate within a unified framework or exhibit context-dependent variations. Thus, future research might investigate both factors in isolation, or uses study designs that are able to disentangle the effects of prediction and attention.

Conclusion

To conclude, the first cortical response of visual processing seemed to be independent of top-down control. Later in the processing hierarchy, top-down signals modulate visual processing. Bottom-up signals (related to error processing) emerge only after the modulatory effects of top-down signals. Furthermore, visual spatial attention seems to modulate oscillatory activity in the anticipation of upcoming visual input. It could be hypothesized that the effects during anticipation are rather broad, subtending a wider assembly of neurons, whereas during stimulation, these effects are limited to a local area which is behaviorally relevant. Future research is needed to disentangle the interaction of prediction and attention effects on stimulus processing.

References

Acharya, J. N., Hani, A. J., Cheek, J., Thirumala, P., & Tsuchida, T. N. (2016). American clinical neurophysiology society guideline 2: Guidelines for standard electrode position nomenclature. *The Neurodiagnostic Journal*, *56*(4), 245–252.

Adjamian, P., Holliday, I. E., Barnes, G. R., Hillebrand, A., Hadjipapas, A., & Singh, K. D. (2004). Induced visual illusions and gamma oscillations in human primary visual cortex. *European Journal of Neuroscience*, *20*(2), 587–592.

Adrian, E. D., & Matthews, B. H. C. (1934). The interpretation of potential waves in the cortex. *The Journal of Physiology*, *81*(4), 440.

Aitken, F., Menelaou, G., Warrington, O., Koolschijn, R. S., Corbin, N., Callaghan, M. F., & Kok, P. (2020). Prior expectations evoke stimulus-specific activity in the deep layers of the primary visual cortex. *PLoS Biology*, *18*(12), e3001023.

Alamia, A., Terral, L., d'Ambra, M. R., & VanRullen, R. (2023). Distinct roles of forward and backward alpha-band waves in spatial visual attention. *Elife, 12,* e85035.

Alilović, J., Timmermans, B., Reteig, L. C., van Gaal, S., & Slagter, H. A. (2019). No evidence that predictions and attention modulate the first feedforward sweep of cortical information processing. *Cerebral Cortex*, *29*(5), 2261–2278.

Alink, A., Schwiedrzik, C. M., Kohler, A., Singer, W., & Muckli, L. (2010). Stimulus predictability reduces responses in primary visual cortex. *Journal of Neuroscience, 30*(8), 2960–2966.

Banzi, M., & Shiloh, M. (2014). *Getting started with Arduino: The open source electronics prototyping platform*. Maker Media, Inc.

Başar, E. (2012). A review of alpha activity in integrative brain function: fundamental physiology, sensory coding, cognition and pathology. *International Journal of Psychophysiology*, *86*(1), 1–24.

Bastos, A. M., Usrey, W. M., Adams, R. A., Mangun, G. R., Fries, P., & Friston, K. J. (2012). Canonical microcircuits for predictive coding. *Neuron*, *76*(4), 695–711.

Bastos, A. M., Vezoli, J., Bosman, C. A., Schoffelen, J.-M., Oostenveld, R., Dowdall, J. R., Weerd, P. de, Kennedy, H., & Fries, P. (2015). Visual areas exert feedforward and feedback influences through distinct frequency channels. *Neuron*, *85*(2), 390–401.

Bauer, M., Kluge, C., Bach, D., Bradbury, D., Heinze, H. J., Dolan, R. J., & Driver, J. (2012). Cholinergic enhancement of visual attention and neural oscillations in the human brain. *Current Biology*, *22*(5), 397–402.

Baumgartner, H. M., Graulty, C. J., Hillyard, S. A., & Pitts, M. A. (2018). Does spatial attention modulate the earliest component of the visual evoked potential? *Cognitive Neuroscience*, *9*(1-2), 4–19.

Bendixen, A., Schröger, E., & Winkler, I. (2009). I heard that coming: Event-related potential evidence for stimulus-driven prediction in the auditory system. *Journal of Neuroscience*, *29*(26), 8447–8451.

Berger, A., Henik, A., & Rafal, R. (2005). Competition between endogenous and exogenous orienting of visual attention. *Journal of Experimental Psychology: General*, *134*(2), 207.

Berger, H. (1929). Über das elektroenkephalogramm des menschen. *Archiv Für Psychiatrie Und Nervenkrankheiten*, *87*(1), 527–570.

Berger, H. (1937). Über das Elektrenkephalogramm des Menschen. XIII. *Archiv Für Psychiatrie Und Nervenkrankheiten*.

Bichot, N. P., Rossi, A. F., & Desimone, R. (2005). Parallel and serial neural mechanisms for visual search in macaque area V4. *Science*, *308*(5721), 529–534.

Brainard, D. H. (1997). The psychophysics toolbox. *Spatial Vision*, *10*(4), 433–436.

Brefczynski, J. A., & DeYoe, E. A. (1999). A physiological correlate of the'spotlight'of visual attention. *Nature Neuroscience*, *2*(4), 370–374.

Buffalo, E. A., Fries, P., Landman, R., Buschman, T. J., & Desimone, R. (2011). Laminar differences in gamma and alpha coherence in the ventral stream. *Proceedings of the National Academy of Sciences*, *108*(27), 11262–11267.

Bullier, J. (2001). Integrated model of visual processing. *Brain Research Reviews*, *36*(2-3), 96–107.

Busch, N. A., Schadow, J., Fründ, I., & Herrmann, C. S. (2006). Time-frequency analysis of target detection reveals an early interface between bottom-up and top-down processes in the gamma-band. *NeuroImage*, *29*(4), 1106–1116.

Carrasco, M. (2011). Visual attention: The past 25 years. *Vision Research*, *51*(13), 1484–1525.

Chalk, M., Herrero, J. L., Gieselmann, M. A., Delicato, L. S., Gotthardt, S., & Thiele, A. (2010). Attention reduces stimulus-driven gamma frequency oscillations and spike field coherence in V1. *Neuron*, *66*(1), 114–125.

Chao, Z. C., Huang, Y. T., & Wu, C.-T. (2022). A quantitative model reveals a frequency ordering of prediction and prediction-error signals in the human brain. *Communications Biology*, *5*(1), 1076.

Chao, Z. C., Takaura, K., Wang, L., Fujii, N., & Dehaene, S. (2018). Large-scale cortical networks for hierarchical prediction and prediction error in the primate brain. *Neuron*, *100*(5), 1252-1266. e3.

Chica, A. B., Bartolomeo, P., & Lupiáñez, J. (2013). Two cognitive and neural systems for endogenous and exogenous spatial attention. *Behavioural Brain Research*, *237*, 107–123.

Chica, A. B., Martín-Arévalo, E., Botta, F., & Lupiánez, J. (2014). The Spatial Orienting paradigm: How to design and interpret spatial attention experiments. *Neuroscience & Biobehavioral Reviews*, *40*, 35–51.

Corbetta, M., & Shulman, G. L. (2002). Control of goal-directed and stimulus-driven attention in the brain. *Nature Reviews Neuroscience*, *3*(3), 201.

Czigler, I., Winkler, I., Pató, L., Várnagy, A., Weisz, J., & Balázs, L. (2006). Visual temporal window of integration as revealed by the visual mismatch negativity event-related potential to stimulus omissions. *Brain Research*, *1104*(1), 129–140.

de Lange, F. P., Heilbron, M., & Kok, P. (2018). How do expectations shape perception? *Trends in Cognitive Sciences*, *22*(9), 764–779.

de Lange, F. P., Rahnev, D. A., Donner, T. H., & Lau, H. (2013). Prestimulus oscillatory activity over motor cortex reflects perceptual expectations. *Journal of Neuroscience, 33*(4), 1400–1410.

Delorme, A., & Makeig, S. (2004). EEGLAB: An open source toolbox for analysis of single-trial EEG dynamics including independent component analysis. *Journal of Neuroscience Methods*, *134*(1), 9–21.

Demarchi, G., Sanchez, G., & Weisz, N. (2019). Automatic and feature-specific prediction-related neural activity in the human auditory system. *Nature Communications*, *10*(1), 1–11.

Den Ouden, H. E. M., Daunizeau, J., Roiser, J., Friston, K. J., & Stephan, K. E. (2010). Striatal prediction error modulates cortical coupling. *Journal of Neuroscience*, *30*(9), 3210–3219.

Den Ouden, H. E. M., Friston, K. J., Daw, N. D., McIntosh, A. R., & Stephan, K. E. (2008). A dual role for prediction error in associative learning. *Cerebral Cortex*, *19*(5), 1175–1185.

Di Russo, F., Martínez, A., & Hillyard, S. A. (2003). Source analysis of event-related cortical activity during visuo-spatial attention. *Cerebral Cortex*, *13*(5), 486–499.

Di Russo, F., Martínez, A., Sereno, M. I., Pitzalis, S., & Hillyard, S. A. (2002). Cortical sources of the early components of the visual evoked potential. *Human Brain Mapping*, *15*(2), 95–111.

Di Russo, F., Stella, A., Spitoni, G., Strappini, F., Sdoia, S., Galati, G., Hillyard, S. A., Spinelli, D., & Pitzalis, S. (2012). Spatiotemporal brain mapping of spatial attention effects on pattern ‐ reversal ERPs. *Human Brain Mapping*, *33*(6), 1334–1351.

DiCarlo, J. J., Zoccolan, D., & Rust, N. C. (2012). How does the brain solve visual object recognition? *Neuron*, *73*(3), 415–434.

Egner, T., Monti, J. M., & Summerfield, C. (2010). Expectation and surprise determine neural population responses in the ventral visual stream. *Journal of Neuroscience*, *30*(49), 16601–16608.

Ekman, M., Kok, P., & Lange, F. P. de (2017). Time-compressed preplay of anticipated events in human primary visual cortex. *Nature Communications*, *8*, 15276.

Engel, A. K., Fries, P., & Singer, W. (2001). Dynamic predictions: Oscillations and synchrony in top–down processing. *Nature Reviews Neuroscience*, *2*(10), 704.

Feldman, H., & Friston, K. J. (2010). Attention, uncertainty, and free-energy. *Frontiers in Human Neuroscience*, *4*, 215.

Ford, J. M., Roth, W. T., & Kopell, B. S. (1976). Attention effects on auditory evoked potentials to infrequent events. *Biological Psychology*, *4*(1), 65–77.

Foxe, J. J., & Snyder, A. C. (2011). The role of alpha-band brain oscillations as a sensory suppression mechanism during selective attention. *Frontiers in Psychology*, *2*, 154.

Fries, P. (2005). A mechanism for cognitive dynamics: neuronal communication through neuronal coherence. *Trends in Cognitive Sciences*, *9*(10), 474–480.

Fries, P. (2009). Neuronal gamma-band synchronization as a fundamental process in cortical computation. *Annual Review of Neuroscience*, *32*, 209–224.

Fries, P. (2015). Rhythms for cognition: communication through coherence. *Neuron*, *88*(1), 220–235.

Fries, P., Reynolds, J. H., Rorie, A. E., & Desimone, R. (2001). Modulation of oscillatory neuronal synchronization by selective visual attention. *Science, 291*(5508), 1560–1563.

Friston, K. (2005). A theory of cortical responses. *Philosophical Transactions of the Royal Society B: Biological Sciences*, *360*(1456), 815–836.

Funes, M. J., Lupiáñez, J., & Milliken, B. (2005). The role of spatial attention and other processes on the magnitude and time course of cueing effects. *Cognitive Processing*, *6*(2), 98–116.

Garrido, M. I., Kilner, J. M., Stephan, K. E., & Friston, K. J. (2009). The mismatch negativity: a review of underlying mechanisms. *Clinical Neurophysiology*, *120*(3), 453–463.

Garrido, M. I., Rowe, E. G., Halász, V., & Mattingley, J. B. (2018). Bayesian mapping reveals that attention boosts neural responses to predicted and unpredicted stimuli. *Cerebral Cortex, 28*(5), 1771–1782.

Gavornik, J. P., & Bear, M. F. (2014). Learned spatiotemporal sequence recognition and prediction in primary visual cortex. *Nature Neuroscience, 17*(5), 732.

Gondan, M., Lange, K., Rösler, F., & Röder, B. (2004). The redundant target effect is affected by modality switch costs. *Psychonomic Bulletin & Review, 11,* 307–313.

Gould, I. C., Rushworth, M. F., & Nobre, A. C. (2011). Indexing the graded allocation of visuospatial attention using anticipatory alpha oscillations. *Journal of Neurophysiology*, *105*(3), 1318–1326.

Grill-Spector, K., Kushnir, T., Hendler, T., & Malach, R. (2000). The dynamics of object-selective activation correlate with recognition performance in humans. *Nature Neuroscience*, *3*(8), 837–843.

Grubb, M. A., White, A. L., Heeger, D. J., & Carrasco, M. (2015). Interactions between voluntary and involuntary attention modulate the quality and temporal dynamics of visual processing. *Psychonomic Bulletin & Review*, *22*, 437–444.

Gruber, T., Müller, M. M., Keil, A., & Elbert, T. (1999). Selective visual-spatial attention alters induced gamma band responses in the human EEG. *Clinical Neurophysiology*, *110*(12), 2074–2085.

Haegens, S., Nácher, V., Luna, R., Romo, R., & Jensen, O. (2011). α-Oscillations in the monkey sensorimotor network influence discrimination performance by rhythmical inhibition of neuronal spiking. *Proceedings of the National Academy of Sciences*, *108*(48), 19377–19382.

Han, C., Wang, T., Yang, Y., Wu, Y., Li, Y., Dai, W., Zhang, Y., Wang, B., Yang, G., & Cao, Z. (2021). Multiple gamma rhythms carry distinct spatial frequency information in primary visual cortex. *PLoS Biology*, *19*(12), e3001466.

Harris, K. D., & Mrsic-Flogel, T. D. (2013). Cortical connectivity and sensory coding. *Nature*, *503*(7474), 51–58.

Herring, J. D., Esterer, S., Marshall, T. R., Jensen, O., & Bergmann, T. O. (2019). Low-frequency alternating current stimulation rhythmically suppresses gamma-band oscillations and impairs perceptual performance. *NeuroImage*, *184*, 440–449.

Hertäg, L., & Clopath, C. (2022). Prediction-error neurons in circuits with multiple neuron types: Formation, refinement, and functional implications. *Proceedings of the National Academy of Sciences*, *119*(13), e2115699119.

Hertäg, L., & Sprekeler, H. (2020). Learning prediction error neurons in a canonical interneuron circuit. *Elife*, *9*, e57541.

Hillyard, S. A., Vogel, E. K., & Luck, S. J. (1998). Sensory gain control (amplification) as a mechanism of selective attention: electrophysiological and neuroimaging evidence. *Philosophical Transactions of the Royal Society B: Biological Sciences*, *353*(1373), 1257–1270.

Hoogenboom, N., Schoffelen, J.-M., Oostenveld, R., & Fries, P. (2010). Visually induced gamma-band activity predicts speed of change detection in humans. *NeuroImage*, *51*(3), 1162–1167.

Hoogenboom, N., Schoffelen, J.-M., Oostenveld, R., Parkes, L. M., & Fries, P. (2006). Localizing human visual gamma-band activity in frequency, time and space. *NeuroImage*, *29*(3), 764–773.

Hopf, J.-M., Boehler, C. N., Luck, S. J., Tsotsos, J. K., Heinze, H.-J., & Schoenfeld, M. A. (2006). Direct neurophysiological evidence for spatial suppression surrounding the focus of attention in vision. *Proceedings of the National Academy of Sciences*, *103*(4), 1053–1058.

Hopfinger, J. B., & Mangun, G. R. (1998). Reflexive attention modulates processing of visual stimuli in human extrastriate cortex. *Psychological Science*, *9*(6), 441–447.

Hopfinger, J. B., & Mangun, G. R. (2001). Tracking the influence of reflexive attention on sensory and cognitive processing. *Cognitive, Affective, & Behavioral Neuroscience*, *1*(1), 56–65.

Hopfinger, J. B., & West, V. M. (2006). Interactions between endogenous and exogenous attention on cortical visual processing. *NeuroImage*, *31*(2), 774–789.

Hsieh, P.-J., Vul, E., & Kanwisher, N. (2010). Recognition alters the spatial pattern of FMRI activation in early retinotopic cortex. *Journal of Neurophysiology*, *103*(3), 1501–1507.

Hubel, D. H., & Wiesel, T. N. (1968). Receptive fields and functional architecture of monkey striate cortex. *The Journal of Physiology*, *195*(1), 215–243.

Hughes, H. C., Darcey, T. M., Barkan, H. I., Williamson, P. D., Roberts, D. W., & Aslin, C. H. (2001). Responses of human auditory association cortex to the omission of an expected acoustic event. *NeuroImage*, *13*(6), 1073–1089.

Intriligator, J., & Cavanagh, P. (2001). The spatial resolution of visual attention. *Cognitive Psychology*, *43*(3), 171–216.

Jabar, S. B., Filipowicz, A., & Anderson, B. (2017). Tuned by experience: How orientation probability modulates early perceptual processing. *Vision Research*, *138*, 86–96.

Jensen, O., Kaiser, J., & Lachaux, J.-P. (2007). Human gamma-frequency oscillations associated with attention and memory. *Trends in Neurosciences*, *30*(7), 317–324.

Jensen, O., & Mazaheri, A. (2010). Shaping functional architecture by oscillatory alpha activity: gating by inhibition. *Frontiers in Human Neuroscience*, *4*, 186.

Jewell, G., & McCourt, M. E. (2000). Pseudoneglect: a review and meta-analysis of performance factors in line bisection tasks. *Neuropsychologia*, *38*(1), 93–110.

Jia, X., Smith, M. A., & Kohn, A. (2011). Stimulus selectivity and spatial coherence of gamma components of the local field potential. *Journal of Neuroscience*, *31*(25), 9390–9403.

Jia, X., Xing, D., & Kohn, A. (2013). No consistent relationship between gamma power and peak frequency in macaque primary visual cortex. *Journal of Neuroscience*, *33*(1), 17–25.

Jiang, J., Summerfield, C., & Egner, T. (2013). Attention sharpens the distinction between expected and unexpected percepts in the visual brain. *Journal of Neuroscience, 33*(47), 18438–18447.

Jiang, Y., Komatsu, M., Chen, Y., Xie, R., Zhang, K., Xia, Y., Gui, P., Liang, Z., & Wang, L. (2022). Constructing the hierarchy of predictive auditory sequences in the marmoset brain. *Elife, 11*, e74653.

Jonides, J. (1981). Voluntary versus automatic control over the mind's eye's movements. *Attention and Performance*.

Jordan, R., & Keller, G. B. (2020). Opposing influence of top-down and bottom-up input on excitatory layer 2/3 neurons in mouse primary visual cortex. *Neuron*, *108*(6), 1194-1206. e5.

Kanwisher, N., & Wojciulik, E. (2000). Visual attention: insights from brain imaging. *Nature Reviews Neuroscience*, *1*(2), 91–100.

Keller, G. B., & Mrsic-Flogel, T. D. (2018). Predictive processing: A canonical cortical computation. *Neuron*, *100*(2), 424–435.

Kelly, S. P., Gomez-Ramirez, M., & Foxe, J. J. (2008). Spatial attention modulates initial afferent activity in human primary visual cortex. *Cerebral Cortex, 18*(11), 2629–2636.

Kelly, S. P., Gomez‐Ramirez, M., & Foxe, J. J. (2009). The strength of anticipatory spatial biasing predicts target discrimination at attended locations: a high‐density EEG study. *European Journal of Neuroscience, 30*(11), 2224–2234.

Kimura, M., Ohira, H., & Schröger, E. (2010). Localizing sensory and cognitive systems for pre-attentive visual deviance detection: an sLORETA analysis of the data of Kimura et al.(2009). *Neuroscience Letters*, *485*(3), 198–203.

Klein, R. M. (2000). Inhibition of return. *Trends in Cognitive Sciences*, *4*(4), 138–147.

Kleiner, M., Brainard, D., & Pelli, D. (2007). What's new in Psychtoolbox-3? Perception 36 ECVP Abstract Supplement. *PLoS One*.

Klimesch, W., Sauseng, P., & Hanslmayr, S. (2007). EEG alpha oscillations: the inhibition–timing hypothesis. *Brain Research Reviews*, *53*(1), 63–88.

Klink, P. C., Dagnino, B., Gariel-Mathis, M.-A., & Roelfsema, P. R. (2017). Distinct feedforward and feedback effects of microstimulation in visual cortex reveal neural mechanisms of texture segregation. *Neuron*, *95*(1), 209-220. e3.

Klinke, R., Fruhstorfer, H., & Finkenzeller, P. (1968). Evoked responses as a function of external and stored information. *Electroencephalography and Clinical Neurophysiology*, *25*(2), 119–122.

Koelewijn, L., Rich, A. N., Muthukumaraswamy, S. D., & Singh, K. D. (2013). Spatial attention increases high-frequency gamma synchronisation in human medial visual cortex. *NeuroImage*, *79*, 295–303.

Kok, P., Bains, L. J., van Mourik, T., Norris, D. G., & Lange, F. P. de (2016). Selective activation of the deep layers of the human primary visual cortex by top-down feedback. *Current Biology*, *26*(3), 371–376.

Kok, P., Failing, M. F., & Lange, F. P. de (2014). Prior expectations evoke stimulus templates in the primary visual cortex. *Journal of Cognitive Neuroscience*, *26*(7), 1546–1554.

Kok, P., Jehee, J. F. M., & Lange, F. P. de (2012). Less is more: Expectation sharpens representations in the primary visual cortex. *Neuron*, *75*(2), 265–270.

Kok, P., Mostert, P., & Lange, F. P. de (2017). Prior expectations induce prestimulus sensory templates. *Proceedings of the National Academy of Sciences*, *114*(39), 10473–10478.

Kok, P., Rahnev, D., Jehee, J. F. M., Lau, H. C., & Lange, F. P. de (2012). Attention reverses the effect of prediction in silencing sensory signals. *Cerebral Cortex*, *22*(9), 2197–2206.

Kucewicz, M. T., Berry, B. M., Kremen, V., Brinkmann, B. H., Sperling, M. R., Jobst, B. C., Gross, R. E., Lega, B., Sheth, S. A., & Stein, J. M. (2017). Dissecting gamma frequency activity during human memory processing. *Brain*, *140*(5), 1337–1350.

Lamme, V. af, Super, H., & Spekreijse, H. (1998). Feedforward, horizontal, and feedback processing in the visual cortex. *Current Opinion in Neurobiology*, *8*(4), 529–535.

Landry, M., Da Silva Castanheira, J., Sackur, J., & Raz, A. (2021). Investigating how the modularity of visuospatial attention shapes conscious perception using type I and type II signal detection theory. *Journal of Experimental Psychology: Human Perception and Performance*, *47*(3), 402.

Lasaponara, S., D’Onofrio, M., Dragone, A., Pinto, M., Caratelli, L., & Doricchi, F. (2017). Changes in predictive cuing modulate the hemispheric distribution of the P1 inhibitory response to attentional targets. *Neuropsychologia*, *99*, 156–164.

Lasaponara, S., Pinto, M., Aiello, M., Tomaiuolo, F., & Doricchi, F. (2019). The hemispheric distribution of α-band EEG activity during orienting of attention in patients with reduced awareness of the left side of space (spatial neglect). *Journal of Neuroscience*, *39*(22), 4332–4343.

Lee, T. S., & Mumford, D. (2003). Hierarchical Bayesian inference in the visual cortex. *JOSA a*, *20*(7), 1434–1448.

Lee, T.-W., Girolami, M., & Sejnowski, T. J. (1999). Independent component analysis using an extended infomax algorithm for mixed subgaussian and supergaussian sources. *Neural Computation*, *11*(2), 417–441.

Magazzini, L., & Singh, K. D. (2018). Spatial attention modulates visual gamma oscillations across the human ventral stream. *NeuroImage*, *166*, 219–229.

Mangun, G. R., & Hillyard, S. A. (1991). Modulations of sensory-evoked brain potentials indicate changes in perceptual processing during visual-spatial priming. *Journal of Experimental Psychology: Human Perception and Performance*, *17*(4), 1057.

Mangun, G. R., Hinrichs, H., Scholz, M., Mueller-Gaertner, H. W., Herzog, H., Krause, B. J., Tellman, L., Kemna, L., & Heinze, H. J. (2001). Integrating electrophysiology and neuroimaging of spatial selective attention to simple isolated visual stimuli. *Vision Research*, *41*(10-11), 1423–1435.

Mangun, G. R., Hopfinger, J. B., Kussmaul, C. L., Fletcher, E. M., & Heinze, H. ‐ J. (1997). Covariations in ERP and PET measures of spatial selective attention in human extrastriate visual cortex. *Human Brain Mapping*, *5*(4), 273–279.

Maris, E., & Oostenveld, R. (2007). Nonparametric statistical testing of EEG-and MEG-data. *Journal of Neuroscience Methods*, *164*(1), 177–190.

Marshall, T. R., O'Shea, J., Jensen, O., & Bergmann, T. O. (2015). Frontal eye fields control attentional modulation of alpha and gamma oscillations in contralateral occipitoparietal cortex. *Journal of Neuroscience*, *35*(4), 1638–1647.

Marshall, T. R., Bergmann, T. O., & Jensen, O. (2015). Frontoparietal structural connectivity mediates the top-down control of neuronal synchronization associated with selective attention. *PLoS Biology*, *13*(10), e1002272.

Martinez, A., Anllo-Vento, L., Sereno, M. I., Frank, L. R., Buxton, R. B., Dubowitz, D. J., Wong, E. C., Hinrichs, H., Heinze, H. J., & Hillyard, S. A. (1999). Involvement of striate and extrastriate visual cortical areas in spatial attention. *Nature Neuroscience, 2*(4), 364–369.

Martınez, A., DiRusso, F., Anllo-Vento, L., Sereno, M. I., Buxton, R. B., & Hillyard, S. A. (2001). Putting spatial attention on the map: timing and localization of stimulus selection processes in striate and extrastriate visual areas. *Vision Research*, *41*(10-11), 1437–1457.

Mayer, A., Schwiedrzik, C. M., Wibral, M., Singer, W., & Melloni, L. (2015). Expecting to see a letter: alpha oscillations as carriers of top-down sensory predictions. *Cerebral Cortex*, *26*(7), 3146–3160.

Meyer, K. (2012). Another remembered present. *Science*, *335*(6067), 415–416.

Meyer, T., & Olson, C. R. (2011). Statistical learning of visual transitions in monkey inferotemporal cortex. *Proceedings of the National Academy of Sciences*, *108*(48), 19401–19406.

Michalareas, G., Vezoli, J., van Pelt, S., Schoffelen, J.-M., Kennedy, H., & Fries, P. (2016). Alpha-beta and gamma rhythms subserve feedback and feedforward influences among human visual cortical areas. *Neuron*, *89*(2), 384–397.

Miller, E. K., Li, L., & Desimone, R. (1991). A neural mechanism for working and recognition memory in inferior temporal cortex. *Science*, *254*(5036), 1377–1379.

Mo, J., Schroeder, C. E., & Ding, M. (2011). Attentional modulation of alpha oscillations in macaque inferotemporal cortex. *Journal of Neuroscience*, *31*(3), 878–882.

Muckli, L., Martino, F. de, Vizioli, L., Petro, L. S., Smith, F. W., Ugurbil, K., Goebel, R., & Yacoub, E. (2015). Contextual Feedback to Superficial Layers of V1. *Current Biology : CB*, *25*(20), 2690–2695. https://doi.org/10.1016/j.cub.2015.08.057

Müller, H. J., & Findlay, J. M. (1988). The effect of visual attention of peripheral discrimination thresholds in single and multiple element displays. *Acta Psychologica*, *69*(2), 129–155.

Müller, H. J., & Rabbitt, P. M. (1989). Reflexive and voluntary orienting of visual attention: time course of activation and resistance to interruption. *Journal of Experimental Psychology: Human Perception and Performance*, *15*(2), 315.

Müller, M. M., Gruber, T., & Keil, A. (2000). Modulation of induced gamma band activity in the human EEG by attention and visual information processing. *International Journal of Psychophysiology*, *38*(3), 283–299.

Müller, N. G., & Kleinschmidt, A. (2004). The attentional 'spotlight's' penumbra: center-surround modulation in striate cortex. *Neuroreport*, *15*(6), 977–980.

Murty, D. V., Shirhatti, V., Ravishankar, P., & Ray, S. (2018). Large visual stimuli induce two distinct gamma oscillations in primate visual cortex. *Journal of Neuroscience, 38*(11), 2730–2744.

Muthukumaraswamy, S. D., & Singh, K. D. (2013). Visual gamma oscillations: the effects of stimulus type, visual field coverage and stimulus motion on MEG and EEG recordings. *NeuroImage*, *69,* 223–230.

Natale, E., Marzi, C. A., & Macaluso, E. (2009). FMRI correlates of visuo‐spatial reorienting investigated with an attention shifting double‐cue paradigm. *Human Brain Mapping*, *30*(8), 2367–2381.

Okazaki, Y. O., Weerd, P. de, Haegens, S., & Jensen, O. (2014). Hemispheric lateralization of posterior alpha reduces distracter interference during face matching. *Brain Research*, *1590,* 56–64.

Oostenveld, R., Fries, P., Maris, E., & Schoffelen, J.-M. (2011). FieldTrip: Open source software for advanced analysis of MEG, EEG, and invasive electrophysiological data. *Computational Intelligence and Neuroscience*, *2011*.

Orekhova, E. V., Butorina, A. V., Sysoeva, O. V., Prokofyev, A. O., Nikolaeva, A. Y., & Stroganova, T. A. (2015). Frequency of gamma oscillations in humans is modulated by velocity of visual motion. *Journal of Neurophysiology*, *114*(1), 244–255.

Park, H.-J., & Friston, K. (2013). Structural and functional brain networks: from connections to cognition. *Science*, *342*(6158), 1238411.

Pfurtscheller, G., Neuper, C., & Mohl, W. (1994). Event-related desynchronization (ERD) during visual processing. *International Journal of Psychophysiology*, *16*(2-3), 147–153.

Pion-Tonachini, L., Kreutz-Delgado, K., & Makeig, S. (2019). ICLabel: An automated electroencephalographic independent component classifier, dataset, and website. *NeuroImage*, *198*, 181–197.

Plöchl, M., Ossandón, J. P., & König, P. (2012). Combining EEG and eye tracking: identification, characterization, and correction of eye movement artifacts in electroencephalographic data. *Frontiers in Human Neuroscience*, *6*, 278.

Poch, C., Campo, P., & Barnes, G. R. (2014). Modulation of alpha and gamma oscillations related to retrospectively orienting attention within working memory. *European Journal of Neuroscience*, *40*(2), 2399–2405.

Popov, T., Gips, B., Kastner, S., & Jensen, O. (2019). Spatial specificity of alpha oscillations in the human visual system. *Human Brain Mapping*, *40*(15), 4432–4440.

Popov, T., Kastner, S., & Jensen, O. (2017). FEF-controlled alpha delay activity precedes stimulus-induced gamma-band activity in visual cortex. *Journal of Neuroscience*, *37*(15), 4117–4127.

Posner, M. I. (1980). Orienting of attention. *Quarterly Journal of Experimental Psychology*, *32*(1), 3–25.

Posner, M. I., Nissen, M. J., & Ogden, W. C. (1978). Attended and unattended processing modes: The role of set for spatial location. *Modes of Perceiving and Processing Information, 137*(158), 2.

Posner, M. I., Rafal, R. D., Choate, L. S., & Vaughan, J. (1985). Inhibition of return: Neural basis and function. *Cognitive Neuropsychology*, *2*(3), 211–228.

Puri, A. M., & Wojciulik, E. (2008). Expectation both helps and hinders object perception. *Vision Research*, *48*(4), 589–597.

Puri, A. M., Wojciulik, E., & Ranganath, C. (2009). Category expectation modulates baseline and stimulus-evoked activity in human inferotemporal cortex. *Brain Research*, *1301*, 89–99.

Rao, R. P. N. (2005). Bayesian inference and attentional modulation in the visual cortex. *Neuroreport*, *16*(16), 1843–1848.

Rao, R. P. N., & Ballard, D. H. (1999). Predictive coding in the visual cortex: a functional interpretation of some extra-classical receptive-field effects. *Nature Neuroscience, 2*(1), 79–87.

Rauss, K., Pourtois, G., Vuilleumier, P., & Schwartz, S. (2012). Effects of attentional load on early visual processing depend on stimulus timing. *Human Brain Mapping, 33*(1), 63–74.

Rauss, K. S., Pourtois, G., Vuilleumier, P., & Schwartz, S. (2009). Attentional load modifies early activity in human primary visual cortex. *Human Brain Mapping, 30*(5), 1723–1733.

Ray, S., & Maunsell, J. H. R. (2010). Differences in gamma frequencies across visual cortex restrict their possible use in computation. *Neuron*, *67*(5), 885–896.

Ray, S., & Maunsell, J. H. R. (2011). Different origins of gamma rhythm and high-gamma activity in macaque visual cortex. *PLoS Biology, 9*(4), e1000610.

Rees, G., Frith, C. D., & Lavie, N. (1997). Modulating irrelevant motion perception by varying attentional load in an unrelated task. *Science*, *278*(5343), 1616–1619.

Riesenhuber, M., & Poggio, T. (1999). Hierarchical models of object recognition in cortex. *Nature Neuroscience*, *2*(11), 1019–1025.

Rihs, T. A., Michel, C. M., & Thut, G. (2007). Mechanisms of selective inhibition in visual spatial attention are indexed by α - band EEG synchronization. *European Journal of Neuroscience*, *25*(2), 603–610.

Rockland, K. S., & Pandya, D. N. (1979). Laminar origins and terminations of cortical connections of the occipital lobe in the rhesus monkey. *Brain Research*, *179*(1), 3–20.

Roelfsema, P. R., Lamme, V. af, & Spekreijse, H. (1998). Object-based attention in the primary visual cortex of the macaque monkey. *Nature*, *395*(6700), 376–381.

Rohenkohl, G., & Nobre, A. C. (2011). Alpha oscillations related to anticipatory attention follow temporal expectations. *Journal of Neuroscience, 31*(40), 14076–14084.

Rungratsameetaweemana, N., Itthipuripat, S., Salazar, A., & Serences, J. T. (2018). Expectations do not alter early sensory processing during perceptual decision-making. *Journal of Neuroscience*, *38*(24), 5632–5648.

Samaha, J., Boutonnet, B., & Lupyan, G. (2016). *How prior knowledge prepares perception: Prestimulus oscillations carry perceptual expectations and influence early visual responses. bioRxiv, 76687.*

SanMiguel, I., Saupe, K., & Schröger, E. (2013). I know what is missing here: Electrophysiological prediction error signals elicited by omissions of predicted" what" but not" when". *Frontiers in Human Neuroscience*, *7*, 407.

Sauseng, P., Klimesch, W., Stadler, W., Schabus, M., Doppelmayr, M., Hanslmayr, S., Gruber, W. R., & Birbaumer, N. (2005). A shift of visual spatial attention is selectively associated with human EEG alpha activity. *European Journal of Neuroscience*, *22*(11), 2917–2926.

Schellekens, W., van Wezel, R. J. A., Petridou, N., Ramsey, N. F., & Raemaekers, M. (2016). Predictive coding for motion stimuli in human early visual cortex. *Brain Structure and Function*, *221*, 879–890.

Schliephake, L. M., Trempler, I., Roehe, M. A., Heins, N., & Schubotz, R. I. (2021). Positive and negative prediction error signals to violated expectations of face and place stimuli distinctively activate FFA and PPA. *NeuroImage*, *236*, 118028.

Siegel, M., Donner, T. H., Oostenveld, R., Fries, P., & Engel, A. K. (2008). Neuronal synchronization along the dorsal visual pathway reflects the focus of spatial attention. *Neuron*, *60*(4), 709–719.

Simson, R., Vaughan Jr, H. G., & Walter, R. (1976). The scalp topography of potentials associated with missing visual or auditory stimuli. *Electroencephalography and Clinical Neurophysiology*, *40*(1), 33–42.

Smout, C. A., Tang, M. F., Garrido, M. I., & Mattingley, J. B. (2019). Attention promotes the neural encoding of prediction errors. *PLoS Biology*, *17*(2), e2006812.

Sourav, S., Bottari, D., Kekunnaya, R., & Röder, B. (2018). Evidence of a retinotopic organization of early visual cortex but impaired extrastriate processing in sight recovery individuals. *Journal of Vision*, *18*(3), 22.

Spratling, M. W. (2008). Predictive coding as a model of biased competition in visual attention. *Vision Research*, *48*(12), 1391–1408.

Stange, L., Ossandón, J. P., & Röder, B. (2022). Crossmodal visual predictions elicit spatially specific early visual cortex activity but later than real visual stimuli. *BioRxiv*, 2022.12. 14.520404.

Stefanics, G., Kremláček, J., & Czigler, I. (2014). Visual mismatch negativity: A predictive coding view. *Frontiers in Human Neuroscience*, *8*, 666.

Stevens, S. A., West, G. L., Al-Aidroos, N., Weger, U. W., & Pratt, J. (2008). Testing whether gaze cues and arrow cues produce reflexive or volitional shifts of attention. *Psychonomic Bulletin & Review*, *15*(6), 1148–1153.

Sulykos, I., & Czigler, I. (2011). One plus one is less than two: Visual features elicit non-additive mismatch-related brain activity. *Brain Research*, *1398*, 64–71.

Summerfield, C., & Egner, T. (2009). Expectation (and attention) in visual cognition. *Trends in Cognitive Sciences*, *13*(9), 403–409.

Summerfield, C., & Koechlin, E. (2008). A neural representation of prior information during perceptual inference. *Neuron*, *59*(2), 336–347.

Summerfield, C., & Lange, F. P. de (2014). Expectation in perceptual decision making: neural and computational mechanisms. *Nature Reviews Neuroscience*, *15*(11), 745–756.

Supèr, H., Spekreijse, H., & Lamme, V. af (2001). Two distinct modes of sensory processing observed in monkey primary visual cortex (V1). *Nature Neuroscience*, *4*(3), 304–310.

Swettenham, J. B., Muthukumaraswamy, S. D., & Singh, K. D. (2009). Spectral properties of induced and evoked gamma oscillations in human early visual cortex to moving and stationary stimuli. *Journal of Neurophysiology*, *102*(2), 1241–1253.

Tallon-Baudry, C. (2009). The roles of gamma-band oscillatory synchrony in human visual cognition. *Frontiers in Bioscience-Landmark*, *14*(1), 321–332.

Thut, G., Nietzel, A., & Pascual-Leone, A. (2006). Differential distribution of alpha-band electroencephalographic (EEG) activity over occipital cortex indexes visuo-spatial attention bias and predicts visual target detection. *J. Neurosci*, *26*, 9494–9502.

Todorovic, A., & Lange, F. P. de (2012). Repetition suppression and expectation suppression are dissociable in time in early auditory evoked fields. *Journal of Neuroscience*, *32*(39), 13389–13395.

Todorovic, A., van Ede, F., Maris, E., & Lange, F. P. de (2011). Prior expectation mediates neural adaptation to repeated sounds in the auditory cortex: An MEG study. *The Journal of Neuroscience : The Official Journal of the Society for Neuroscience*, *31*(25), 9118–9123. https://doi.org/10.1523/JNEUROSCI.1425-11.2011

Trempler, I., Bürkner, P.-C., El-Sourani, N., Binder, E., Reker, P., Fink, G. R., & Schubotz, R. I. (2020). Impaired context-sensitive adjustment of behaviour in Parkinson's disease patients tested on and off medication: An fMRI study. *NeuroImage*, *212*, 116674.

Treue, S. (2001). Neural correlates of attention in primate visual cortex. *Trends in Neurosciences*, *24*(5), 295–300.

van Dijk, H., Schoffelen, J.-M., Oostenveld, R., & Jensen, O. (2008). Prestimulus oscillatory activity in the alpha band predicts visual discrimination ability. *Journal of Neuroscience*, *28*(8), 1816–1823.

van Es, M. W. J., Gross, J., & Schoffelen, J.-M. (2020). Investigating the effects of pre-stimulus cortical oscillatory activity on behavior. *NeuroImage*, *223*, 117351.

van Kerkoerle, T., Self, M. W., Dagnino, B., Gariel-Mathis, M.-A., Poort, J., van der Togt, C., & Roelfsema, P. R. (2014). Alpha and gamma oscillations characterize feedback and feedforward processing in monkey visual cortex. *Proceedings of the National Academy of Sciences*, *111*(40), 14332–14341.

van Pelt, S., & Fries, P. (2013). Visual stimulus eccentricity affects human gamma peak frequency. *NeuroImage*, *78*, 439–447.

van Velzen, J., & Eimer, M. (2003). Early posterior ERP components do not reflect the control of attentional shifts toward expected peripheral events. *Psychophysiology*, *40*(5), 827–831.

Vinck, M., Uran, C., & Canales-Johnson, A. (2022). The neural dynamics of feedforward and feedback interactions in predictive processing.

Vogel, E. K., & Luck, S. J. (2000). The visual N1 component as an index of a discrimination process. *Psychophysiology*, *37*(2), 190–203.

Wacongne, C., Labyt, E., van Wassenhove, V., Bekinschtein, T., Naccache, L., & Dehaene, S. (2011). Evidence for a hierarchy of predictions and prediction errors in human cortex. *Proceedings of the National Academy of Sciences*, *108*(51), 20754–20759.

Walsh, K. S., McGovern, D. P., Clark, A., & O'Connell, R. G. (2020). Evaluating the neurophysiological evidence for predictive processing as a model of perception. *Annals of the New York Academy of Sciences*, *1464*(1), 242.

Wang, C., Rajagovindan, R., Han, S.-M., & Ding, M. (2016). Top-down control of visual alpha oscillations: Sources of control signals and their mechanisms of action. *Frontiers in Human Neuroscience*, *10*, 15.

Wang, Y., Wu, J., Fu, S., & Luo, Y. (2010). Orienting and focusing in voluntary and involuntary visuospatial attention conditions: An event-related potential study. *Journal of Psychophysiology*, *24*(3), 198.

Williams, S. H., & Johnston, D. (1991). Kinetic properties of two anatomically distinct excitatory synapses in hippocampal CA3 pyramidal neurons. *Journal of Neurophysiology*, *66*(3), 1010–1020.

Winkler, I. (2007). Interpreting the mismatch negativity. *Journal of Psychophysiology*, *21*(3-4), 147–163.

Womelsdorf, T., & Fries, P. (2007). The role of neuronal synchronization in selective attention. *Current Opinion in Neurobiology*, *17*(2), 154–160.

Worden, M. S., Foxe, J. J., Wang, N., & Simpson, G. V. (2000). Anticipatory biasing of visuospatial attention indexed by retinotopically specific alpha-band electroencephalography increases over occipital cortex. *Journal of Neuroscience, 20*(6), RC63-RC63.

Wright, R. D., & Ward, L. M. (2008). *Orienting of attention*. Oxford University Press.

Zumer, J. M., Scheeringa, R., Schoffelen, J.-M., Norris, D. G., & Jensen, O. (2014). Occipital alpha activity during stimulus processing gates the information flow to object-selective cortex. *PLoS Biology*, *12*(10), e1001965.

Appendix

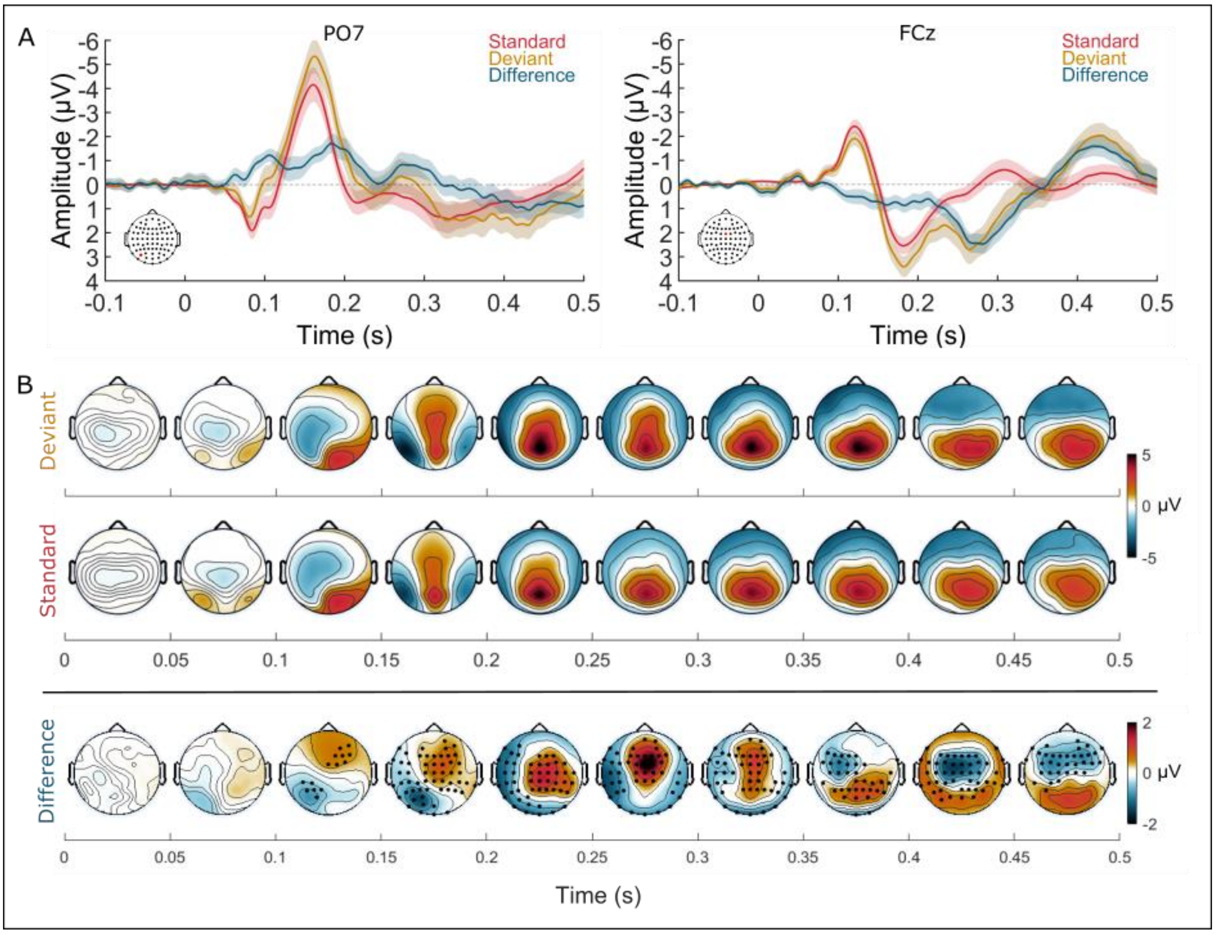

Figure A.1. Grand averages of the ERPs to bottom right (BR) Standards and Deviants. (A) ERPs to BR Standards (red) and Deviants (yellow) and the difference ERP (blue) derived by subtracting ERPs to BR Deviants from ERPs to BR Standards at electrodes PO8 (left) and FCz (right) (see red marked electrodes in the schematic drawing of the electrode montage). Error bands represent the standard error of the mean. Time zero is the moment of the background switch. (B) ERP topographies display the ERPs to BR Deviants (first row) and Standards (second row) and the difference of ERPs to BR Standards minus ERPs to BR Deviants (last row) for the post background switch time epoch 0 to 500 ms in 50 ms steps. Stars in the ERP topographies in the last row indicate electrodes that survived tests for multiple comparisons (p < .05).

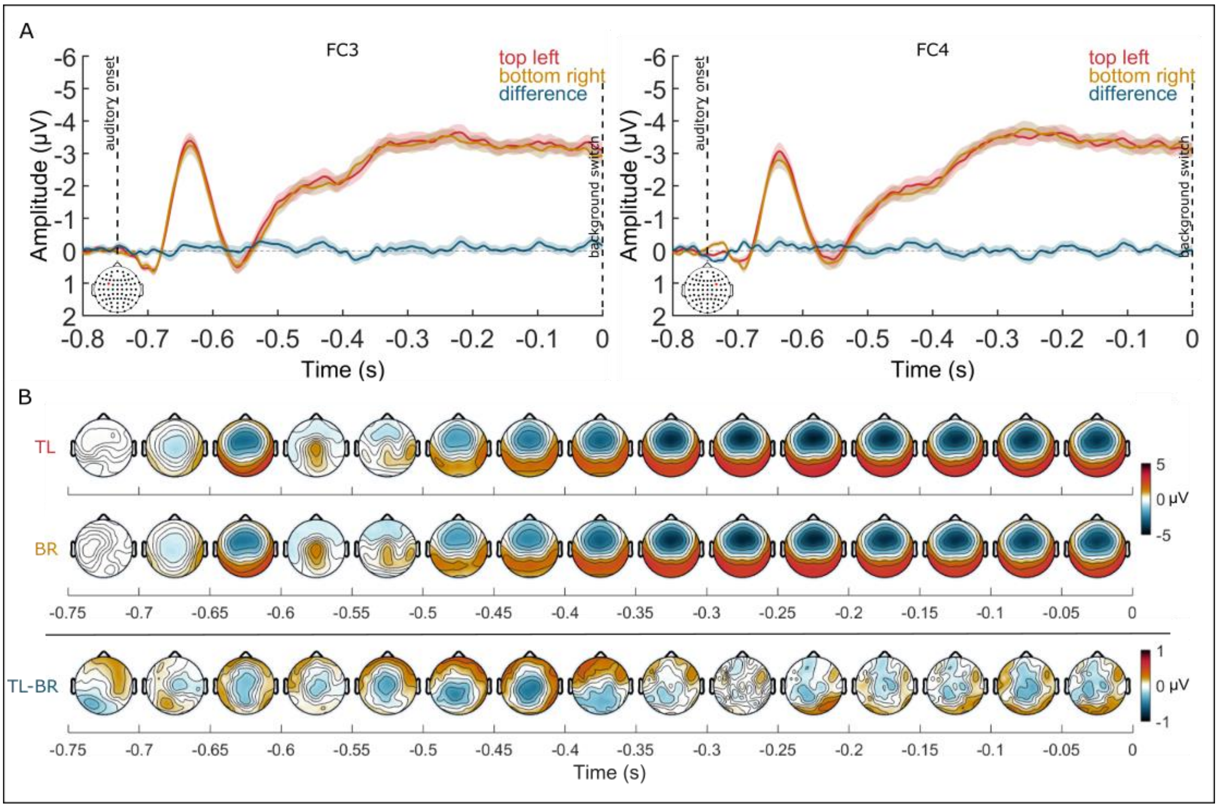

Figure A.2. Grand averages of the ERPs to auditory stimulation in the Auditory only run associated with top left (TL) and bottom right (BR) locations in the crossmodal run. (A) ERPs following auditory stimulation associated with TL (red) and BR (yellow) locations and the difference TL-BR (blue) at electrodes FC3 (left) and FC4 (right) (see red marked electrodes in the schematic drawing of the electrode montage). Error bands represent the standard error of the mean. The first dashed line indicates the onset of auditory stimulus. Time zero is the moment of the background switch. (B) ERP topographies to auditory stimuli (A1/A2) associated with the TL (first row) and BR (second row) location as well as the difference ERP of both conditions (TL-BR; last row) for the pre-background switch time epoch -750 to 0 ms in 50 ms steps. Stars in the ERP topographies in the last row indicate electrodes that survived tests for multiple comparisons (p < .05).

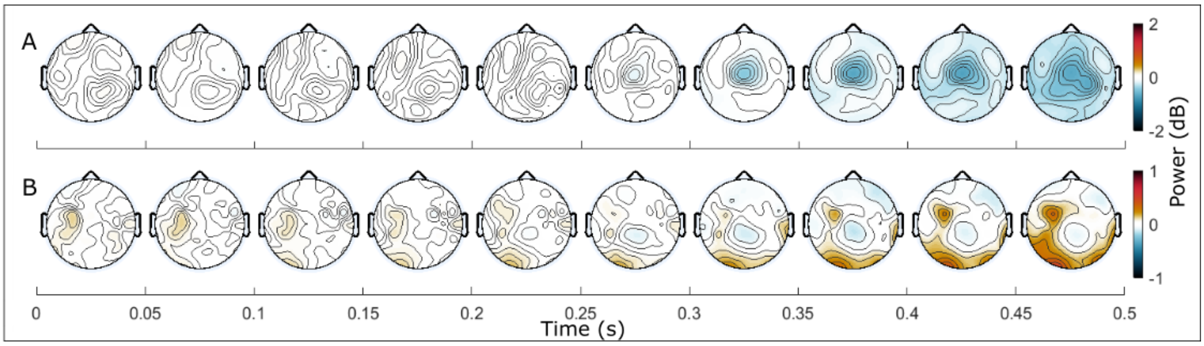

Figure B.1. Modulation of alpha-band (8 to 12 Hz) and gamma-band (50 to 74 Hz) power by target presentation. Time zero represents the onset of the target stimuli. (A) Average EEG topographies of alpha power across participants of the effect of target vs. non-target trials. (B) Average EEG topographies of gamma power across participants of the effect of target vs. non-target trials

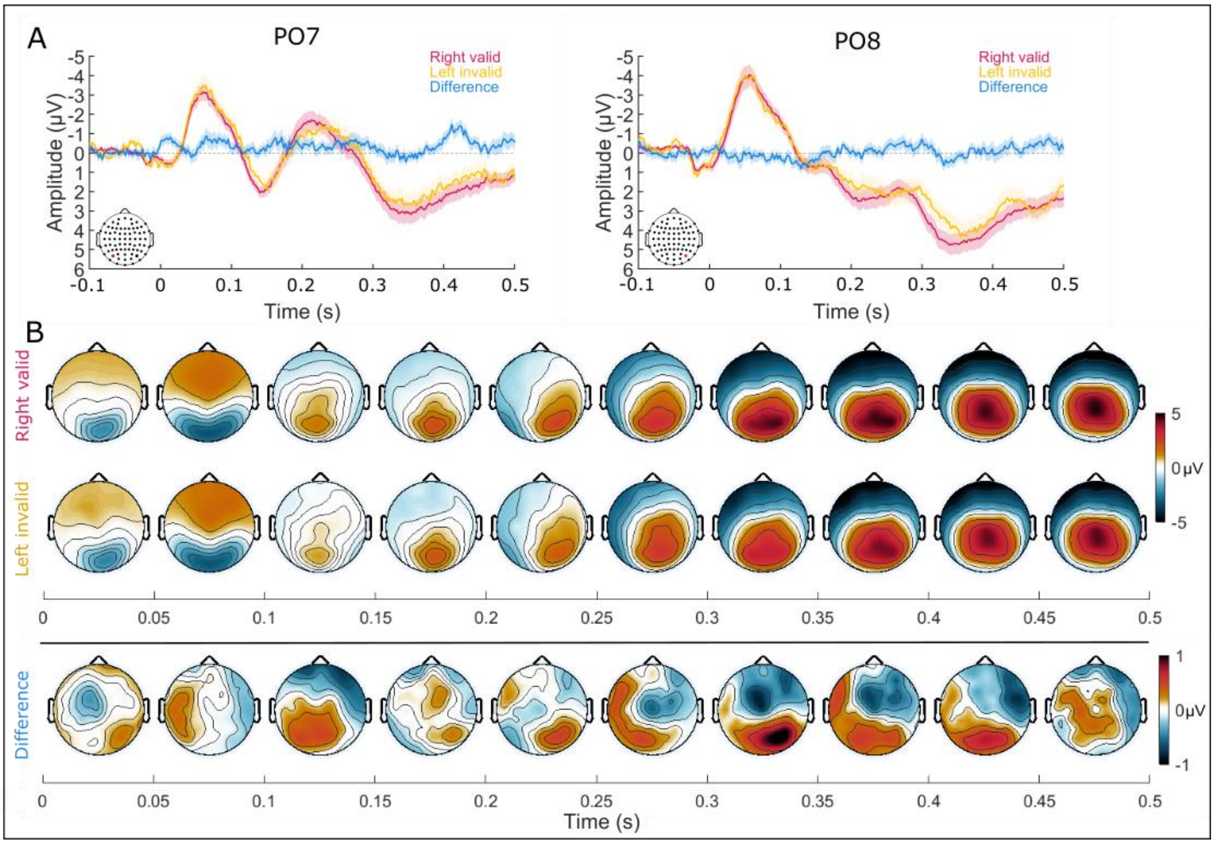

Figure B.2. Grand averages of the ERPs for valid and invalid endogenously cued rightward targets. (A) ERPs to right valid (red), left invalid (yellow) endogenous cues and the difference ERP (blue) derived by subtracting ERPs to left invalid from ERPs to right valid endogenous cues at electrode PO7 (left) and PO8 (right) (see red marked electrodes in the schematic drawing of the electrode montage). Error bands represent the standard error of the mean. At time point zero, the target stimulus was presented. (B) ERP topographies to right valid (first row) and left invalid (second row) endogenous cues as well as the difference ERP (ERP(right valid) minus ERP(left invalid); last row) for the post-exogenous epoch 0 to 500 ms in 50 ms steps. Dots on the ERP topography in the last row indicate electrodes that survived tests for multiple comparisons (p < .05).

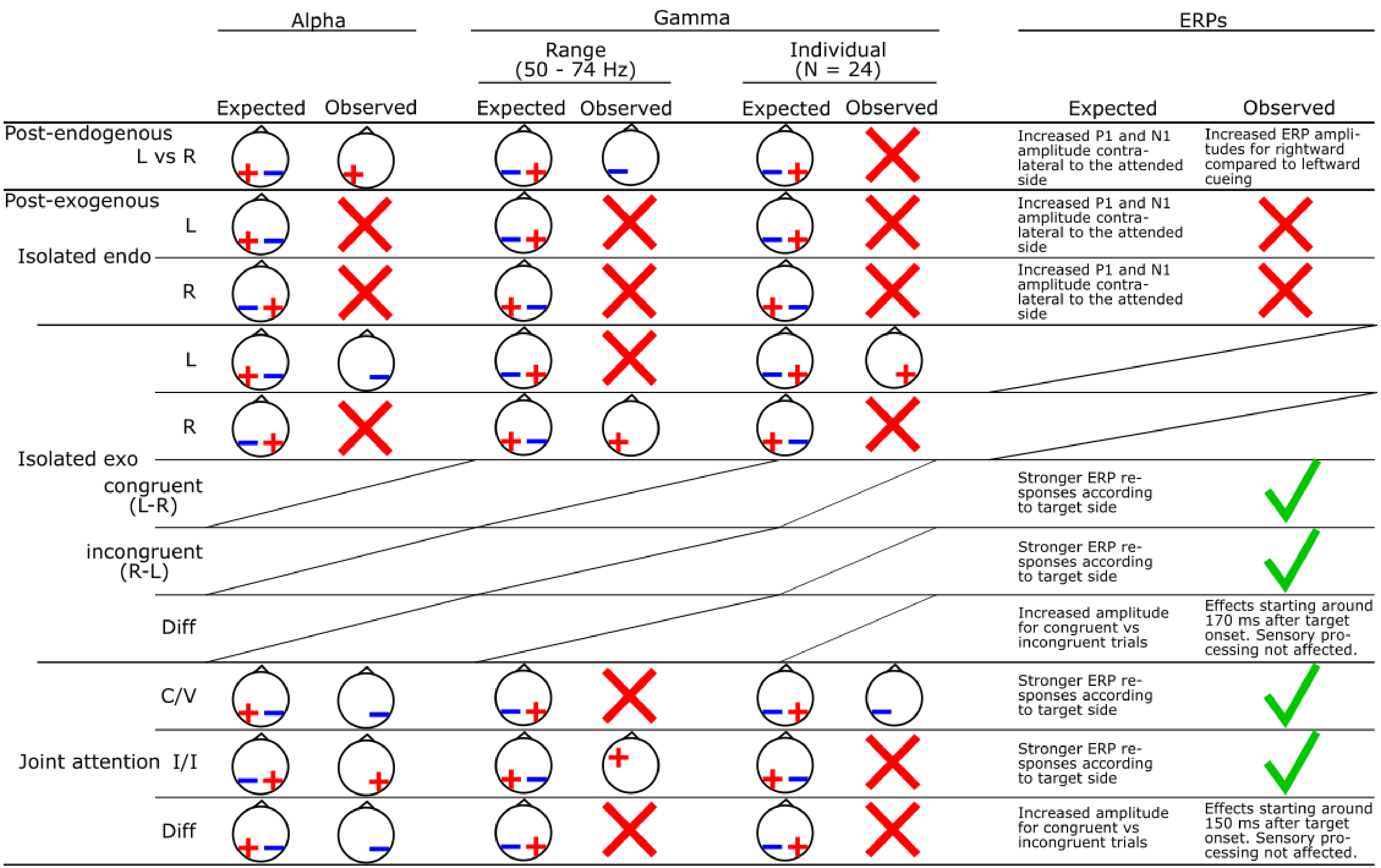

Figure B.3. Illustration of an extract of expected and observed effects of oscillatory activity in the alpha and gamma band, gamma peak frequency, as well as ERPs. Red crosses represent no significant findings, whereas green picks represent that the expected effects were observed. Blue minus symbols represent negative differences, whereas red plus symbols represent positive differences.

Acknowledgments

Ich möchte mich herzlichst bei meiner Betreuerin Brigitte Röder, welche mir die Möglichkeit eröffnet hat zu promovieren und diese erfolgreich zu beenden, und all meinen Kommitesmitgliedern Christian Moll, Viola Störmer, Anja Riesel und Frank Rösler bedanken.

Des Weiteren möcht ich mich bei José P. Ossandón, für seine Unterstützung und sein offenes Ohr, und allen lieben Kolleg*innen in der BPN bedanken. Besonders möchte ich mich bei Andreas Weiß, Madita Linke, Rashi Pant und Alexander Kramer, die ich nicht nur Kolleg*innen, sondern auch Freund*innen nennen darf, bedanken. Des Weiteren möchte ich mich bei Cordula Hölig bedanken, die mich auf den wissenschaftlichen Weg gebracht hat, aber mir immer einen ehrlichen Einblick gab. Viel Dank und Liebe schicke ich auch an unsere ehemaligen Kolleginnen Veronika Zweckerl und Valentina Marcazzan. Der größte Dank geht an meine liebste Kollegin und Arbeitsehefrau Daniela Schönberger, ohne sie hätte es dieses Schriftstück wohl nie gegeben.

Vielen Dank an meine Familie und die besten Freund*innen, die es immer geschafft haben, mich auch aus dem größten Loch rauszuholen! Ich danke meiner Mutter Angela Hoppe für das Selbstvertrauen und den Selbstwert den sie mir mitgegeben hat. Meinem Papa Lutz Hoppe, der mich immer wieder auf den Boden bringt und mich dazu anhält auch eine andere Perspektive einzunehmen. An meinen Bruder Lars Zwetzschke, der auch weit weg auf der anderen Seite der Erde, immer ein Teil meines Lebens geblieben ist. Meiner Schwester Ines Paravia, bei der ich runterkommen kann und die Diss, sowie mein Leben in Hamburg einfach mal ruhen lassen kann. Ich möchte mich bei Timo Stange bedanken, der all die Jahre an meiner Seite war und mich sowohl bei Höhen als auch Tiefen immer wieder geerdet hat. Des Weiteren danke ich: Verena Dillenberger, Malte Jacob, Sarah Valentiner, Frauke Gotzhein, Hanna Stoffregen, Sören Loley, Géraud Ploix, Guido Jakoby, Oliver Petersen, Laura Tzschach, Luisa Siedler, Lukas Voß, Corbin Zander, Annika Lüth, Lena Elwers, Masha Mae Arakeljan, Melina und Annabel, dafür, dass sie einfach die weltbesten Freund*innen sind und mich immer alle so individuell wie sie sind unterstützt und aufgefangen haben!

Universität Hamburg
DER FORSCHUNG | DER LEHRE | DER BILDUNG

FAKULTÄT
FÜR PSYCHOLOGIE UND
BEWEGUNGSWISSENSCHAFT
Institut für Bewegungswissenschaft
Institut für Psychologie

Erklärung gemäß ***(bitte Zutreffendes ankreuzen)***

☐ **§ 4 (1c) der Promotionsordnung des Instituts für Bewegungswissenschaft der Universität Hamburg vom 18.08.2010**

☒ **§ 5 (4d) der Promotionsordnung des Instituts für Psychologie der Universität Hamburg vom 20.08.2003**

Hiermit erkläre ich,

Liesa Stange (Vorname, Nachname),

dass ich mich an einer anderen Universität oder Fakultät noch keiner Doktorprüfung unterzogen oder mich um Zulassung zu einer Doktorprüfung bemüht habe.

Hamburg, 28.04.2023
Ort, Datum

Unterschrift

Universität Hamburg
DER FORSCHUNG | DER LEHRE | DER BILDUNG

FAKULTÄT
FÜR PSYCHOLOGIE UND
BEWEGUNGSWISSENSCHAFT
Institut für Bewegungswissenschaft
Institut für Psychologie

Eidesstattliche Erklärung nach ***(bitte Zutreffendes ankreuzen)***

☐ **§ 7 (4) der Promotionsordnung des Instituts für Bewegungswissenschaft der Universität Hamburg vom 18.08.2010**

☒ **§ 9 (1c und 1d) der Promotionsordnung des Instituts für Psychologie der Universität Hamburg vom 20.08.2003**

Hiermit erkläre ich an Eides statt,

1. dass die von mir vorgelegte Dissertation nicht Gegenstand eines anderen Prüfungsverfahrens gewesen oder in einem solchen Verfahren als ungenügend beurteilt worden ist.
2. dass ich die von mir vorgelegte Dissertation selbst verfasst, keine anderen als die angegebenen Quellen und Hilfsmittel benutzt und keine kommerzielle Promotionsberatung in Anspruch genommen habe. Die wörtlich oder inhaltlich übernommenen Stellen habe ich als solche kenntlich gemacht.

Hamburg, 28.04.2023

Ort, Datum

Unterschrift